THE ROLE OF SKIN DEFORMATION FEEDBACK IN HAPTIC PERCEPTION OF VIRTUAL OBJECTS

A DISSERTATION
SUBMITTED TO THE DEPARTMENT OF MECHANICAL ENGINEERING
AND THE COMMITTEE ON GRADUATE STUDIES
OF STANFORD UNIVERSITY
IN PARTIAL FULFILLMENT OF THE REQUIREMENTS
FOR THE DEGREE OF
DOCTOR OF PHILOSOPHY

Jacob Suchoski

July 2019

This dissertation is online at: http://purl.stanford.edu/zw037mr9511

I certify that I have read this dissertation and that, in my opinion, it is fully adequate in scope and quality as a dissertation for the degree of Doctor of Philosophy.

Allison Okamura, Primary Adviser

I certify that I have read this dissertation and that, in my opinion, it is fully adequate in scope and quality as a dissertation for the degree of Doctor of Philosophy.

Mark Cutkosky

I certify that I have read this dissertation and that, in my opinion, it is fully adequate in scope and quality as a dissertation for the degree of Doctor of Philosophy.

Sean Follmer

Approved for the Stanford University Committee on Graduate Studies.

Patricia J. Gumport, Vice Provost for Graduate Education

This signature page was generated electronically upon submission of this dissertation in electronic format. An original signed hard copy of the signature page is on file in University Archives.

Abstract

Through exploration and interaction, we rely on haptic information to help perceive the world around us. Haptic devices, which can provide controlled touch feedback, have the potential to improve the realism and utility of virtual environments. Traditional haptic devices impart forces and torques on the user, often through a world-grounded kinesthetic force feedback device. However, it is difficult for these world-grounded devices to match the unrestricted movement of head-mounted virtual reality displays due to the increased cost, friction, and inertia that comes with increased size. Skin deformation feedback offers an alternative, user-grounded form of haptic feedback that, when worn on the fingers, can mimic the cutaneous interaction forces experienced during object manipulation. These devices are not without their own limitations; size and weight constraints often limit the available force output applied to the fingerpad, and thus, the physical properties of a virtual object conveyed to a user. This thesis elucidates the role of skin deformation feedback in human perception of virtual objects to inform haptic device design and rendering algorithms.

We started by studying the relative contributions of skin deformation and kinesthetic forces to weight perception. We designed mechanical thimbles to amplify the skin deformation forces felt on the fingerpad when grasping and lifting a real world object, and demonstrated that this changes the weight perceived by human participants. We then augmented an existing three-degree-of-freedom wearable skin deformation device, which provides feedback in the directions shear and normal to the fingerpad, with contact-event based haptics. Then, we showed that adding a high-frequency contact cue to shear-only skin deformation can serve as an alternative to shear-plus-normal skin deformation for a grasp-lift-and-place task of a "fragile" virtual object.

We also found that adding a contact cue to shear-plus-normal skin deformation feedback did not improve the performance of this task. Next, we developed a haptic illusion to alter the perceived weight of virtual objects by scaling inertial forces when using skin deformation haptic feedback. Through human participant experiments, we measured the changes in perceived virtual weight and validated the effect of the illusion. Finally, we combined our scaled inertial forces haptic weight illusion with a visuo-haptic weight illusion, non-unity control-to-display ratio, in complementary and conflicting manners to further alter the perceived virtual weight of virtual objects when using skin deformation haptic devices. These results give insight into how to use the limited available force output of skin deformation feedback devices to help users better perceive virtual worlds.

Acknowledgements

The only person I can think to start off this very long thank-you train is my advisor, Professor Allison Okamura. It is easy to say without her, my path in life would be radically different. When I first came to Stanford, I was woefully unprepared for the rigors of grad school, not to mention the fact that when I arrived on campus I thought "Standford" was the correct spelling of the university I chose to attend. I had thoughts of doing a Phd but no real idea about how to make that happen. Furthermore, after my third week of being on campus, which coincided with my 22nd birthday, I started exhibiting symptoms of what turned out to be chronic kidney disease. During this time, I was supposed to be working on a research rotation project for Allison, jockeying with several other graduate students for one of the few position in her revered lab. Instead, my life got flipped upside down, sending me into a spiral that, quite frankly, I didn't know how to deal with. When things did finally settle, during the fall of my second year of grad school, it seemed a little too late to pursue my goal of a PhD from Stanford (at this point I learned the correct spelling). I approached Allison, soliciting advice about what to do next. She offered me a chance to do another rotation project to bolster my application for other universities' PhD programs. That project happened to lead to a conference paper, and then, a funding opportunity for a PhD student. Allison offered me the funded position, which came days before I needed to confer my masters degree and leave Stanford. Allison didn't have to help me by offering me that research project. She didn't have to offer me that PhD position. She didn't owe me anything and had a line of grad students hoping to have her as their PI. But she saw something in me, and for that, I am eternally grateful. What followed was four of the greatest years of my life. She put up with my

jokes and called me out on my bs. She helped me grow as a student and as a person. I would not be the person I am today if it wasn't for her. So thank you Allison for everything you've done for me.

I would also like to thank my reading committee, Dr. Mark Cutkosky and Dr. Sean Follmer. Thank you for your time with regards to all the presentations, edits, and dialog that helped me round out my work as I completed this thesis. I would also like to thank Dr. Jamie Paik and Dr. Anson Lowe for being a part of my defence committee.

Huge shoutout to the CHARM lab. Everybody in the lab has impacted my life in a positive way. You all are some of the most supportive and genuine people I have ever met. Thanks for putting up with me for 4+ years. Special thank you to Dr. Sam Schorr for being an awesome research mentor and an even better friend. Another special thank you to Sean Sketch for teaching me stats, setting the gold standard for presentations, and for always making time to answer my questions.

Thank you Joe for being the best big brother. You've always had my back and I hope you know that I'll always have yours.

Last, but not least, I want to thank my mom and dad. Thank you for always believing in me. Thank you for supporting me through every up and down. I know I am truly lucky to have you both as parents and words will never be able to convey my gratitude for all things you've done for me and for all the love you've shown me. This is for you.

Nomenclature

β	Coefficient of generalized linear mixed-effects (model)
D_V	Dependent variable of generalized linear mixed-effects (model)
w	Weighting factor of tacile contribution
C/D	Control-to-display ratio
GLME	Generalized linear mixed-effects (model)
ICC	Impulse contact cue
JND	Just noticeable difference
NoCC	No contact cue
PA	Peak acceleration
PGF	Peak grip force
PGFR	Peak grip force rate
POE	Point of objective equality
PSE	Point of subjective equality
SCC	Decaying sinusoid contact cue
SN	Shear-plus-normal skin deformation feedback
SO	Shear-only skin deformation feedback

W Weight of variable-weight object

Contents

List of Tables

List of Figures

Chapter 1

Introduction

Virtual reality systems offer users visually rich and expansive worlds in which to explore and interact. The exploration and interaction experiences are heightened when users are provided haptic feedback, which allows them to feel elements of the virtual world. The combination of haptics with virtual reality not only provides larger entertainment value, such as improving the user experience of playing a virtual piano [16], but can also be used to create useful training simulators for assembly tasks [17] and medical procedures [18]. Furthermore, displaying the physical properties, such as stiffness or weight, of a virtual object through a haptic device has proven useful for conveying certain information, such as tissue consistency in medical training simulators [19], or for decreasing completion times of assembly related tasks when compared to vision only [20].

Traditional haptic devices apply kinesthetic force feedback from world-grounded desktop-based devices. These forces are often applied through a manipulandum that provides the user with both kinesthetic and cutaneous stimuli in an intuitive manner but limits the type of interactions the user can have with the virtual environment. Additionally, these devices suffer from friction and inertial effects when trying to scale the workspace to match the unrestricted movement allowed by current inside-out head-mounted virtual reality displays.

Tactile feedback devices, which provide cutaneous stimuli similar to traditional haptic devices without the kinesthetic force component, can be used as an alternative

to kinesthetic force feedback. They can provide both force direction and magnitude information to the user in an intuitive manner [21, 22]. These devices can be user-grounded, allowing for a wearable form factor and enabling a potentially infinite workspace.

This thesis focuses on a specific type of tactile feedback, skin deformation feedback, which locally deforms the skin of the fingerpad to mimic the cutaneous interaction forces experienced when manipulating a real world object. In particular, we examine the role of skin deformation feedback in perception through design, development, and human participant experiments.

1.1 Motivation

Advancements in head-mounted display technology combined with lower prices have resulted in virtual reality systems reaching a wider range of consumers. Complementary haptic systems have not seen the same level of commercial availability and consumer adoption beyond basic vibration feedback in handheld controllers or smart phones. One main reason for this is cost. Traditional world-grounded kinesthetic force feedback haptic devices require high quality motors to produce high fidelity, high force outputs to the user. Another reason for lack of adoption is available workspace. Achieving a large workspace with a world-grounded device to accompany the movement allowed by current head-mounted displays is hindered by increased inertial and frictional effects that come with increased size.

Skin deformation feedback, a form of tactile feedback, is an alternative to traditional kinesthetic force feedback that offers a user-grounded feedback modality which can complement the free movement enabled by current head-mounted displays. A common design goal for such wearable devices, particularly devices worn on the fingertip, is a lightweight package that does not restrict the movement of the user. To achieve this goal, small, lightweight motors are used, which have a limited force output. Adding gearboxes would increase the force output but decrease the bandwidth, which hinders device performance and rendering accuracy, and increase the weight of a device. This limited force output, in turn, limits the amount of virtual weight

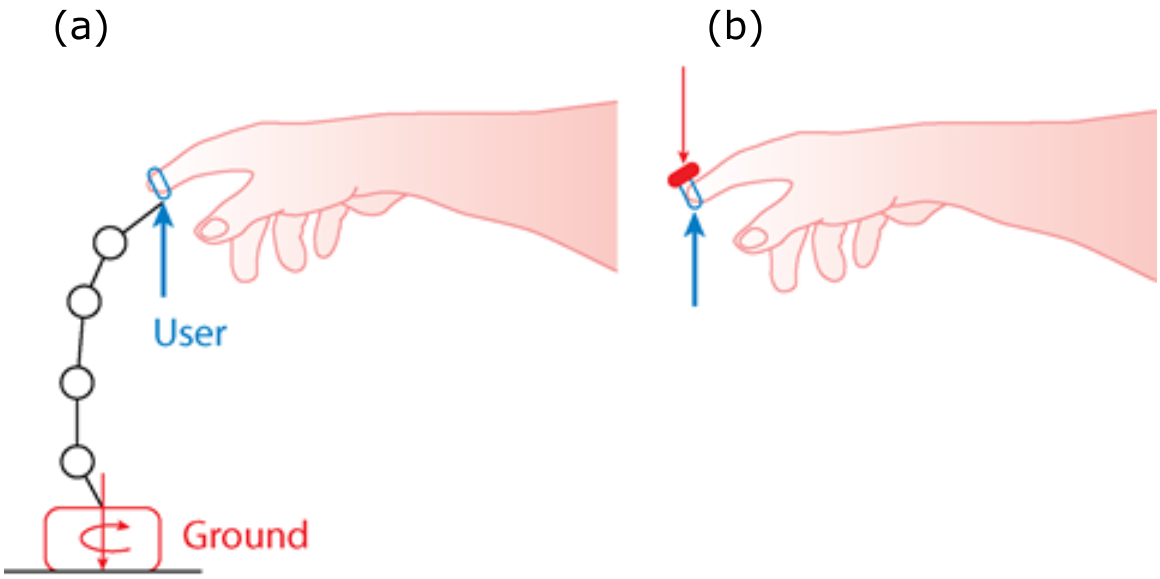

Figure 1.1: (a) Kinesthetic force feedback is often applied by a desktop-base device that is grounded to the world. (b) Skin deformation devices provide an alternative form of feedback that can be grounded to the user. Adapted from [1] © 2013 IEEE.

that can be conveyed to a user in virtual reality when holding a virtual object with wearable skin deformation feedback devices. Thus, it is important to understand the role of skin deformation in virtual reality perception to inform both device design and rendering algorithms that utilize the limited force capabilities of fingertip-wearable, skin deformation feedback devices.

1.2 Contributions

The major contributions of this dissertation are summarized as follows:

- *Design of mechanical thimbles that amplify the amount of skin deformation when picking up real-world objects to measure, through human participant experiments, the relative contributions of skin deformation and kinesthetic forces for object weight perception.* We develop a set of mechanical thimbles that amplify the amount of skin deformation when picking up real-world objects. We

demonstrate, though human participant experiments, that amplified skin deformation forces increase human weight perception of an object. We measure points of subjective equality for multiple ratios of skin deformation forces to kinesthetic forces to estimate their relative contributions in object weight perception and show human weight perception is largely dominated by kinesthetic forces.

- *Integrate and validate contact-event based haptics with a wearable skin deformation haptic device.* We integrate a piezoelectric actuator with an existing skin deformation device to provide contact-event based haptics for testing combinations of three-degree-of-freedom, two-degree-of-freedom shear-only, and no skin deformation feedback with either an impulse-based or decaying sinusoid contact cue. We demonstrate, through human participant experiments, that augmenting three translational degrees of freedom of skin deformation feedback on the fingerpad with a contact-event based cue does not improve task performance of a grasp-lift-and-place task of a "fragile" virtual object. We also demonstrate, through human participant experiments, that adding a high frequency contact-event based vibrotactile contact cue to two shear degrees of freedom of skin deformation feedback improves performance of a grasp-lift-and-place task of the "fragile" virtual object.

- *Implement haptic illusions to alter virtual weight perception during a grasp-lift-and-place task.* We develop an inertial scaling haptic weight illusion, leveraging an existing physics framework for virtual reality environments. We demonstrate and measure, through human participant experiments, a change in perceived virtual weight when using the inertial scaling method with wearable skin deformation haptic feedback devices, increasing the range of perceivable weights that can be rendered. We also demonstrate and measure, through human participant experiments, the change in virtual weight perception when combining haptic and visuo-haptic weight illusion methods, scaled inertial forces and non-unity control-to-display ratio, in complementary and conflicting manners, further increasing the range of perceivable weights that can be rendered.

1.3 Previous Work

This section provides an overview of existing relevant research. We first discuss research on weight perception and weight illusions. We then give an overview of skin deformation feedback and wearable skin deformation haptic devices.

1.3.1 Weight Perception and Illusions

Gaining insight into how humans form weight percepts can help render more believable objects in virtual reality via haptic feedback. Knowing how various haptic signals effect perception can help determine which types of haptic feedback are important. Haptic classification of objects begins with a grasp-and-lift routine, shown in Fig. 1.2, as the first stage of exploration [23]. As the fingers begin to grasp the object, there is a contact cue followed by the reaction forces from the object on the fingers. As we prepare to lift the object, we grasp the object firmly enough, generating enough friction force between the fingers and the object, to support the weight of the object. Upon liftoff, the entire weight of the object is supported between the two fingers, deforming the skin locally, and this weight is felt through the muscles in the arm and hand used to generate the lifting motion. During a grasp and lift task, a person's weight representation of an object is updated by transient afferent responses (e.g., from Pacinian afferents) that occur when the lifting force overcomes gravity [24]. Typically these updates are complete after one or two lifting trials [24].

Weight perception has long been studied, dating back more than a hundred years to when Ernst Weber observed that weight discrimination is more precise if a weight is lifted by the hand as opposed to setting a weight on the hand while the hand is supported by a table. It was further shown that weight discrimination is more sensitive under voluntary muscle contractions compared to muscle contractions elicited via galvanic or faradic excitation of the motor nerve [25]. This indicates that an efferent copy of our muscle commands during a lifting task contributes to our weight perception of an object.

Gibson [26] introduces the idea of affordance, later expanded upon by Turvey et al.

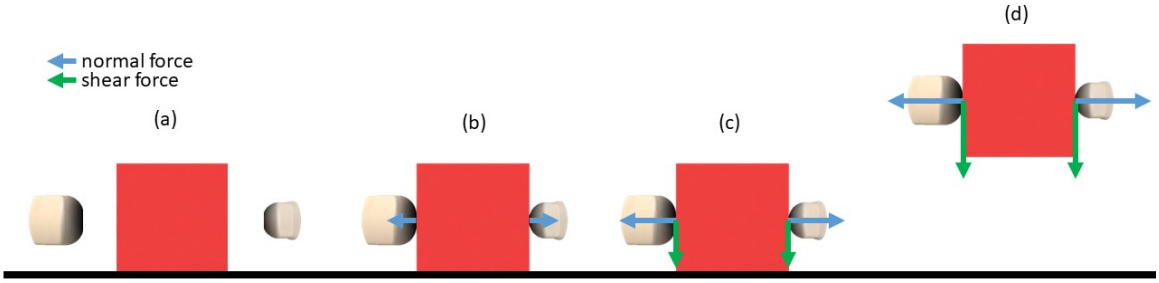

Figure 1.2: An example of a grasp-and-lift task using a pinch grip. (a) The task starts with the thumb and index finger approaching the sides of the object. (b) As contact is made, the normal force increases. (c) Before liftoff, the shear and normal forces on the fingers increase as the lifting force starts to overcome the weight of the object. (d) After liftoff, the weight of the object is supported through the shear forces on the fingers.

[27], with respect to an object's perceived heaviness, which is the consideration of the relation of an object's inertial properties to properties of the human movement system. Turvey et al. show that the perceived heaviness of an object is, in part, determined by the linear combination of the object's mass and particular scalar variables calculated from the object's inertia tensor [27]. This idea of perceived heaviness with respect to the context of inertia and movement is further expanded by Carello et al. [28] where they state "singular properties such as heaviness is more properly construed as 'heaviness while doing X' or 'movable in a particular way.'" This principle agrees with the work done by Amazeen and Tuvey [29] which shows that an object's perceived heaviness when wielded depends on an object's rotational inertia, proving that an object's perceived weight is not just a function of mass but also the effort to wield the object. This body of work emphasizes that weight perception or perceived heaviness must be taken in the context of the action or manipulation taking place and the effort needed to perform the action or manipulation.

The visual aspect of the rotational movement when wielding an object was also shown to have an effect on weight perception when Streit et al. [30] scaled the displayed rotational displacement of a real world object being wielded compared to the actual rotational displacement of the object. This scaling of motion is similar the work presented by Dominjon et al. [31], in which they scale the position of a visual

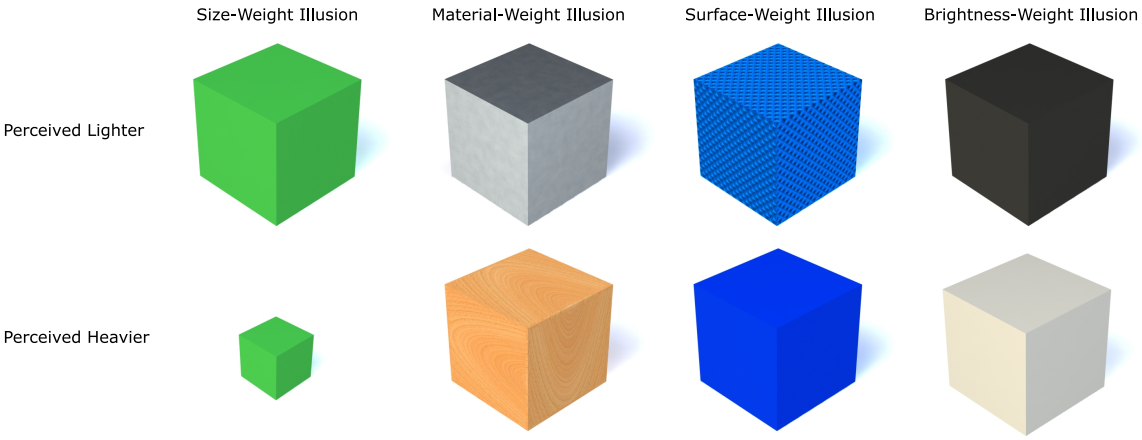

Figure 1.3: Examples of several known weight illusions that show that various physical properties, such as size [2], density [3, 4], surface texture [5, 6], and color brightness [7], can have an effect on weight perception.

avatar of an object being manipulated in virtual reality during a weight discrimination task which alters the virtual object's perceived weight. This scaling value is referred to as the control-to-display ratio.

Differences in certain physical properties, other than the mass of the objects, have been shown to affect weight discrimination and thus play a role in forming the weight percept of an object. Examples of these can be seen in Fig. 1.3. The size-weight illusion, also known as the Charpentier illusion, shows us that an object's size affects its perceived weight [2]. Flanagan and Beltzer [32] showed that one's perceptual system can operate independently from the sensorimotor system based on the persistence of the size-weight illusion even after the sensorimotor system has adapted to the weight of each object from multiple lifts. Wolfe [3] showed that objects made of denser materials, such as brass and steel, are perceived to be lighter than objects made of less dense material, such as wood. Buckingham et al. [4] showed this illusion can be induced from expectation alone by allowing participants to see the object before performing the lift without visual feedback. Furthermore, objects with low friction (smooth) surfaces are likely to be judged to be heavier than objects with high friction (rough) surfaces [5, 6]. Flanagan et al. [5] theorized this is due to the increased grip force required to hold a smother object of the same weight. Even

color has been shown to have a slight effect on weight perception, with lighter and brighter colored objects seeming to be heavier than darker colored objects [7, 33, 34]. Walker et al. [7] showed that darker objects were visually judged to be heavier but it is unknown if this had an effect on the weight perception during a lifting task. While these various physical properties can affect an object's perceived weight, there is no research that has decoupled the tactile shear force from the object's weight – which is experienced kinesthetically – and analyzed their relative contributions to the object's perceived weight.

1.3.2 Skin Deformation Feedback

Adding haptics to virtual reality systems adds the sense of touch to an already visually rich experience. One of the most common and compelling haptic modalities is kinesthetic force feedback. Kinesthetic force feedback is traditionally applied to the user via a world-grounded desktop-based robotic platform, typically through a manipulandum. A classic example of a three-degree-of-freedom kinesthetic haptic device is the Phantom, developed in the early 1990s [35]. Phantoms are often used with a stylus or thimble end-effector, the latter of which is worn by a user on the fingertip. Such devices can often produce large forces and render high virtual stiffnesses but only in a limited workspace. Problems with friction, inertia, and cost hinder the scalability of these devices.

Tactile feedback is another haptic modality that can provide meaningful feedback to a user, particularly on the glabrous skin of the hand and fingerpad where there is a high density of mechanoreceptors [36, 37]. Vibrations applied to the user, also known as vibrotactile feedback, have been used in virtual reality and teleoperation to convey various information such as contact events [38, 39] and force magnitude [40]. Low spatial resolution of human vibration perception increases the difficulty of conveying direction in a compact form with vibrotactile feedback.

Skin deformation feedback is a form of tactile feedback that deforms the skin of the user by stretching or pressing on it with a tactor. Some of the first devices that provided pure skin deformation feedback used a tactor moving in an aperture. In

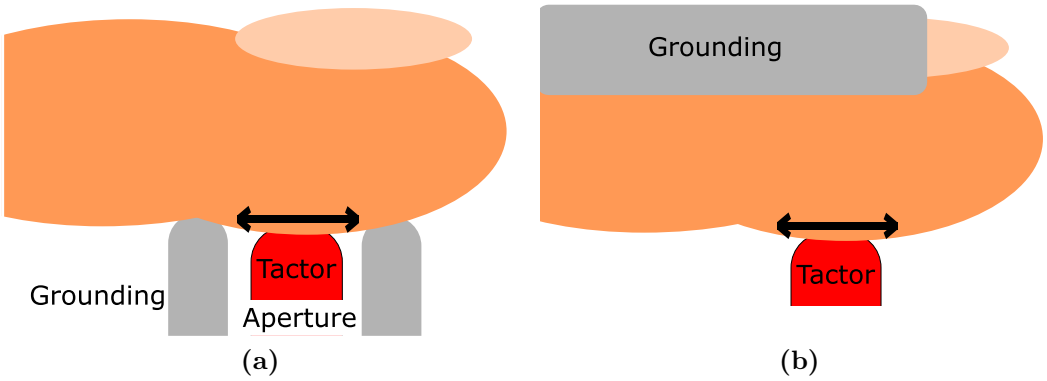

Figure 1.4: (a) The grounding forces for a tactor-aperture based approach to skin deformation feedback are local to the contact area of the tactor, similar to the devices presented in [8, 9]. (b) For non-tactor-aperture approaches, the grounding forces are further away, such as on the backside of the finger, and ideally more distributed.

this approach, which can be seen in Fig. 1.4a, the user places their fingerpad over an opening in which the tactor moves to deform the skin. The edges of the opening provide localized reactions forces to the fingerpad; thus there is no net force on the finger. It was shown that when using this tactor-aperture approach, both magnitude and direction can be conveyed by skin deformation feedback [21,22]. Skin deformation feedback has also been used to increase the perceived friction and stiffness of a virtual surface using a tactor-aperture device mounted to a traditional kinesthetic force feedback device [8,41]. A three-degree-of-freedom version of these devices was used to augment kinesthetic force feedback when following a path; users showed improvement in a path-following task when using the combination of skin deformation feedback and kinesthetic force feedback over kinesthetic force feedback alone [9]. Mounting these these particular tactor-aperture devices to a desktop-based kinesthetic force feedback device requires the user to grip the device in a specific manner to ensure the fingerpad lies over the aperture, limiting the manipulation of virtual objects.

Because pure skin deformation feedback, i.e. feedback that deforms the skin with no kinesthetic component, is intrinsically user grounded, it presents the possibility to be implemented in a wearable-type device, using grounding methods similar to that presented in Fig. 1.4b. Recently, a number of wearable skin deformation feedback

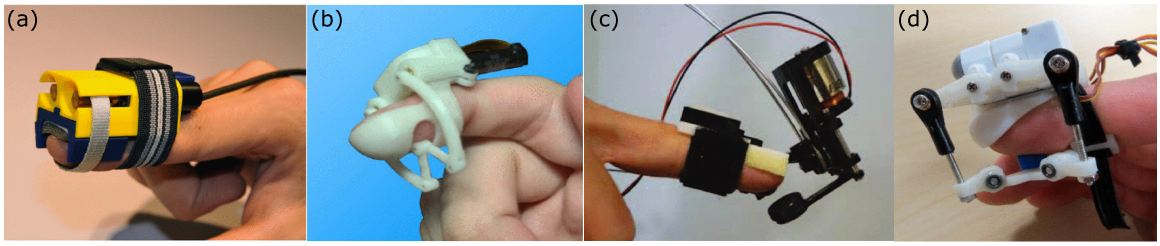

Figure 1.5: Examples of previous skin deformation devices. In (a), the device uses a belt to generate shear skin deformation in one degree of freedom [10]. The device in (b) uses a two-degree-of-freedom linkage to apply one-direction shear and normal force to the fingerpad with the ability to make and break contact [11]. The device in (c) shows another approach to making and breaking contact with the fingerpad, using a solenoid actuator near the tip of the finger [12]. Lastly, (d) shows a device with a three-degree-of-freedom RSR parallel mechanism that applies two-direction shear and normal skin deformation feedback [13].

devices have been developed, such as those shown in Fig. 1.5, including several devices that use two motors and a belt that wraps around the finger to provide shear and normal force feedback [42,43]. Using a similar device on the fingertip, Minamizawa et al. [10] were able to render the sensation of weight when statically grasping a virtual object. Tsetserukou et al. [11] developed a device that provides two-degree-of-freedom force feedback, one shear and one normal to the fingerpad, using rigid links, which also allows the device to make and break contact with the user. Solazzi et al. [12] present another multi-degree-of-freedom wearable device that can make and break contact with the finger at different locations. This device was improved upon by reducing the weight and improving the portability and wearability [44]. Some devices, such as the ones presented in [45] and [1], use cables to orient a platform that contacts the fingerpad in the normal direction. Other wearable skin deformation devices, such as the one presented in Chinello et al. [46], use parallel mechanisms, in this case a 3-RRS (revolute-revolute-spherical) mechanism, instead of cables to simulate contact with arbitrarily oriented surfaces. None of these devices provides feedback in both shear directions and the direction normal to the fingerpad. Rendering shear forces is useful for providing users with a sense of the weight of a virtual object during manipulations, especially with a lack of kinesthetic force feedback.

Leonardis et al. [13] presented a three-degree-of-freedom skin deformation device that can provide both shear and radial-to-the-fingerpad skin deformation feedback, but due to the RSR (revolute-spherical-revolute) configuration, the shear directions are coupled with the orientation which could effect the perception of shear forces, such as those caused by the weight of a virtual object in a grasp-and-lift task. Schorr and Okamura [47] presented a wearable device that provided three purely translational degrees of freedom of skin deformation feedback. This device was improved upon in [14] with the addition of gecko-inspired dry adhesive [48] on the end-effector to eliminate the need of the previous tactor to be indented into the finger pad to prevent slip.

These devices are not without their own drawbacks such as limited force output due to the small motors required to keep the devices lightweight. This puts a limit on the amount of virtual weight that is able to be rendered through the devices when manipulating a virtual object. Adding large gear boxes would increase the maximum force output but would negatively impact the bandwidth of a device and increase the device's weight. To increase the range of perceivable weights experienced by the users, other methods must be explored that do not require radical changes to hardware. Another drawback is that all these devices lack the ability to prevent the finger from penetrating too far into a virtual surface, causing the devices to saturate their force output and creating an unrealistic experience for the user. This is in contrast to kinesthetic force feedback devices, which provide a physical resistance or, if the force output is large enough, a physical constraint that prevents the finger from penetrating the virtual surface. While users can learn over time to grasp a virtual object in a more gentle manner to avoid penetrating too deep into the virtual object, we consider if there is a way to intrinsically help the user moderate their grip by providing a haptic contact cue in addition to skin deformation feedback.

1.4 Dissertation Overview

This thesis is composed of five chapters. In Chapter 1, we introduce the motivation for this work, a summary of the contributions included in this thesis, and a review of

prior work relevant to weight perception and skin deformation feedback.

Chapter 2 describes our work to determine the relative contributions of tactile and kinesthetic force for weight perception. We developed a set of mechanical thimbles to amplify the skin deformation forces experienced when lifting a real world object. We performed a human participant experiment to measure the change in perceived weight during a grasp-and-lift task when using these mechanical thimbles.

Chapter 3 describes the augmentation of an existing three-degree-of-freedom, wearable skin deformation haptic device with contact-event based haptics. We conducted an experiment to assess the performance of human participants in completing a grasp-lift-and-place task with a "fragile" virtual object with combinations of skin deformation and contact cues in an effort to either augment or replace existing degrees of freedom of the skin deformation device with the contact cues.

Chapter 4 presents a novel haptic weight illusion in which we scale the inertial forces experienced during virtual object interactions to alter the virtual weight perceived by the user through wearable skin deformation devices in virtual reality. A human participant experiment was performed to measure the change in perceived weight when virtual objects are rendered with increased inertial forces. A second experiment was performed in which we measured the effect on perceived virtual weight when decreasing inertial forces while also measuring the effects of the complementary and conflicting combinations of the scaled inertial forces haptic weight illusion with the non-unity control-to-display ratio visuo-haptic weight illusion.

Finally, Chapter 5 summarizes the results of this work and reviews the contributions of this thesis. It concludes by discussing possibilities for future research related to this work.

Chapter 2

Skin Deformation Contribution to Weight Perception

In this chapter we investigate how weight percepts change when the amount of force applied to the finger pad is amplified during grasping and lifting of an object. We designed two pairs of mechanical thimbles to be worn on the thumb and index finger of each hand. The thimbles apply an amplified force to the finger pads when the subject lifts an object. We performed two experiments to calculate the Points of Subjective Equality (PSEs) for various skin deformation force amplification levels. The first experiment was done as an initial investigation into amplified skin deformation forces, and the second experiment followed up to find any effects of saturation. A two-alternative, forced-choice paradigm with a double-random, 1-up, 1-down adaptive staircase method was used to calculate the PSEs. Instrumented objects were used to measure subjects' grip force and acceleration during the experiment to assess any correlation between these measurements and the change in weight perception. We described the different contributions of tactile percepts and kinesthetic percepts to the user's weight perception with a simple function. We found that amplifying the forces on the skin during the grasp-and-lift task did have an effect on the user's perceived weight of the object. This work has been submitted for publication as [49].

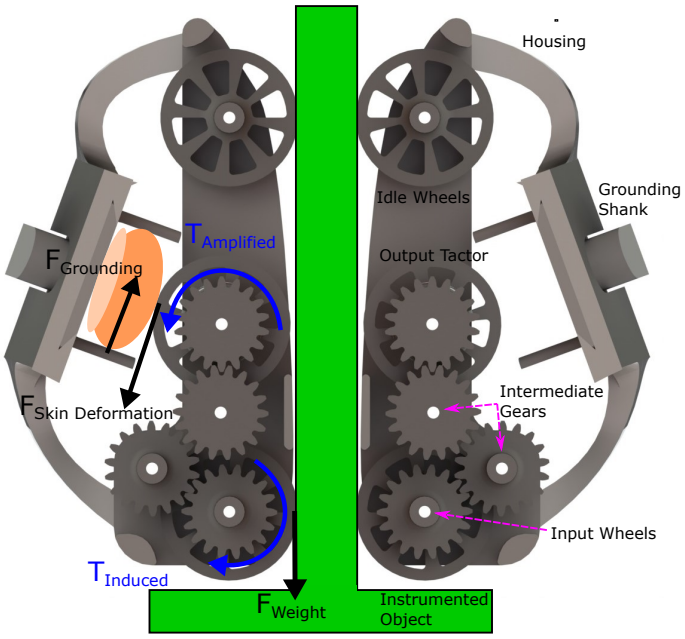

Figure 2.1: The mechanical thimbles amplify the skin deformation forces using a gear train from the input wheels, which make contact with the object, to the output tactor, which makes contact with the finger pad. The idle wheels of the mechanical thimble help with grasping the instrumented object without transmitting any of the lift force. A cut-away view of a pair of mechanical thimbles with a simple free-body diagram showing the forces and torques associated with the skin deformation amplification.

2.1 Study Description

To understand the role of skin deformation in weight perception when grasping and lifting objects, we performed an experiment to determine a PSE of weight between nominal skin deformation (1:1) and amplified skin deformation (N:1, where N is the amplification factor) when grasping and lifting objects. The first experiment was performed using a lower range of amplification ratios (N = 1, 1.6, 2, 3.1, and 4), and a second experiment was performed using a higher and wider range of amplification ratios (N = 2, 4, 6.2, 8). The protocols for both experiments were approved by the Stanford University Institutional Review Board.

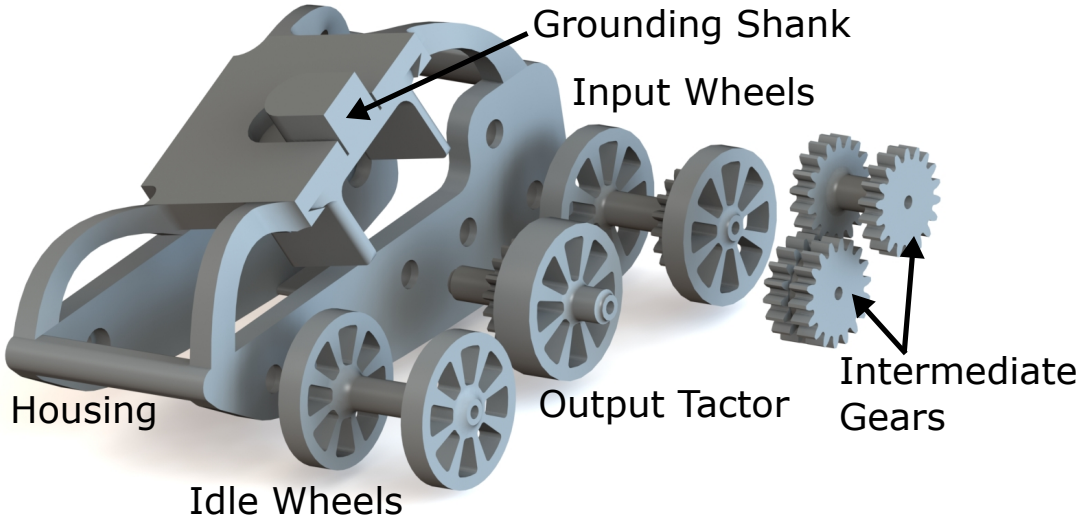

Figure 2.2: An exploded view shows the three stages of the mechanical thimble gear train, each of which can be changed to allow for a range of skin deformation amplification levels.

2.1.1 Experiment Setup

2.1.1.1 Mechanical Thimbles

We designed two pairs of mechanical thimbles, one pair for each hand, to amplify the force applied to the finger pad when grasping and lifting an object. The force applied on the finger pad is transmitted by a three-stage gear train consisting of input wheels, intermediate gears, and an output tactor; all of which are interchangeable. The idle wheels simply provide stability. The input stage and the idle wheels both have two wheels to stabilize the thimbles when grasping the instrumented objects. A cut-away view of the mechanical thimbles with tactor and grounding forces can be seen in Fig. 2.1. Each stage of the gear train and idle wheels is mounted on a shaft with ball bearings pressed into the housing of the thimble. The wheels, gears, housing, and grounding shank were all 3D printed using an ABS-like material. An exploded view of the thimbles and gear train can be seen in Fig. 2.2. Fig. 2.3 and Fig. 2.4 shows a user grasping and lifting an object while wearing the mechanical

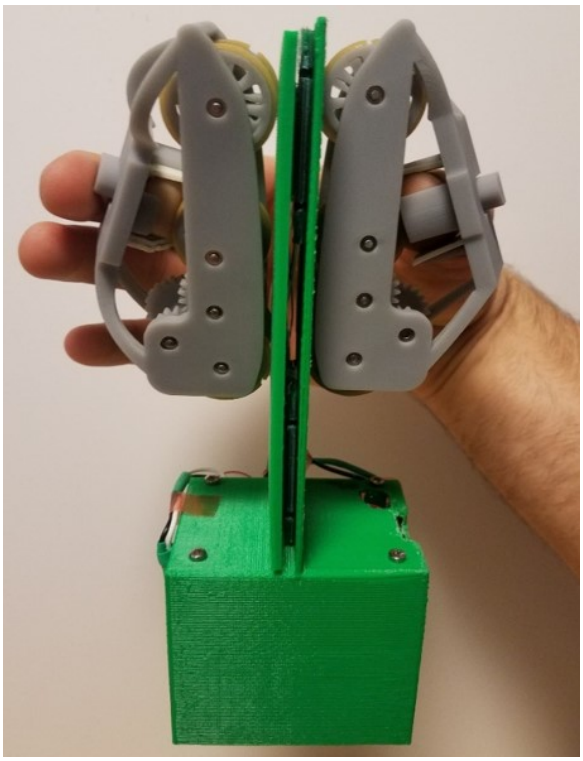

Figure 2.3: Subjects wore a pair of mechanical thimbles on the thumb and index finger of each hand.

thimbles. The subject slides their finger or thumb into the thimble and their digit rests on the tactor wheel connected to the output of the gear train. The four wheels of the thimble and the tactor are wrapped in high-friction rubber to help with the grip on both the finger and the instrumented object. Each thimble has a grounding shank fitted with a semi-soft foam which makes contact with the sides of the digit to provide localized grounding of the shear forces. The index finger thimbles have a mass between 48.5 g and 50.3 g and the thumb thimbles have a mass between 50.2 g and 52.3 g.

2.1.1.2 Instrumented Objects

We built a pair of nearly identical instrumented objects (Fig. 2.5). Each one contains a compartment to hold weighted slugs, so that we could vary the actual weight of the object, and an array of sensors: two 3-axis force sensors [50], a force sensitive resistor

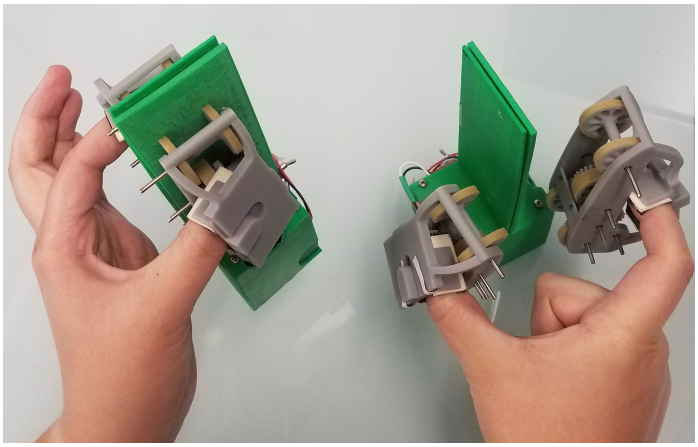

Figure 2.4: A subject wearing two sets of mechanical thimbles during a weight discrimination task. Subjects could only lift one object at a time.

(FSR), and a 6-axis inertial measurement unit (IMU). The two force sensors, which we used to measure grip force during the lifting of the instrumented objects, are less than 3 mm thick each and are mounted between the body of the instrumented object and a plate to allow the grip force to be distributed across the two sensors. The thin form factor of these sensors prevented the aperture distance between the subjects thumb and index finger from being unnaturally large for a grasp and lift task. The minimum aperture distance using the mechanical thimbles, i.e. the distance between the index finger and thumb when the wheels of a set of mechanical thimbles are touching, is 48.3 mm. The thickness of the instrumented object and plate with the force sensors mounted in between is 7 mm. Thus, the overall aperture distance for the grasp and lift task while wearing mechanical thimbles was 55.3 mm. The sensors have a resolution of 40 mN, although the sensors can measure up to $\pm$100 N in the normal direction, we calibrated each of our sensors for $\pm$50 N. The FSR is used to determine when the instrumented object has been lifted off the surface. The 6-axis IMU is used to analyze the accelerations of the instrumented object during a lift. Fig. 2.6 shows how the signal from the FSR was used to segment the acceleration and grip force data during a trial. The data was compiled by an Arduino micro-controller and sent over Bluetooth to a computer where it was recorded in MATLAB at 54 Hz. Each instrumented object, with no added weights, has a mass of 175 g.

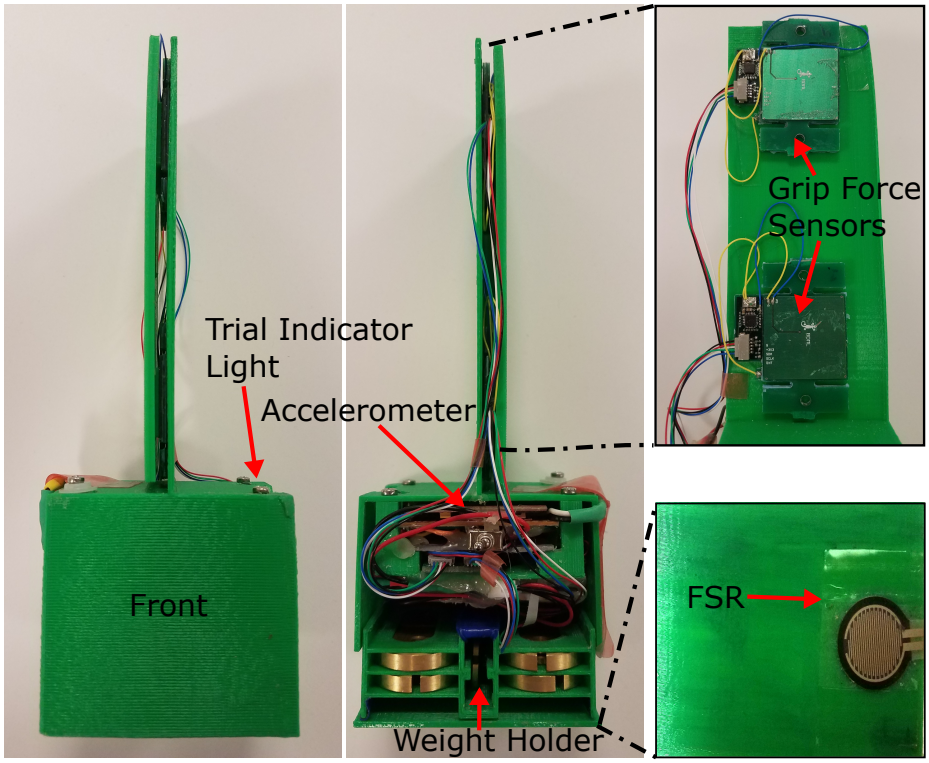

Figure 2.5: Instrumented object lifted by subjects wearing mechanical thimbles. A weight holder compartment allows the experimenter to vary the actual weight of the object. The object contains sensors to measure grip force, acceleration, and surface contact. The object streams collected data wirelessly to a micro-controller; the wireless connection was used to prevent subjects from perceiving any additional weight due to an electrical cord.

2.1.2 Experiment Procedure

To determine the PSE between nominal skin deformation and amplified skin deformation, we employed a two-alternative, forced-choice paradigm using a double-random, 1-up, 1-down adaptive staircase method. Subjects were seated across from the experimenter and presented with a pair of mechanical thimbles for each hand. One pair of mechanical thimbles, the reference thimbles, always had a 1:1 gear ratio, while we interchanged the other pair of thimbles depending on the gear ratio. The hand wearing the reference thimbles was always presented with the reference object; the

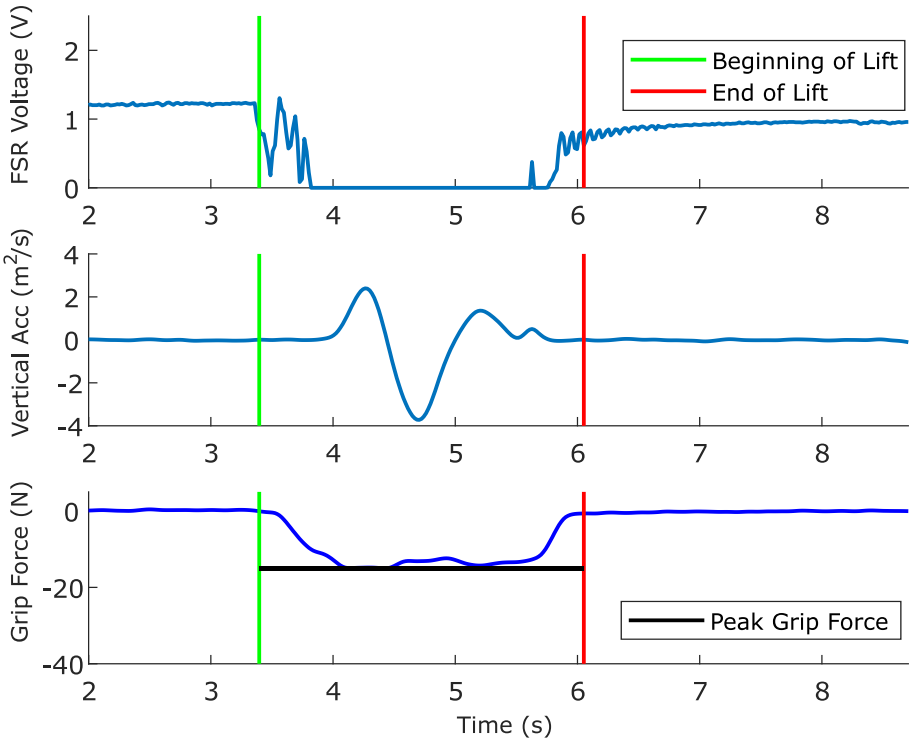

Figure 2.6: Grip force and vertical acceleration data from one grasp-and-lift of one subject. A lift detection algorithm was implemented to segment the grip force and vertical acceleration data using the signal from the FSR located on the bottom of the instrumented object so that it made contact with the experiment surface when the subject set it down. From this segmentation, we evaluated average grip force and peak acceleration during a lift.

hand wearing the other thimbles was always presented with the variable-weight object. In our experiments we varied two variables: the weight of the variable-weight object and the gear ratios of the thimbles. In each trial, the subject was presented with these two, nearly identical objects and asked to determine which object "overall feels heavier."

Subjects were not allowed to lift both objects at the same time. Subjects were also asked to only grasp, lift, and set down the objects, and not shake the objects, in order to eliminate any effect of backlash from the gear train. There was no limit to the number of lifts a subject could perform before making a decision, and no order

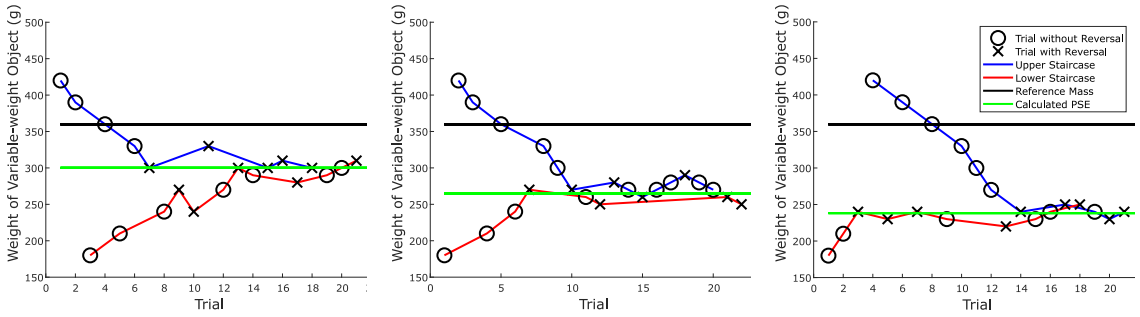

(a) **(b)** **(c)**

Figure 2.7: These plots show three separate subjects' responses when comparing the weight of two objects during (a) Experiment 1 using a 4:1 gear ratio, (b) Experiment 2 using a 6.2:1 gear ratio, and (c) Experiment 2 using a 8:1 gear ratio. The subjects' responses are shown as an $\times$ or as a circle. The $\times$ represents a reversal in direction from the subject's response on the previous step of that staircase (either ascending or descending); a circle represents no reversal. The Point of Subject Equality (PSE) was calculated by averaging the user's last three reversals on each staircase.

in lifting of the instrumented objects was enforced. Subjects were also permitted to maintain their grasp on an object throughout the trial due to the difficulty in aligning the wheels of the thimbles vertically over multiple quick grasps. The trial ended when the subject gave an answer; this answer was recorded in a graphical user interface, and the experiment program then generated the next weight of the variable-weight object. Both instrumented objects were then taken behind a divider where the weight of the variable-weight object was changed and then presented back to the subject for the next trial. Subjects were unaware that one of the objects was a reference object whose weight remained constant. Subjects were asked to wear noise-reducing ear muffs in order to prevent auditory cues, caused by the experimenter changing the object's weight, from affecting their decisions.

For both experiments, the weight of the variable-weight object was determined for each trial by using a double-random, 1-up, 1-down adaptive staircase.

In a single staircase method, the stimulus presented to a subject changes (increases or decreases) based on the subject's answer to the previous trial (the previous "step"). A staircase can be ascending or descending. An ascending staircase means the initial

stimulus (step 1) is much lower than the reference stimulus. In our experiment, this means the weight of the variable-weight object started less than the weight of the reference object; if a subject said that the reference object felt heavier, then the weight of the variable-weight object would be increased by one step size. If a subject said that the variable-weight object felt heavier, then the weight of the variable-weight object would be decreased by one step size. A descending staircase means the initial stimulus (step 1) is much higher than the reference stimulus.

However, when a single staircase method is used, a human subject can quickly figure out how the stimuli are being ordered and anticipate the next step. To remove this bias, we used two staircases (an ascending and a descending staircase) concurrently during a single round of lifts, and we randomly intermixed steps from each staircase. In this method, the experimenter keeps track of which step on each staircase the subject is on; when it is time to take the next step on the ascending staircase, for example, the experimenter refers to the subject's previous response on the ascending staircase and adjusts the variable-weight object accordingly.

The initial values of each staircase were determined during a pilot study to ensure that the PSE values of each skin deformation amplification ratio was within the prescribed range. If the subject answered that the variable-weight object felt heavier, the weight of that object was decreased by one step size on the current staircase. The step size for both experiments started at 30 g and decreased to 10 g after a number of reversals for that staircase occurred. The round for a particular amplification ratio concluded when each staircase reached a predetermined number of reversals. The weight of the reference object was 360 g and the weight of the variable-weight object started at 180 g for the ascending staircase and 420 g for the descending staircase. In Fig. 2.7, we see the staircase results (for three separate subjects) for amplification ratios 4:1, 6.2:1, and 8:1. In both experiments, we calculated a PSE of weight between nominal and amplified skin deformation across a range of amplification ratios by averaging the last 3 reversals of both staircases. The PSE values were then averaged across all participants for each amplification ratio.

During pilot studies, subjects who identified as engineers often noted, either verbally or in their post-experiment survey, that they had a hard time making decisions

between the two presented weights after "figuring out" how the mechanical thimbles worked. This suggests that when a subject is aware of the amplification method and, therefore, the difference in cues between kinesthetic and skin deformation, the decision is much more cognitive than perceptual. This led to the recruitment of non-engineers for both experiments because they were less likely to "figure out" how the mechanical thimbles worked, either from lack of knowledge or lack of desire to do so.

2.1.2.1 First Experiment

The first experiment consisted of five separate rounds, using gear ratios 1:1, 1.6:1, 2:1, 3.1:1, and 4:1. To help subjects become familiar with picking up the objects with the mechanical thimbles, each subject's first round of grasp-and-lift comparisons was done with two pairs of 1:1 geared thimbles. This also allowed us to evaluate any possible bias introduced by the mechanical thimbles. We ordered the remaining four rounds of geared thimbles using a Latin square and alternated which hand was equipped with the reference thimbles during the experiment, to balance for handedness as well as to limit fatigue in either hand. Each round ended after five reversals in each staircase. The step size reduced from 30 g to 10 g after the second reversal. Each subject took approximately two hours to complete the five rounds with breaks included to reduce fatigue. A total of 8 participants (1 male and 7 female) between the ages of 25 and 31 participated in this experiment after giving informed consent. All 8 participants were right-hand dominant.

2.1.2.2 Second Experiment

A second experiment was carried out to investigate the effects of amplified skin deformation over a wider range of gear ratios. This experiment consisted of four separate rounds, using gear ratios of 2:1, 4:1, 6.2:1, and 8:1. Again we ordered the rounds using a Latin square. For this experiment the reference thimbles were always worn on the subject's left hand. Each round ended after four reversals in each staircase. The step size reduced from 30 g to 10 g after the first reversal. Each subject took approximately one and a half hours to complete the four rounds, which included breaks

to reduce fatigue. A total of 4 participants (2 male and 2 female) between the ages of 18 and 28 participated in this experiment after giving informed consent. All 4 participants were right-hand dominant.

2.1.2.3 Statistical Analysis

For all ratios, a t-test was performed on the PSEs across all participants against the reference weight of 360 g. A Bonferroni correction for multiple comparisons was used in assessing statistical significance.

We fit five generalized linear mixed effect (GLME) models to assess: the effect of the gear ratio on the perceived weight (PSE), the number of lifts per trial, the peak grip force rate, the peak grip force, and the peak acceleration during each lift.

Perceived weight. The first GLME model assessed the significance of the gear ratio parameters on the perceived weight (PSE) using an identity link function for Experiment 1. Instead of using the PSE calculated for each subject, which is averaged across the last 3 reversals of each staircase, we decided to use each reversal value across all subjects for each gear ratio for our model. This was done with the understanding that reversals are not exact measurements of the PSE, but it stands to reason that it is an approximation with a measurement resolution equal to one step size of the staircase. The gear ratio is treated as a fixed effect to simulate its effect across participants, and subject was treated as a random effect. Each ratio was entered into the model as one less than the gear ratio, N-1, to account for the nominal amount of skin deformation that occurs when the ratio is 1:1. This means we expect the intercept term of the model to be close to the reference weight. We used the same GLME model on the resulting reversals used to calculate the PSEs of gear ratios from Experiment 2, first for the full set of gear ratios (2:1, 4:1, 6.2:1, and 8:1) and then on the gear ratios above 2:1 (4:1, 6.2:1, and 8:1).

During each trial, grip force and acceleration were recorded on both objects. We used the FSR signal in conjunction with the accelerometer and force sensors to determine when the objects were lifted and set back down, and we segmented the data of each trial into individual lifts. An example trial showing how we sectioned the grip force and accelerometer data for each lift can be seen in Fig. 2.6. This allowed us to

analyze the number of lifts as well as the peak grip force rate, the peak grip force, and the max upward acceleration during each lift. For analyzing these variables, we combined the data from Experiments 1 and 2.

Number of lifts. The second GLME model analyzed the number of lifts per trial of both objects. Fixed effects were the gear ratio and the absolute value of the difference in weight of the variable-weight object and the PSE, of the gear ratio used in each trial, Δ(PSE); the random effect was the subject.

Peak grip force rate. The third GLME model analyzed the peak grip force rate during a lift, using gear ratio and weight of the variable-weight object as fixed effects, and the subject as a random effect. Since the experimenters did not require subjects to completely release either object while the other was being lifted, only the first lift from each trial was used to analyze peak grip force rate.

Peak grip force during lift. The fourth GLME model analyzed the peak grip force during a lift. Fixed effects were gear ratio, weight of the variable-weight object, the object's peak acceleration, and an indicator variable (represented by 0 or 1), denoting if the lift was the first one performed on the object in the trial; the random effect was the subject. Each object has at least one lift per trial, and therefore each object has one lift with the indicator variable value as 1. The purpose of the indicator variable is to account for subjects using less grip force on the object after they have already lifted it once. The peak acceleration was included because there is a natural relationship between lift force and acceleration, and lift force is limited by the grip force due to friction, provided the object does not slip in the grasp.

Peak acceleration during lift. Lastly, the fifth GLME model analyzed the peak acceleration during each lift. The fixed effects were gear ratio, weight of the variable-weight object, and an indicator variable denoting if the lift was the first one performed on the object in the trial; the random effect was the subject.

The analysis of peak grip force rate, peak grip force, and peak acceleration was done separately for the reference object and for the variable-weight object. Table 2.1 shows the factors used in the various generalized linear mixed-effects models.

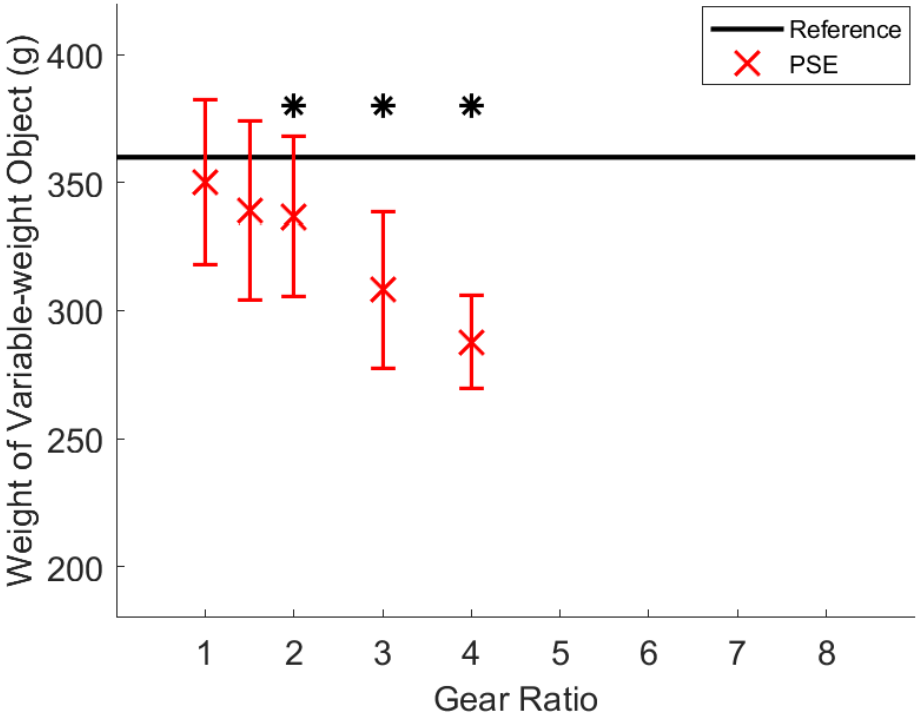

Figure 2.8: The PSE decreases as the gear ratio increases for a reference weight of 360 g from Experiment 1. The asterisk (*) denotes statistical significance, after Bonferroni correction for multiple comparisons, for PSEs across all participants in Experiment 1 when compared to the reference weight of 360 g.

2.2 Results

Perceived weight. The PSEs calculated for each experiment are given in Table 2.2. The effects of the gear ratios tested in the first experiment can be seen in Fig. 2.8, where the PSEs calculated for a reference weight of 360 g decrease as the gear ratio increases. The PSEs are plotted with error bars corresponding to plus/minus one standard deviation. The PSEs calculated from the second experiment can be seen in Fig. 2.9 which shows that higher gear ratios have a significant effect on PSE, but the effect seems to saturate for ratios above 4:1. For all ratios, a t-test was performed against the reference weight of 360 g. All ratios, except for 1:1 and 1.6:1, have PSEs significantly different from 360 g ($p<0.05$) after a Bonferroni correction for multiple

Table 2.1: Linear mixed-effects model components

Factor	Categorical/ Continuous	Within/ Between Subjects	df
Fixed Effects			
Gear Ratio	Continuous	Within	1
W	Continuous	Within	1
PA	Continuous	Within	1
First Lift	Categorical	Within	1
Δ(PSE)	Continuous	Within	1
Random			
Subject	Categorical	–	12

W is weight of variable-weight object, *PA* is peak acceleration, Δ*(PSE)* is absolute difference between weight of variable-weight object and the measured PSE, *df* is degrees of freedom

comparisons.

The results of a generalized linear mixed-effects model for Experiment 1 showed that the gear ratio has a statistically significant effect on the PSE ($p<0.05$) with a coefficient of -21.2 g $\pm$ 3.35 g and an intercept term of 351.9 g $\pm$ 8.7 g. Using the same model on Experiment 2 for all gear ratios, we found that the gear ratio had a significant effect on PSE ($p<0.05$), but when the model is analyzed for gear ratios above 2:1 (4:1, 6.2:1, and 8:1), we found that gear ratio no longer has a significant effect ($p>0.05$). This shows there is a saturation of the effect of amplified skin deformation on perceived weight above ratios of 4:1. We theorize that this is due to saturation in the stretch of the skin of the finger pad. In our case, the saturation of the stretch of the skin appears to occur when the tactile force felt by the user is greater than 5.6 N on each finger pad which comes from calculating the force on each finger pad when lifting a 285.4 g object using thimbles containing gears with a 4:1 gear ratio.

Number of lifts. From our generalized linear mixed-effects model used to analyze the number of lifts in total, combined for both objects per trial, we found a significant

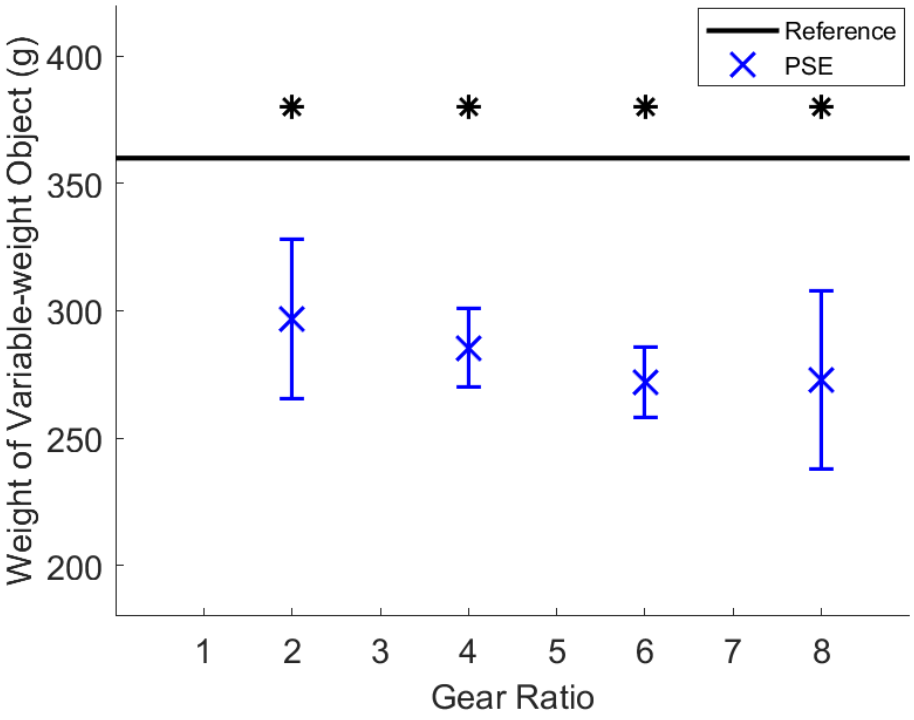

Figure 2.9: Subjects' Point of Subjective Equality (PSE) when comparing a variable-weight object with a reference object weighing 360 g from Experiment 2. Amplified gear ratios continue to have an effect on a user's perception of weight at higher ratios, although the effect starts to saturate above gear ratios of 4:1. This is possibly due to the limits in the stretch of the skin of the finger pad. The asterisk (*) denotes statistical significance after Bonferroni correction for multiple comparisons for PSEs for all participants in Experiment 2 when compared to the reference weight of 360 g.

effect from both the gear ratio ($p<0.05$) and Δ(PSE) ($p<0.05$).

Peak grip force rate. For the peak grip force rate, we also found the gear ratio to have a significant effect for both the reference object and the variable-weight object ($p<0.05$). The weight of the variable-weight object only had a significant effect on peak grip force rate for the variable-weight object ($p<0.05$) but not on the peak grip force rate for the reference object ($p>0.05$).

Peak grip force during lift. For the peak grip force during a lift of the reference object, the gear ratio, weight of the variable weight object, peak acceleration and first

Table 2.2: PSEs for each skin deformation amplification ratio calculated from both experiments

Experiment	Ratio N (N:1)	Mean PSE (g) with Reference Weight 360 g	STD (g)
1 (8 subjects)	1	350.2	32.2
	1.6	339.2	35.1
	2	336.7	31.3
	3.1	308.1	30.6
	4	287.7	18.2
2 (4 subjects)	2	296.7	31.3
	4	285.4	15.3
	6.2	272.1	13.8
	8	272.9	35.1

lift indicator had a significant effect ($p<0.05$). For the variable weight object, the gear ratio, weight of the variable weight object, and first lift indicator had a significant effect on the peak grip force, while the peak acceleration did not ($p>0.05$).

Peak acceleration during lift. Lastly, analyzing the peak acceleration during a lift, we found that the gear ratio and first lift indicator had significant effects on both the reference object and the variable-weight object ($p<0.05$). The weight of the variable-weight object had a significant effect on the peak acceleration of the variable-weight object ($p<0.05$) but did not have a significant effect on the peak acceleration of the reference object($p>0.05$).

A statistical summary of each GLME model can be seen in Table 2.3, and the resulting estimated coefficients of the fixed effects can be seen in Table 2.4

We chose to quantify the amount of influence the tactile sensation has on weight perception by fitting a simple function

$$POE = w * PSE * N + (1 - w) * PSE \tag{2.1}$$

where POE is the Point of Objective Equality (i.e., the reference weight), N is the gear ratio, and w is the tactile contribution coefficient, to the PSEs from Experiment 1. The fit resulted in a weighting coefficient of 0.083 with an r-squared value of 0.94.

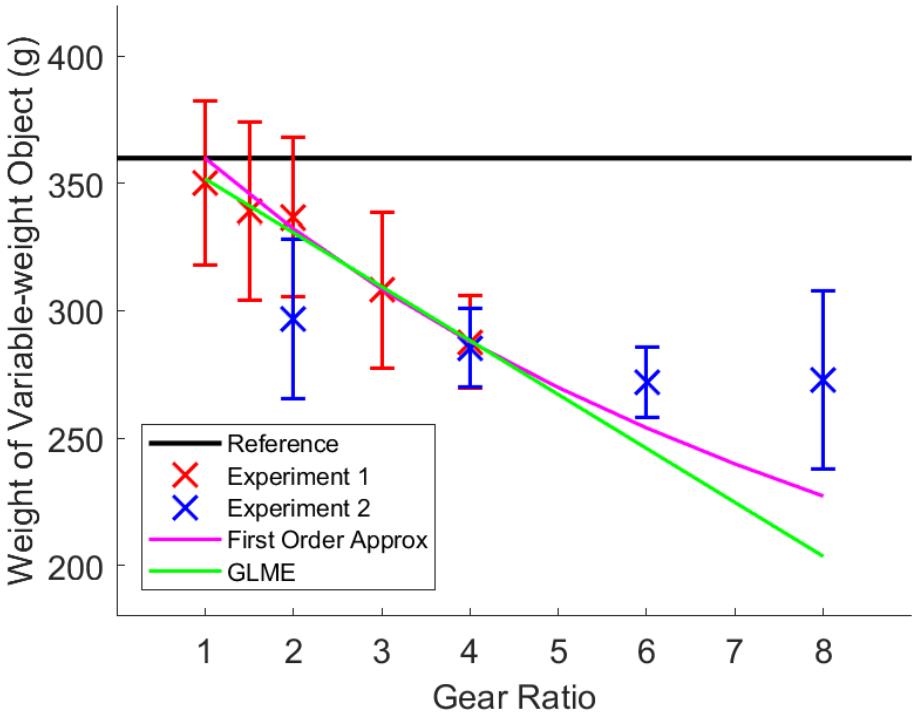

Figure 2.10: Our first order approximation for perceived weight with a tactile contribution coefficient of 0.083 plotted with the resulting fit of the GLME and the data from both experiments.

The function can be seen plotted in Fig. 2.10 along with the results from Experiments 1 and 2 as well as the resulting GLME fit. The PSEs from Experiment 2 were excluded from the tactile contribution coefficient fit due to the saturation of the effect of skin deformation amplification which causes the tactile contribution coefficient to drop to less than 0.05 at a gear ratio of 8:1. Fig. 2.11 shows the tactile contribution coefficients plotted for each gear ratio.

2.3 Discussion

Perceived weight. The PSEs generated from both experiments show that amplifying the amount of skin deformation during a grasp-and-lift task makes an object feel heavier. Using non-electro-mechanical thimbles for the experiment gives an advantage

Table 2.3: Statistical summary of generalized linear mixed-effects models

Metric	Gear Ratio Range/Object (df)	Effect	Gear Ratio	W	First Lift	Δ(PSE)
PSE (reversals) Exp. 1	1:1, 1.6:1, 2:1, 3.1:1, 4:1 (1,238)	F	**155.2**	–	–	–
		p	**<0.001**	–	–	–
PSE (reversals) Exp. 2	2:1, 4:1, 6.2:1, 8:1 (1,94)	F	**15.1**	–	–	–
		p	**<0.001**	–	–	–
	4:1, 6.2:1, 8:1 (1,70)	F	3.8	–	–	–
		p	0.05	–	–	–
Lifts	(1,1309)	F	**8.2**	–	–	**54.3**
		p	**0.004**	–	–	**<0.001**
Peak Grip Force Rate	Ref (1,1182)	F	**32.6**	3.18	–	–
		p	**<0.001**	0.07	–	–
	VW (1,1182)	F	**7.4**	**8.04**	–	–
		p	**0.007**	**0.005**	–	–
Peak Grip Force	Ref (1,1627)	F	**67.4**	3.5	**32.7**	–
		p	**<0.001**	0.06	**<0.001**	–
	VW (1,1627)	F	**765.5**	**21.6**	**59.7**	–
		p	**<0.001**	**<0.001**	**<0.001**	–
Peak Acceleration	Ref (1,1939)	F	**30.6**	2.0	**21.2**	–
		p	**<0.001**	0.15	**<0.001**	–
	VW (1,993)	F	**139.3**	**92.5**	**17.9**	–
		p	**<0.001**	**<0.001**	**<0.001**	–

W is weight of variable-weight object, *PA* is peak acceleration, *Δ(PSE)* is absolute difference between weight of variable-weight object and the measured PSE, *Ref* is reference object, *VW* is variable-weight object, *df* is degrees of freedom. Bold type denotes statistically significant factors at p<0.05 threshold.

Table 2.4: Estimated coefficients of generalized linear mixed-effects model fixed effects

			Coefficients			
Metric	Gear Ratio Range/Object	Intercept	Gear Ratio	W (g)	First Lift	Δ(PSE) (g)
PSE (reversals) (g) Exp. 1	1:1, 1.6:1, 2:1, 3.1:1, 4:1	351.9	**-21.2**	–	–	–
PSE (reversals) (g) Exp. 2	2:1, 4:1, 6.2:1, 8:1	302.9	-4.2	–	–	–
	4:1, 6.2:1, 8:1	295.6	**-3.1**	–	–	–
Lifts	–	3.2	**0.065**	–	–	**-6.4e-3**
Peak Grip Force Rate (N/s)	Ref	0.09	**0.005**	-4.4e-5	–	–
	VW	0.15	**0.005**	**1.4e-4**	–	–
Peak Grip Force (N)	Ref	6.1	**0.40**	**2.7e-3**	**1.12**	–
	VW	8.0	**2.6**	**0.015**	**2.59**	–
Peak Acceleration (m/s^2)	Ref	1.3	**0.031**	-2.3e-4	**-0.10**	–
	VW	1.9	**-0.065**	**-1.5e-3**	**-0.087**	–

W is weight of variable-weight object, *PA* is peak acceleration, *Δ(PSE)* is absolute difference between weight of variable-weight object and the measured PSE, Ref reference object, *VW* is variable-weight object. Bold type denotes statistically significant factors at $p<0.05$ threshold.

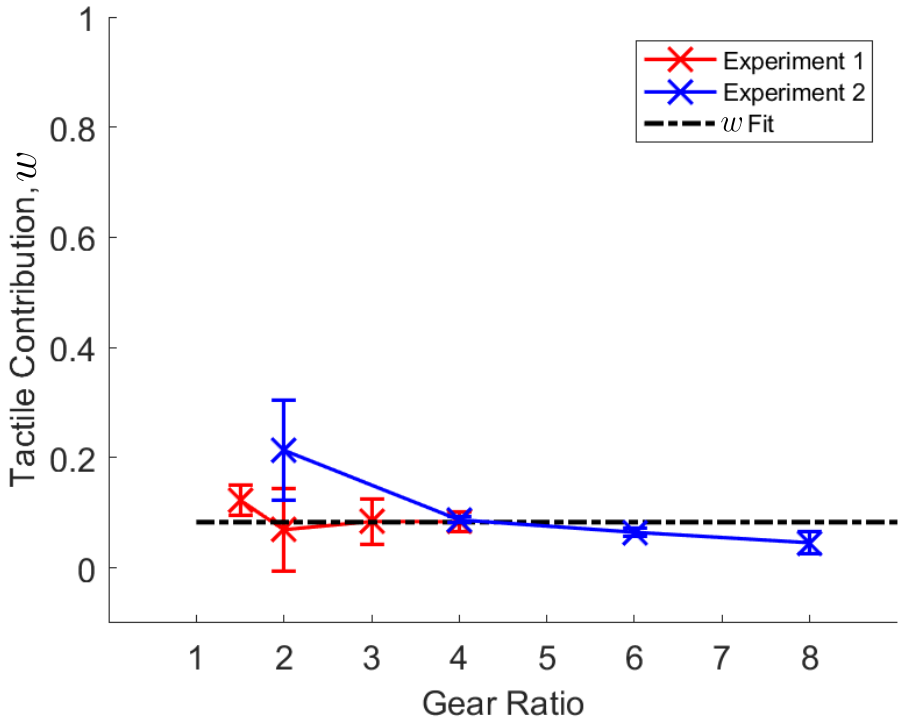

Figure 2.11: As the gear ratio increases and the effect of skin deformation becomes saturated, the tactile contribution coefficient drops to less than 0.05. The discrepancy at the 2:1 ratio may be caused by fewer subjects participating in the second experiment, which has a wider range of gear ratios.

over an electro-mechanical system by eliminating any transient effects that a controller or power supply could have on the experimental results. Similarly, by having the objects wirelessly transmit data, we eliminate any unintended weight or inertial effects a cable might have on the results.

By fitting a generalized linear mixed-effects model, we found that amplifying skin deformation has a statistically significant effect on weight perception. To determine the relative contributions of skin deformation and kinesthetic force on perceived weight, we developed a simple function based on the influences of each. The fit of the first-order approximation resulted in a tactile contribution coefficient of 0.083. For ratios above 4:1, there is a slight roll-off due to saturation of the effect of skin deformation on perceived weight. The discrepancy between PSEs for the 2:1 ratio

may be caused by fewer subjects participating in the second experiment, causing an outlier to have a larger effect on the calculated value.

The saturation of the effect of skin deformation on weight perception can be attributed to the limits of skin pliability of the finger pad. We theorize that the increase in applied normal force required to lift an object that is picked up with mechanical thimbles that are amplifying the shear skin deformation forces, contributes to the saturation of the skin deformation in conjunction with the applied shear forces. Such an increase in normal force will cause the finger pad to deform in the normal direction, thereby limiting the amount the finger pad can deform in the shear direction. If we used a material with higher friction, thus lowering the required normal force to lift, it could change the magnitude of the shift in perceived weight under skin deformation amplification.

Though the weight of the mechanical thimbles are not negligible, with each weighing about 50 g, we believe they are comparable to those of current skin deformation feedback devices [1, 13, 47] and still help inform the design of new skin deformation feedback devices.

Number of lifts. In analyzing the total number of lifts per trial, we reason that the number of lifts corresponds to how easy it is to choose which object feels heavier during the trial. Thus, we included the difference in weight of the variable-weight object from the PSE in our GLME model, theorizing that as the weight approached the fit of the GLME, per the staircase method, the choice would become more difficult for subjects and thus the number of lifts would increase. The resulting coefficient from the GLME model, shown in Table 2.4 supports this theory only to the degree that the number of lifts does increase as the weight of the variable-weight object gets closer to the PSE.

Peak grip force rate. The results from the GLME model for peak grip force rate show that the gear ratio has a similar sized effect on both objects, though only the thimbles lifting the variable-weight object have the amplification of force. For the peak grip force rate of the variable-weight object, weight also had a significant effect. This could be due to the gear train traveling more along the object as the skin of the finger pad stretches, possibly inducing a more rapid increase of force for heavier

objects, more so at higher gear ratios and larger weights.

Peak grip force during lift. From the analysis of the peak grip force during a lift, it is interesting to note that the gear ratio had a significant effect on both objects albeit much less of an effect on the reference object. This effect of the gear ratio causing an increase in grip force on the reference object, which is always lifted with a 1:1 gear ratio, is possibly due to the expectation of a heavier feeling weight from interactions with the variable-weight object and the force-amplifying thimbles. When considering the larger positive effect from the first lift indicator, it appears that subjects, after lifting the object once, lessened their grip force, thus reducing the amount of strain on the finger pad caused by the normal force to possibly elicit more of the tactile sensation.

Acceleration during lift. The results of the GLME model for peak acceleration also show an increase in object acceleration after the first lift for both objects supporting the modulation of grip force and acceleration in an exploratory strategy when discriminating the weight of two unknown objects. The negative effect of the weight of the variable-weight object on its own peak acceleration suggests that subjects have a predetermined lifting force that underestimates the weight of the object. Seeing an effect of gear ratio on the acceleration of both objects, albeit in opposite directions, is interesting. The gears amplify the forces felt on the finger pad but do not affect the kinesthetic load experienced by the subject.

2.4 Conclusion

We performed experiments to measure the change in subjects' weight perception when the skin deformation of their finger pads was amplified. We designed non-electrical (passive) mechanical thimbles with interchangeable gears that amplified the skin deformation felt by a user when grasping and lifting an object. We also designed instrumented objects which measured grip force and vertical acceleration. In the first experiment, we measured a subject's changed perception of the weight of a variable-weight object compared with a reference object weighing 360 g, and we repeated the comparison using five different gear ratios of 1:1, 1.6:1, 2:1, 3.1:1,

and 4:1. We furthered this investigation in a second experiment where we repeated the comparisons using gear ratios of 2:1, 4:1, 6.2:1, and 8:1. We found that the change in perceived weight for a reference weight of 360 g becomes saturated for skin deformation amplification ratios above 4:1 with a PSE of 285.4 g. Using this value, we calculated the shear force on each finger pad to be 5.6 N in a quasi static holding grasp.

We analyzed the lifting metrics of total number of lifts, peak grip force rate, peak grip force, and peak acceleration and found the gear ratio had a significant effect on each one. We also found that for trials where the subject lifted each object more than once, the subject reduced their grip and increased their acceleration, likely in an attempt to elicit more tactile sensation.

These results inform the design and control of wearable skin deformation feedback devices by giving insight into how our perception of weight changes as the skin deformation is increased. This is important for wearable tactile haptic feedback devices using skin deformation because the kinesthetic load for the user does not change while rendering the skin deformation forces associated with picking up a virtual object.

Chapter 3

Augmentation and Replacement of Skin Deformation Feedback with Vibrotactile Contact Cues

In Chapter 1, we reviewed several wearable skin deformation feedback devices. All these devices lack a kinesthetic force that prevents the finger from penetrating too far into a virtual surface, which causes the devices to saturate their force output and creates an unrealistic experience for the user. While users can learn over time to grasp a virtual object in a more gentle manner to avoid penetrating too deep into the virtual object, we consider if there is a way to intrinsically help the user moderate their grip by providing a haptic contact cue in addition to skin deformation feedback. Furthermore, we want to investigate the effect of the contact cue without skin deformation feedback in the normal-to-the-fingerpad direction on virtual object penetration. Doing so informs whether we can *replace* the normal-to-the-fingerpad feedback with a contact cue in an effort to reduce the complexity of skin deformation devices.

In this chapter, we investigate whether augmenting our current skin deformation feedback device, a fingertip wearable device with three translational degrees of freedom shown in Fig. 3.1, with contact event-based haptic methods could reduce the penetration depth, and thus the virtual grip force, when manipulating a virtual

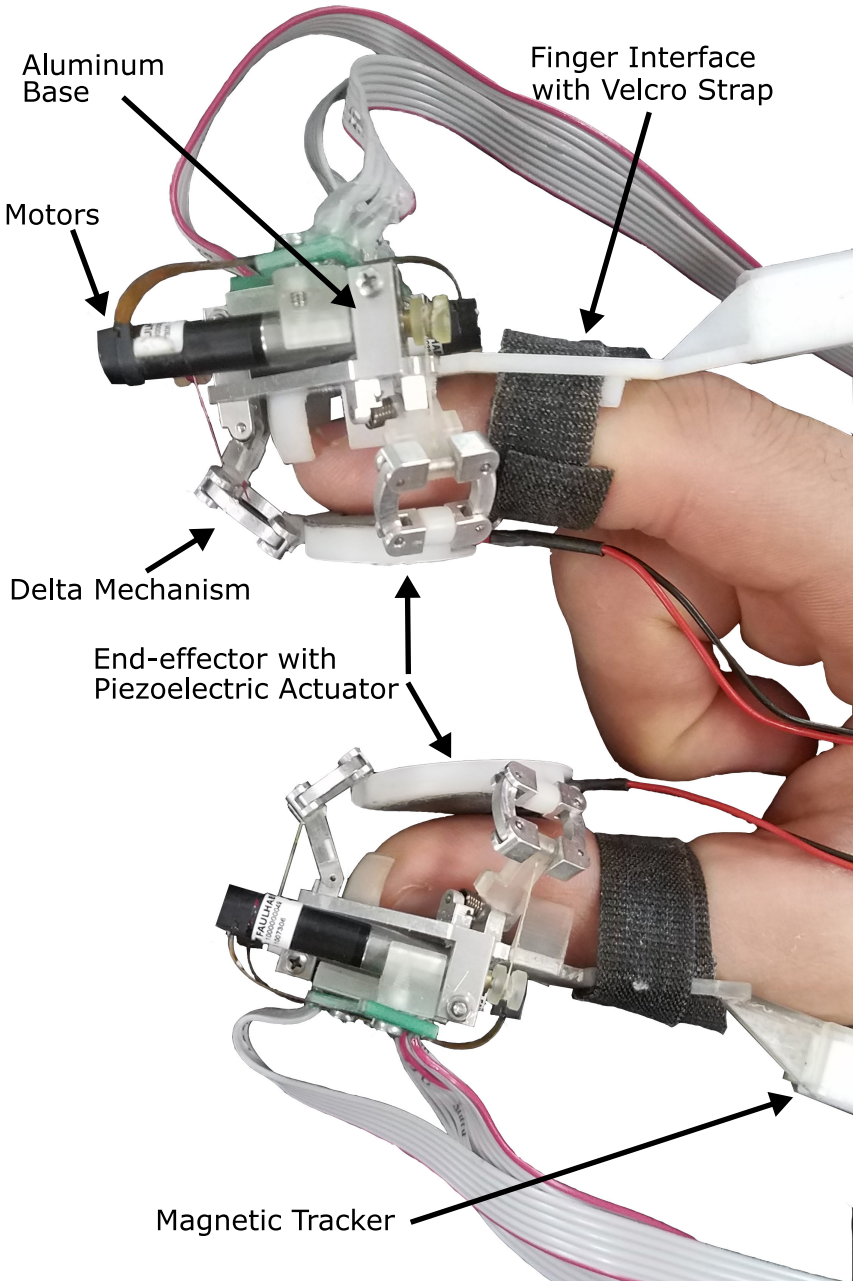

Figure 3.1: For this study, participants wore 3-DoF skin deformation devices on their index finger and thumb modified from [14], with the addition of a piezoelectric actuator embedded in each end-effector. These actuators provide one of the two vibrotactile contact cues we tested.

object. We also investigate whether using these contact cues could serve as a replacement for skin deformation feedback normal-to-the-fingerpad, in an effort to reduce the complexity and cost of current multi degrees of freedom (DoF) skin deformation feedback devices. We chose two contact event-based haptic cues (contact cues): a fixed-width force pulse (impulse) rendered through the skin deformation device and a decaying sinusoid rendered through a piezoelectric actuator. The impulse is meant to mimic the lower frequency, higher displacement component of skin deformation that occurs when contacting an object, i.e., the noticeable skin deformation in the direction of contact, while the decaying sinusoid is meant to mimic the higher frequency, lower displacement component of transient accelerations that occur when contacting an object.

3.1 Contact Cues

Vibration feedback has been used to enhance haptic perception of teleoperated robots and virtual environments, particularly when making contact with a surface or object. One method that was explored began with collecting real-world data on the vibrations, forces, and velocities that occur when using a stylus to tap on various materials, stroke a variety textures, and puncture membranes (as might be done in medical procedures). From this data, empirical models were created of vibration waveforms and it was shown that users interacting with this vibration feedback system performed better than chance in a virtual surface discrimination task [51]. This work was continued, showing that using a decaying sinusoid as an approximation for the contact vibrations still allowed users to identify three different virtual materials when rendering vibration alone [52]. Using a simpler method, Hwang et al. [53] showed that they could increase effective stiffness by rendering a short force pulse through the haptic device. Event-based haptic feedback has been shown to improve the realism of contact events; Kuchenbecker et al. [38] used an inverse model of a desktop-based haptic device to render prerecorded acceleration profiles that resemble transients that occur when tapping an object with a stylus. This method was compared to previous methods of rendering decaying sinusoids and open-loop force pulses. All three methods showed an

improvement in the realism of the tapping and a decrease in virtual object penetration depth over traditional haptic rendering, which uses no contact cue.

Based on this result from [38], we chose, for our experiments, two different contact cues: a fixed-width force pulse (impulse) and a decaying sinusoid. To render the decaying sinusoid, we decided to augment the device with a piezoelectric actuator in the end-effector because the contact vibrations we chose require a bandwidth of 100 Hz or more, which is much higher than the capabilities of our wearable skin deformation device.

3.2 Study Description

The purpose of this study was to determine if reducing the degrees of freedom of skin deformation feedback and adding vibrotactile contact cues had any effect on a user's ability to complete a grasp-lift-and-place task with a "fragile" virtual object. This grasp-lift-and-place task of a "fragile" virtual object involves the dynamic movement of an object while having users focus on virtual grip force and, therefore, penetration depth into the virtual object. It simulates actions we perform on a regular basis in the real world while also providing a task which can be accomplished with no haptic feedback to be used for comparison.

A total of 18 participants (9 male and 9 female) between the ages of 19 and 31 participated in this experiment after giving informed consent. All 18 participants were right-hand dominant. The protocol was approved by the Stanford University Institutional Review Board.

3.2.1 Device

The skin deformation devices used for this experiment were modified from the ones presented in [14]. Each wearable device provides three translational degrees of freedom of skin deformation force feedback to the user's fingertip – two degrees of freedom in shear directions and one degree of freedom normal to the fingerpad. Three motors with encoders are located on the backside of the finger and actuate the joints of the

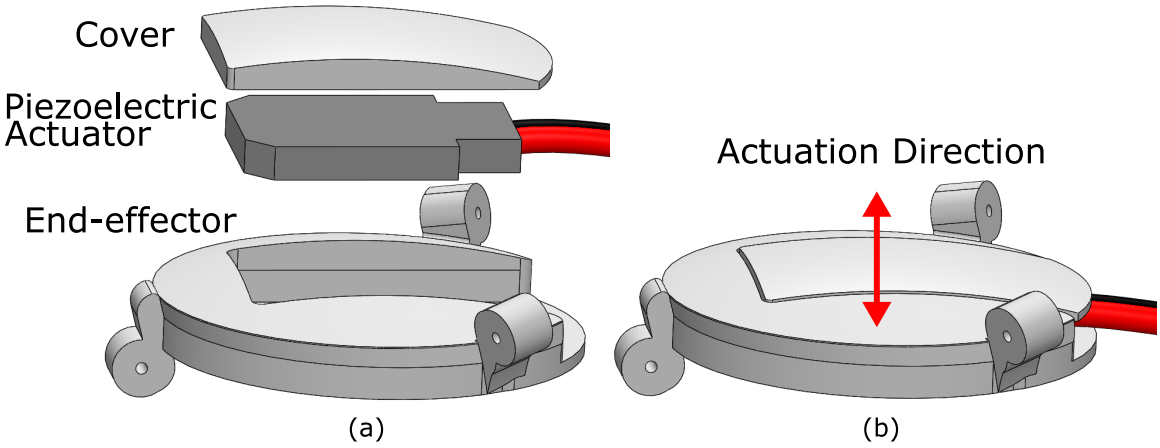

Figure 3.2: (a) The piezoelectric actuator is embedded inside the end-effector of the skin deformation device to provide the decaying sinusoid contact cue. (b) The piezoelectric actuator is covered to maintain the contour of the end-effector as it presses against the fingerpad. The cover is attached only to the piezoelectric actuator, making it free to move relative to the end-effector when displaying the sinusoidal contact cue.

delta mechanism using a bias-spring-tether transmission. The aluminum base of the device slides onto finger interfaces that are sized for the participant. See Fig. 3.1. The strap of the finger interface is wrapped around the middle of the user's finger, and the finger interface contacts the back and sides of the user's fingertip. Once the devices are fixed to the user's index finger and thumb, the neutral position of each device (desired position of the end-effector when rendering zero force) is set so the end-effector barely makes contact with the fingerpad. A PowerHap 7G piezoelectric actuator made by TDK was embedded in the end-effector of the device as shown in Fig. 3.2.

A probe from an Ascension 3D Guidance trakSTAR system was fixed to each finger interface and measures the position and orientation of the fingers with an update rate of 200 Hz. The virtual environment was rendered using the CHAI3D framework [54] and had an update rate of 1.6 kHz. The environment was displayed to participants on an Oculus Rift DK2 head-mounted virtual reality system. The devices are position-controlled and have a 10 Hz bandwidth. The controller takes the

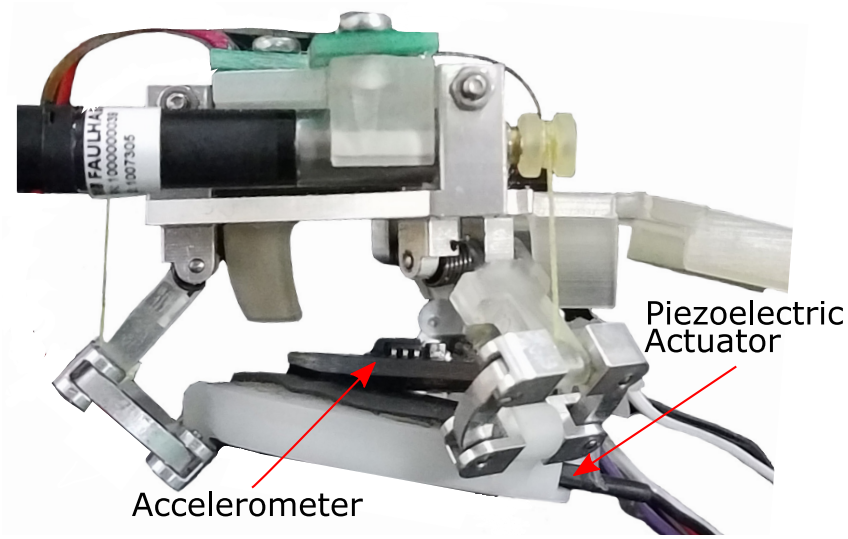

Figure 3.3: The device was mounted horizontally, with the accelerometer attached to the end-effector to measure the accelerations of the contact cues.

forces calculated using the physics engine of CHAI3D in the virtual environment and converts them into desired device positions using a constant of 2.1 mm/N, which is based on the reported mean lateral stiffness of the fingerpad [55]. Because this is a position-controlled device with a fixed force-to-displacement gain, the virtual weights and forces applied to the participants are specific for this set-up.

3.2.2 Haptic Conditions

The haptic conditions tested in this experiment combine two elements: skin deformation feedback and contact cues (Table 3.1). The skin deformation feedback category is composed of three conditions: no skin deformation feedback, shear-only skin deformation feedback, and shear-plus-normal skin deformation feedback. The shear-only skin deformation feedback condition rendered force feedback to the user using only the two shear degrees of freedom of the skin deformation devices (Conditions 4, 5, and 6). The normal force was set to a small value of 0.25 N to ensure the end-effector

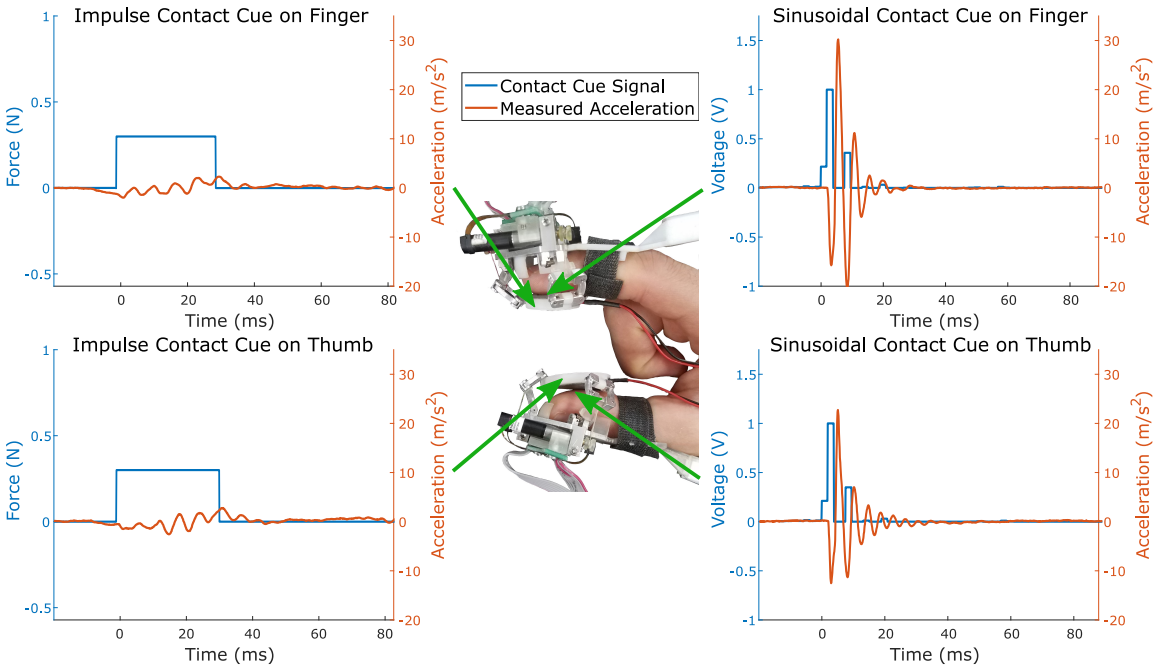

Figure 3.4: The impulse contact cue (ICC) signals and the sinusoidal contact cue (SCC) signals (in orange) and the resulting accelerometer measurements (in blue) for each device (finger and thumb).

contacted the finger and did not slip when rendering the shear forces. The shear-plus-normal skin deformation feedback conditions (Conditions 7, 8, and 9) used all three degrees of freedom of the skin deformation devices.

The contact cue category is also composed of three conditions: no contact cue (NoCC), an impulse contact cue played through the skin deformation device rendered in the normal-to-the-fingerpad direction (ICC), and a decaying sinusoid contact cue (SCC) rendered with a piezoelectric actuator, embedded in the end-effector of the skin deformation device shown in Fig. 3.2. We used the device itself to produce the impulse (Conditions 2, 5, and 8), but, since we have limited bandwidth, we chose an additional actuator to play the decaying sinusoid (Conditions 3, 6, and 9). The signal used to render the decaying sinusoid consisted of two sequential impulses, with the second impulse having a smaller amplitude than the first. For the impulse contact cue condition, the skin deformation device was given a 0.3 N force signal normal to the

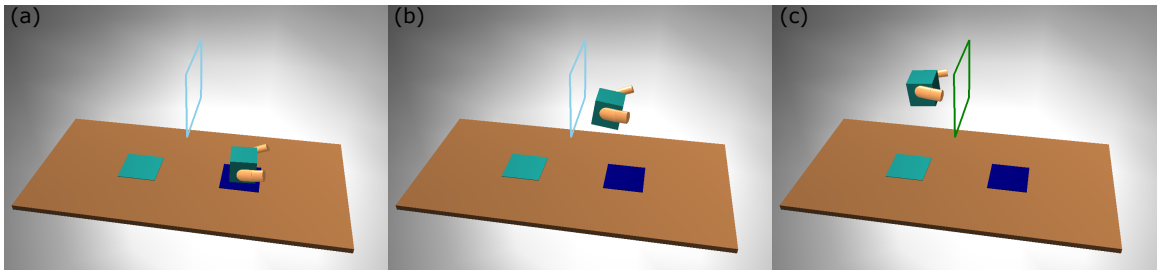

Figure 3.5: The task for the experiment consisted of grasping a virtual block (a), lifting the block (b), passing it through a hoop (c), and then placing the block back down on the table.

Table 3.1: The nine haptic conditions combine skin deformation feedback and contact cues

Condition	Skin Deformation Feedback	Contact Cue
1	None	None
2		Impulse Force
3		Decaying Sinusoid
4	Shear directions only	None
5		Impulse Force
6		Decaying Sinusoid
7	Shear directions plus normal direction	None
8		Impulse Force
9		Decaying Sinusoid

fingerpad in addition to the forces rendered from the haptic interactions for 30 ms. Since the end-effector is set to make contact with the user when rendering zero force, we eliminate the inherent contact cue provided by the device when rendering forces in the normal-to-the-fingerpad direction. Neither contact cue signal amplitude was varied based on velocity. The experimenters reasoned that the approaches to grasping and lifting a "fragile" virtual block would be of a low velocity contact and thus some signals would not be noticeable if the amplitude varied with velocity. Instead the amplitudes of each signal were chosen so that the contact cues felt similar in magnitude on the finger.

An accelerometer was attached to each end-effector to record the accelerations of the contact cues. Measurements were taken at 17 kHz with a ADXL335 three-axis accelerometer. The on-board capacitors were replaced to increase the cutoff frequency of the RC filter from 50 Hz to 500 Hz. The devices were mounted horizontally using a finger interface for the device (Fig. 3.3). Fig. 3.4 shows signals used to command the skin deformation device and the piezoelectric actuator, along with the resulting acceleration waveforms.

3.2.3 Procedure

Prior to the start of the experiment, participants were given three minutes to interact with a virtual block while wearing the skin deformation devices to help familiarize them with the devices and the virtual reality headset. During this time, all three degrees of skin deformation feedback were rendered and no contact cues were rendered.

For the experiment, participants were asked to complete a grasp-lift-and-place task with a "fragile" virtual block without breaking it. Each participant performed this task under all nine haptic conditions. The order that the haptic conditions were presented to participants was based on Latin squares. For each of the nine conditions, participants completed 30 trials, for a total of 270 trials. For each haptic condition, the 30 trials were divided into three 10-trial segments, and for each segment, participants used one of three different weighted blocks (100 g, 200 g, and 300 g). The order of the 10-trial segments was pseudo-randomized.

A single trial consisted of grasping a virtual block from the right-hand side of a virtual table, lifting it up, passing it through a 5 cm x 5 cm hoop rendered 10 cm in the air at the center of the table, and placing it in a square on the left-hand side of the table, as shown in Fig. 3.5. The color of the hoop turned from blue to green when the block passed through. There was no haptic feedback rendered from interactions with the hoop. Participants were informed at the end of each trial whether or not they "broke" the virtual block by squeezing it too hard. Each of the three different weighted blocks had their own grip force thresholds for determining a break; the thresholds were selected from pilot data and are 1.62 N, 1.70 N, and

1.93 N corresponding to the 100 g, 200 g, and 300 g blocks respectively. Before the start of each 10-trial segment, participants were informed of the weight of the block verbally by the experimenter with the labels "light," "medium," and "heavy," but participants were not informed of which haptic condition was being rendered during the trial.

At the end of each haptic condition, participants were asked to rate the realism of the condition on a scale of 1 to 7 with 1 being "not real" and 7 being "real." Participants took a two-minute break between haptic conditions and a five-minute break after the fifth haptic condition. Data from the virtual environment was recorded at 300 Hz during each trial.

3.3 Results

During the experiment, we recorded position data of the magnetic tracker for each finger, the interaction forces to be rendered on the haptic devices, and the position of the virtual block for each trial, along with whether or not the virtual block was "broken" during the trial. The total number of breakages by condition can be seen in Fig. 3.6. The total number of breakages by order of presentation can be seen in Fig. 3.7. Using the virtual force data, we calculated the maximum grip force when completing the task, i.e., moving the virtual block through the hoop. We then averaged the maximum grip force across all trials and all participants for each condition (Fig. 3.8). We also calculated the maximum grip force that occurred before the block was lifted off the virtual table and averaged this across all trials and all participants for each condition (Fig. 3.9).

We fit a generalized linear mixed-effects model to analyze effects of each haptic condition on max grip force during the lift, max grip force before the lift, and number of breakages, using the FitGLME function in MATLAB. We used an identity link function and assumed a normal distribution, as seen in Equation (3.1), for the two grip force models where D_V is the dependent variable used for the fit. In the case of modeling the breakages, we used a logit link function for a binomial distribution as

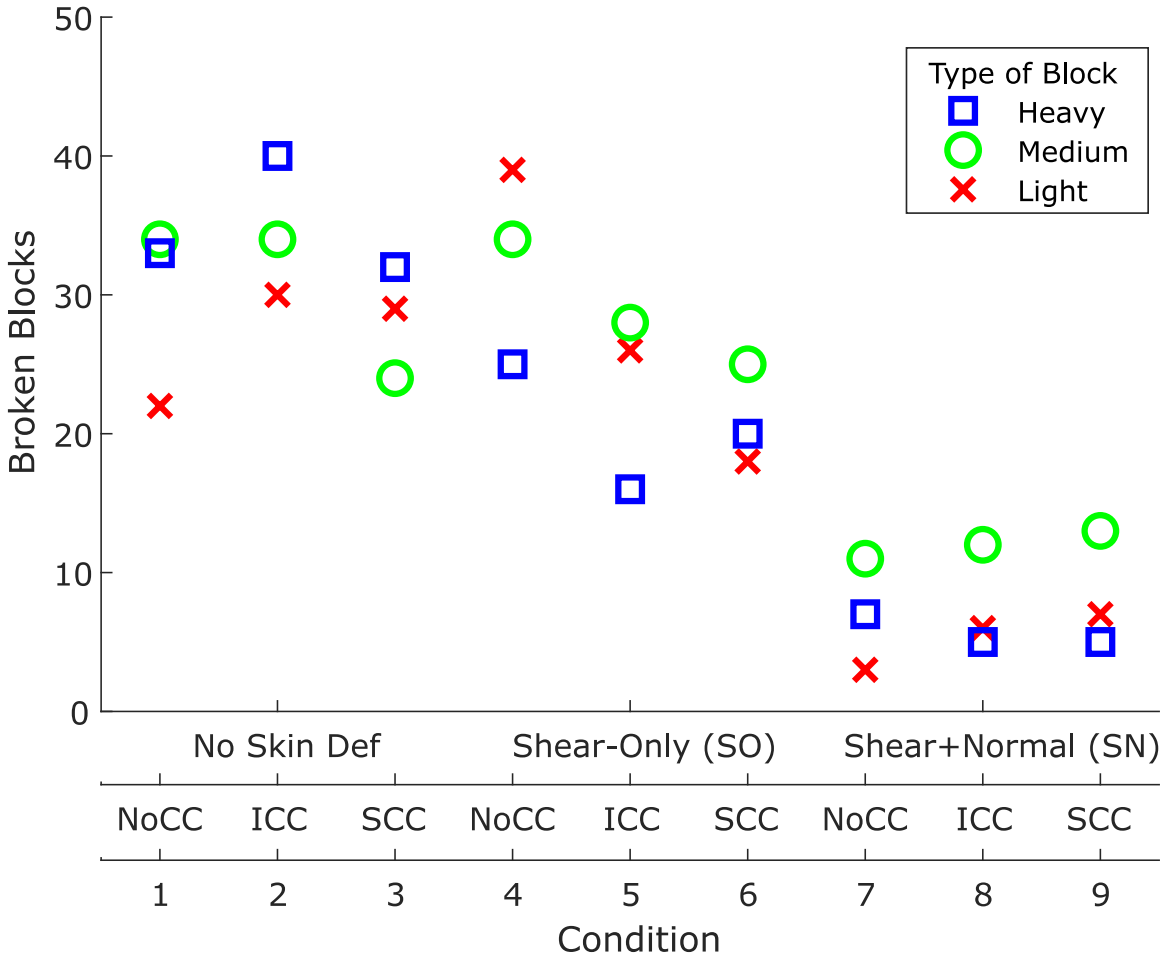

Figure 3.6: There is a significant drop in the number of broken blocks when participants were given shear-plus-normal skin deformation feedback.

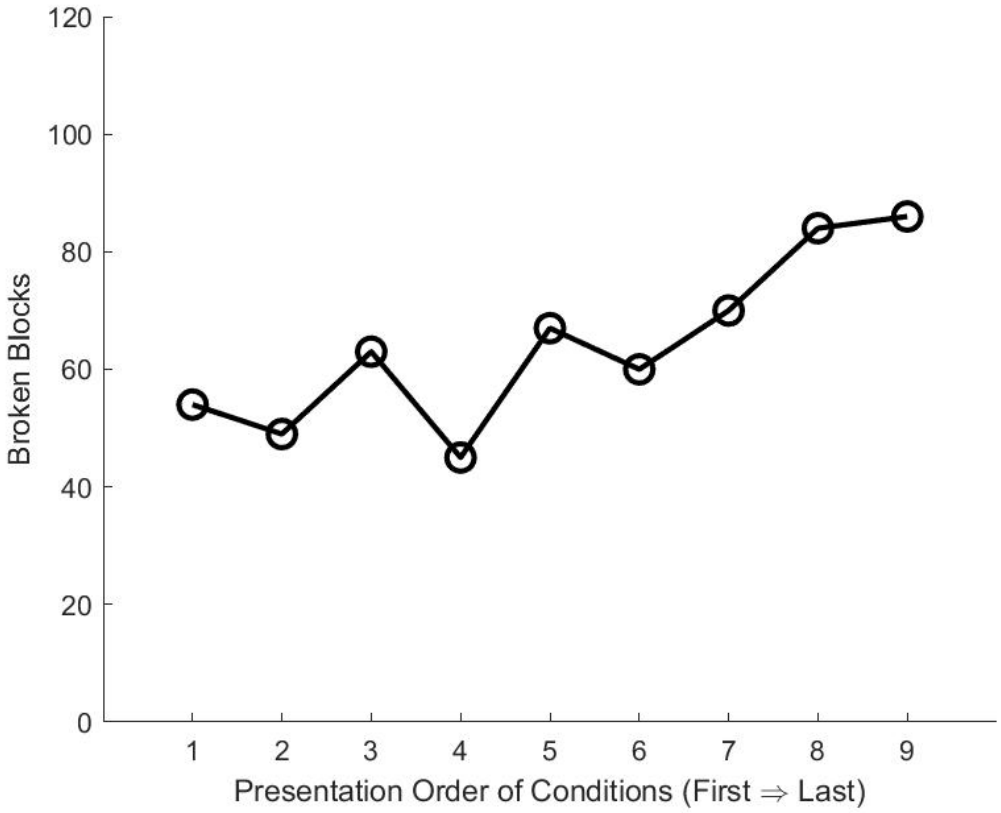

Figure 3.7: The number of broken blocks is larger for haptic conditions presented later in the experiment, suggesting participants may have experienced some fatigue.

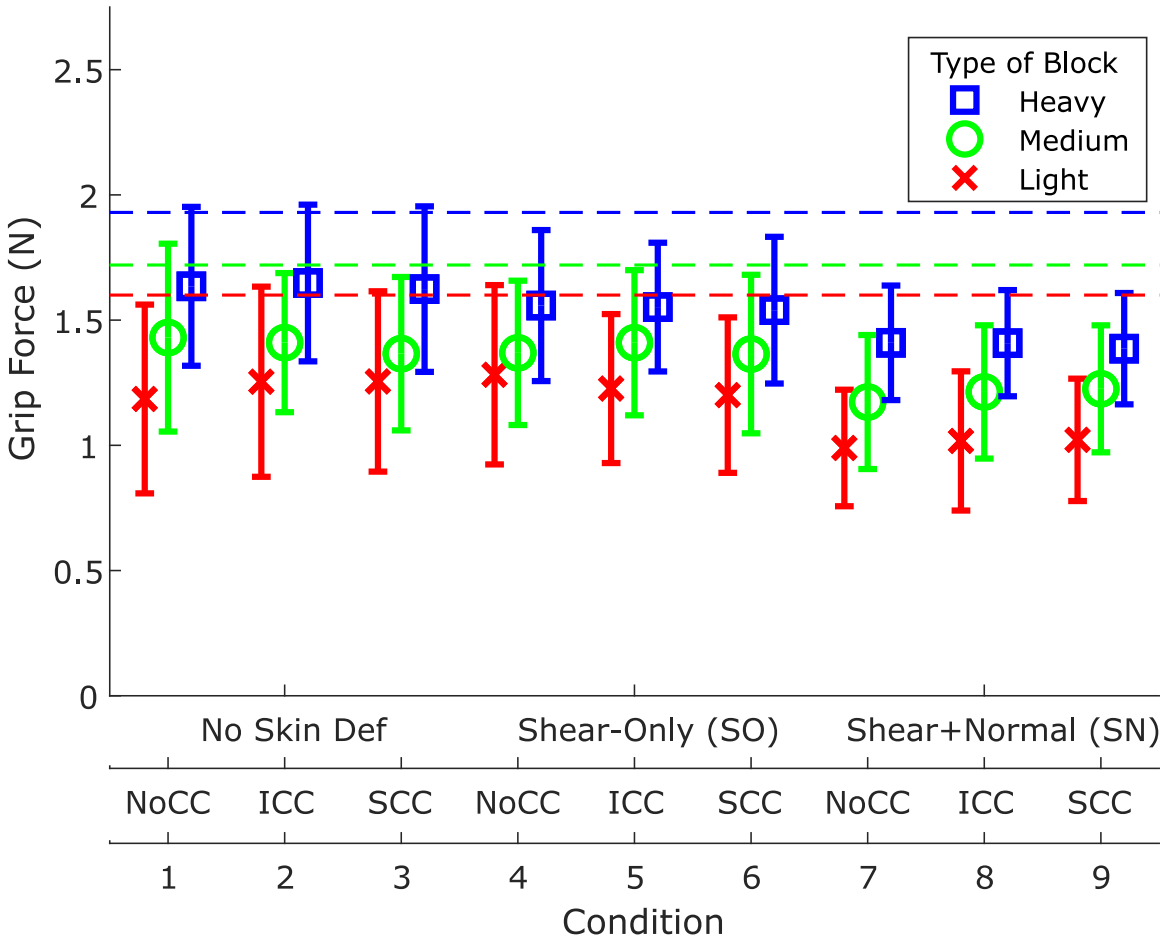

Figure 3.8: The max grip force during the task was averaged across all participants and is shown here with errorbars representing plus/minus one standard deviation and the dashed lines representing the force threshold used for the breaking of the virtual objects. The max grip force is significantly lower for shear-plus-normal skin deformation feedback (Conditions 7, 8, and 9) than for the no skin deformation feedback condition (Condition 1).

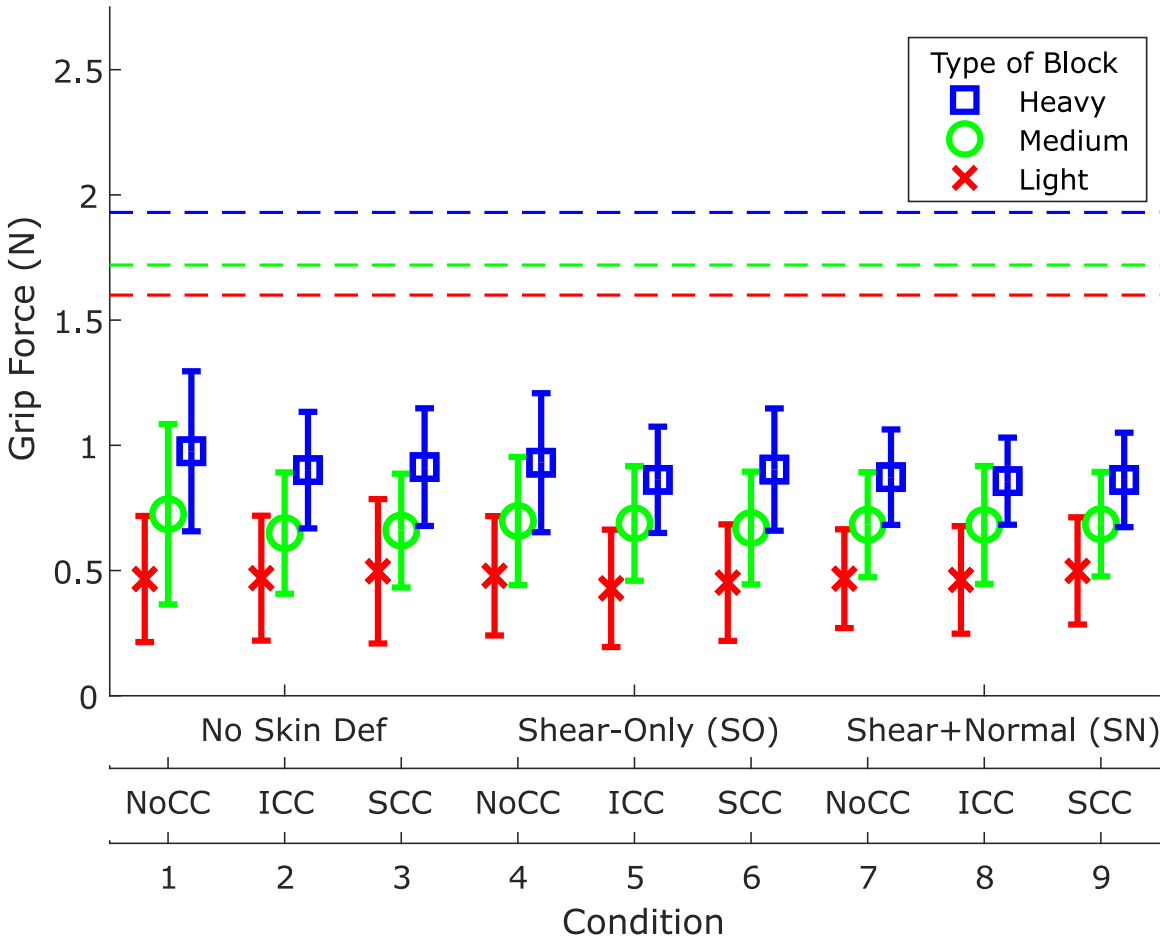

Figure 3.9: The max grip force before liftoff was averaged across all participants and is shown here with errorbars representing plus/minus one standard deviation and the dashed lines representing the force threshold used for the breaking of the virtual objects. The max grip force before liftoff is significantly lower for all haptic conditions except Condition 4 (the shear-only skin deformation feedback condition with no contact cue) than for the no feedback condition (Condition 1).

seen in Equation (3.2). We modeled the haptics conditions using four indicator variables. Those four indicator variables, H_{SO} for shear-only skin deformation feedback, H_{SN} for shear-plus-normal skin deformation feedback, H_{ICC} for the impulse rendered through the skin deformation device, and H_{SCC} for the decaying sinusoid rendered through the piezoelectric actuator, are used to represent the combinations of skin deformation feedback and contact cues. The ":" denotes the interaction effects between two variables. Each indicator variable was assigned either 1 or 0 depending on which haptic condition was being rendered for a particular trial. The no skin deformation and no contact cue condition was coded as 0's in all four indicator variables. The weights of the block were coded as two indicator variables, H_M for the "medium" block and H_H for the "heavy" block, with the "light" block occurring when H_M and H_H are set to 0.

$$\begin{aligned} D_V = {} & \beta_0 + \beta_M(H_M) + \beta_H(H_H) \\ & + \beta_{ICC}(H_{ICC}) + \beta_{SCC}(H_{SCC}) \\ & + \beta_{SO}(H_{SO}) + \beta_{SN}(H_{SN}) \\ & + \beta_{SO:ICC}(H_{SO} : H_{ICC}) \\ & + \beta_{SO:SCC}(H_{SO} : H_{SCC}) \\ & + \beta_{SN:ICC}(H_{SN} : H_{ICC}) \\ & + \beta_{SN:SCC}(H_{SN} : H_{SCC}) \end{aligned} \tag{3.1}$$

$$\begin{aligned}\log \frac{D_V}{1-D_V} &= \beta_0 + \beta_M(H_M) + \beta_H(H_H) \\ &+ \beta_{ICC}(H_{ICC}) + \beta_{SCC}(H_{SCC}) \\ &+ \beta_{SO}(H_{SO}) + \beta_{SN}(H_{SN}) \\ &+ \beta_{SO:ICC}(H_{SO} : H_{ICC}) \\ &+ \beta_{SO:SCC}(H_{SO} : H_{SCC}) \\ &+ \beta_{SN:ICC}(H_{SN} : H_{ICC}) \\ &+ \beta_{SN:SCC}(H_{SN} : H_{SCC})\end{aligned} \tag{3.2}$$

We then sum the coefficients of the four indicator variables and the interaction effects, as seen in Equation (3.3), to get the total effect of each combination of skin deformation feedback with each contact cue.

$$\begin{aligned}\beta_{SO\ w/\ ICC} &= \beta_{SO} + \beta_{ICC} + \beta_{SO:ICC} \\ \beta_{SO\ w/\ SCC} &= \beta_{SO} + \beta_{SCC} + \beta_{SO:SCC} \\ \beta_{SN\ w/\ ICC} &= \beta_{SN} + \beta_{ICC} + \beta_{SN:ICC} \\ \beta_{SN\ w/\ SCC} &= \beta_{SN} + \beta_{SCC} + \beta_{SN:SCC}\end{aligned} \tag{3.3}$$

The coefficients of each generalized linear mixed-effects model, including the interaction terms, can be found in Figs. 3.10, 3.11, and 3.12 with asterisks representing a significant difference ($p<0.05$) compared to the reference condition, which is lifting the "light" block with no skin deformation feedback and no contact cue.

The realism ratings for each condition were also averaged across all participants and are plotted in Fig. 3.13. We tested for significant effects of skin deformation feedback and contact cues on the realism rating using a Friedman Test which is a non-parametric alternative to the one-way ANOVA used when the dependent variable is ordinal. We found that skin deformation feedback has a significant effect on realism rating ($p< 0.01$) while the contact cues did not have a significant effect ($p = 0.72$).

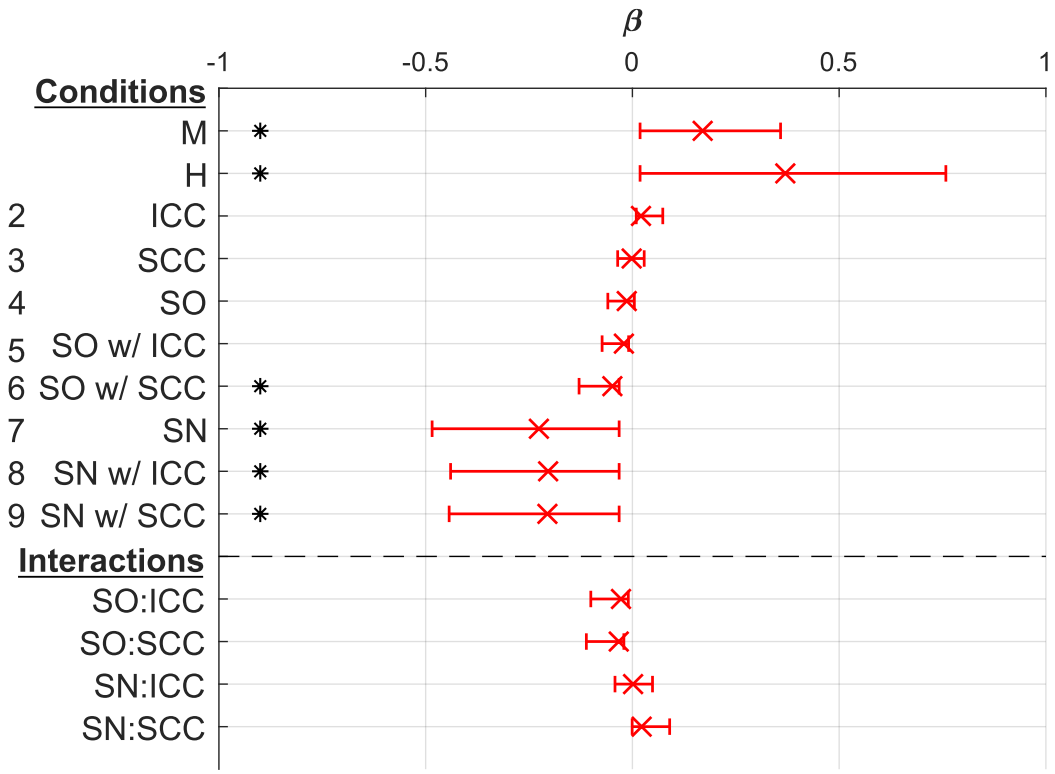

Figure 3.10: The coefficients of the GLMEs, presented in Equation (3.1) and Equation (3.3), modeling the max grip force throughout the task are shown here. The values below the horizontal line represent the interaction effects between skin deformation feedback conditions and the vibrotactile feedback conditions. Condition 1 is not presented because it is the reference condition for GLME. The *'s represent coefficients significantly different ($p < 0.05$) from the no feedback condition, Condition 1. The errorbars represent the 95% confidence interval reported by the fit of the GLME.

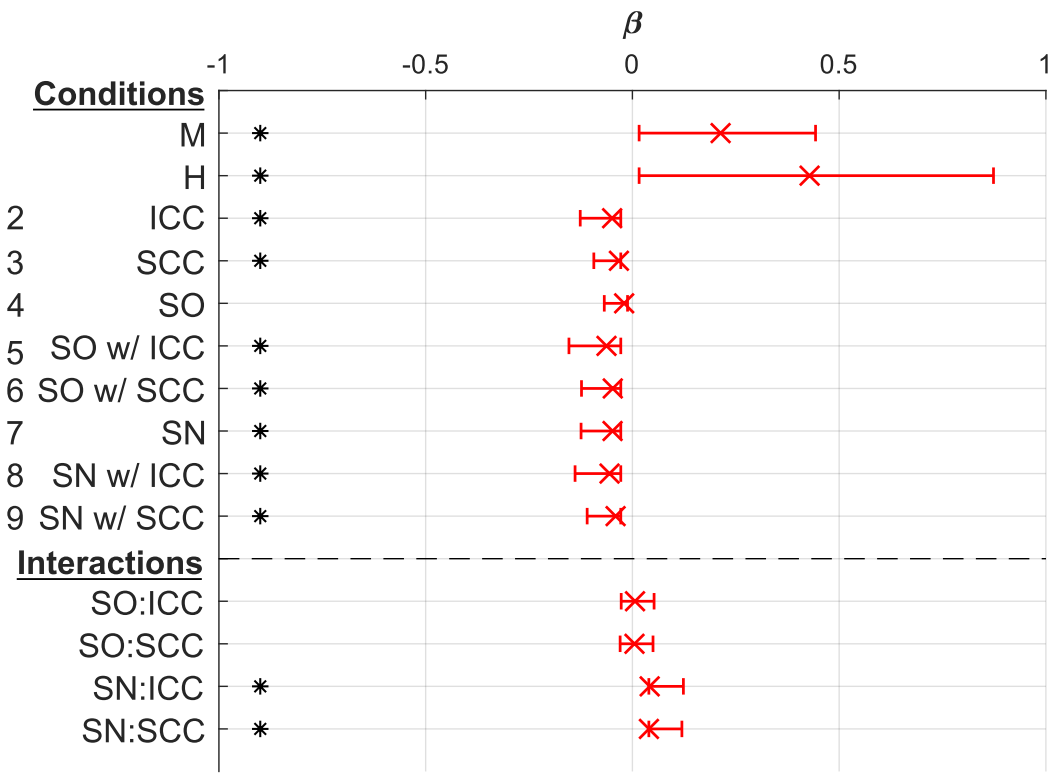

Figure 3.11: The coefficients of the GLMEs, presented in Equation (3.1) and Equation (3.3), modeling the max grip force before liftoff are shown here. The values below the horizontal line represent the interaction effects between skin deformation feedback conditions and the vibrotactile feedback conditions. Condition 1 is not presented because it is the reference condition for GLME. The *'s represent coefficients significantly different ($p < 0.05$) from the no feedback condition, Condition 1. The errorbars represent the 95% confidence interval reported by the fit of the GLME.

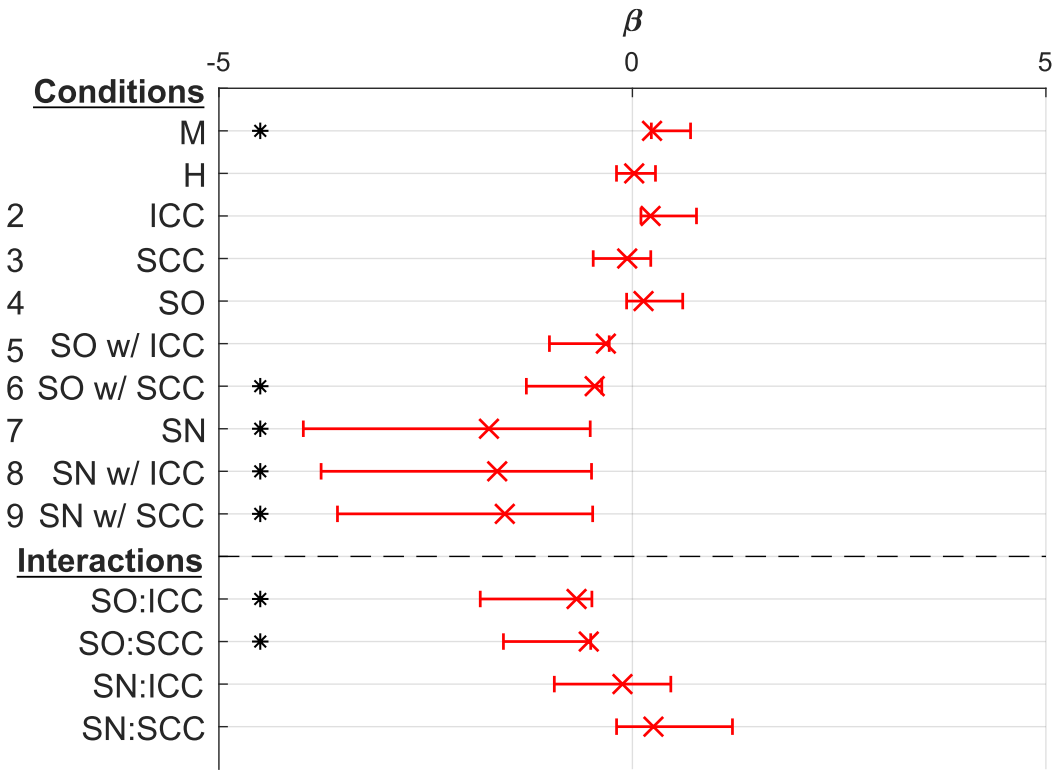

Figure 3.12: The coefficients of the GLMEs, presented in Equation (3.2) and Equation (3.3), modeling the likelihood the virtual block was broken are shown here. The values below the horizontal line represent the interaction effects between skin deformation feedback conditions and the vibrotactile feedback conditions. Condition 1 is not presented because it is the reference condition for GLME. The *'s represent coefficients significantly different ($p < 0.05$) from the no feedback condition, Condition 1. The errorbars represent the 95% confidence interval reported by the fit of the GLME.

Using a Mann–Whitney U test for post hoc analysis, the results show that the shear-plus-normal skin deformation feedback was significantly different from both shear-only skin deformation feedback ($p< 0.01$) and no skin deformation feedback ($p< 0.01$), and the results show that shear-only skin deformation feedback was significantly different from no skin deformation feedback ($p< 0.01$).

3.4 Discussion

The results of this experiment show that a user is significantly less likely to break the virtual block when receiving shear-plus-normal skin deformation feedback (Condition 7). The results also show that the haptic conditions combining shear-plus-normal skin deformation feedback with a vibrotactile contact cue (Conditions 8 and 9) significantly reduce the likelihood of breaking the virtual block. However, the primary effect for shear-plus-normal skin deformation feedback with a vibrotactile contact cue (Conditions 8 and 9) on likelihood of breaking the block comes from the shear-plus-normal skin deformation feedback and not from the contact cue or from the interaction between the two. This is because, as seen in Fig. 3.12, β_{SN} is larger than β_{ICC}, β_{SCC}, and the interaction coefficients, $\beta_{SN:ICC}$ and $\beta_{SN:SCC}$. It is noteworthy that the shear-only skin deformation feedback combined with the contact cue rendered through the piezoelectric actuator (Condition 6) also significantly reduces the user's chance of breaking the block. When looking at the interaction terms, we see that the interaction between shear-only and both contact cues (Conditions 5 and 6) have a significant effect on reducing the chance of breaking the block. We also see that the medium weight block has a significant effect on the likelihood of breaking the virtual block. This can be attributed to the breaking threshold not being equally spaced between the light block and the heavy block. These thresholds were determined from a pilot study and thus do not have a linear relationship with virtual weight.

Fig. 3.11, the maximum grip force before the virtual block is lifted off the table, shows that all the tested conditions, except for the shear-only skin deformation feedback condition (Condition 5), have a significant effect on reducing the maximum grip force applied to the block before liftoff. This result concurs with the results presented

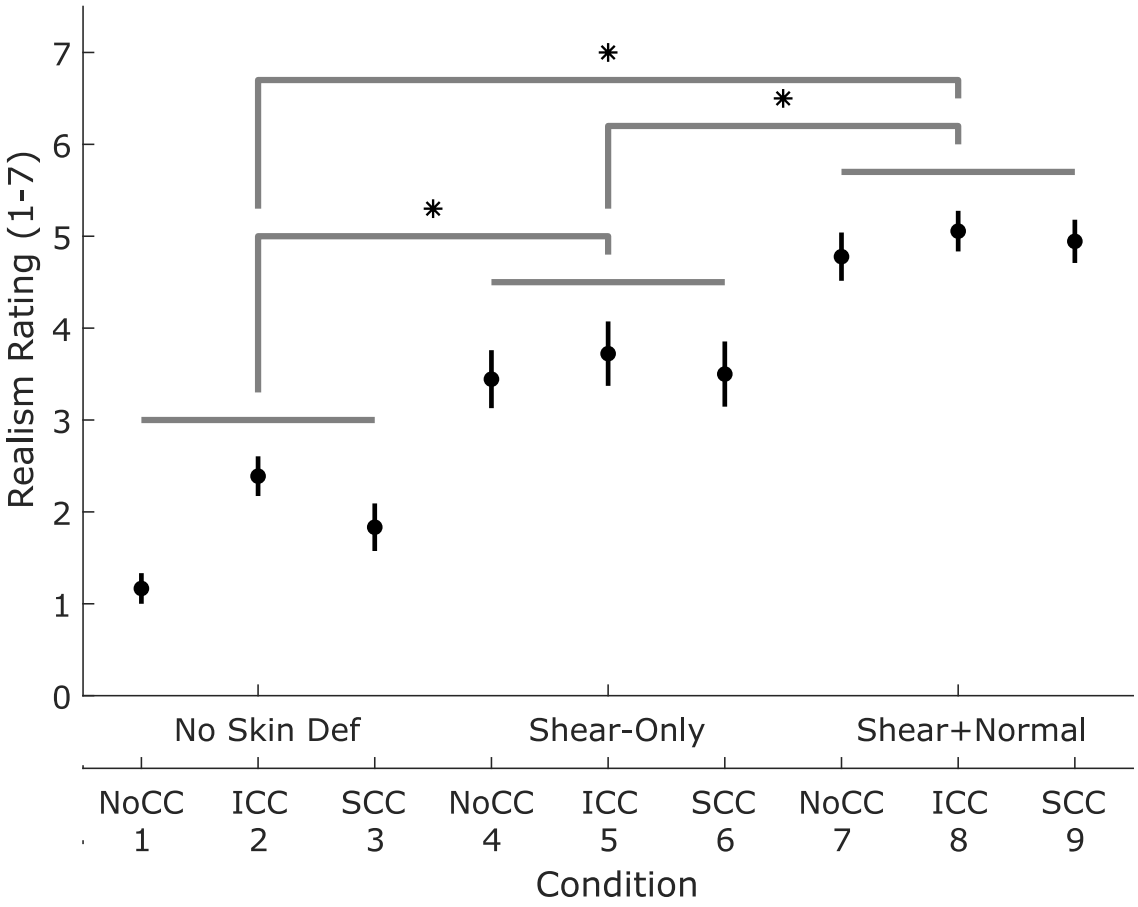

Figure 3.13: The realism rating for each haptic condition was averaged across all participants and is shown here with errorbars representing the standard error. The addition of shear-only (Conditions 4, 5, and 6) and shear-plus-normal (Conditions 7, 8, and 9) skin deformation feedback significantly increases the realism rating ($p < 0.05$), denoted above by the *'s, while the addition of an impulse contact cue (Conditions 2, 5, and 8) or a sinusoidal contact cue (Conditions 3, 6, and 9) has no significant effect on the realism rating.

in [38] where adding a contact cue reduces the penetration depth into the virtual objects. The absence of a significant effect from Condition 5 is expected because shear-only skin deformation feedback is the only haptic condition that does not apply any feedback until the block is starting to lift off the table. This means that the shear forces experienced during the lifting of the block are not enough feedback to reduce the maximum grip force experienced by the block. When looking at the interaction terms between the types of skin deformation feedback and the contact cues, we see that there is a significant effect for combining shear-plus-normal skin deformation feedback and both contact cues. However the coefficient is positive with relatively the same magnitude as both the shear-plus-normal skin deformation feedback and each contact cue by itself. This suggests that when combining shear-plus-normal skin deformation feedback with a contact cue, their effects do not add together; rather one of the two feedback modalities dominates the effect on max grip force before lift off. We also notice that the coefficients for the haptic conditions which combine shear-only skin deformation feedback and each of the contact cues (Conditions 5 and 6) are significantly lower than the reference condition (Condition 1), but the interaction terms are not significant. This suggests that the majority of the effect of the combination of shear-only skin deformation and contact cues on max grip force before liftoff comes from the contact cue.

While the addition of either contact cue does significantly reduce the grip force before liftoff, and thus the initial penetration depth, only Conditions 6, 7, 8, and 9 have a significantly lower max grip force through the task. Interestingly, neither contact cue on their own is enough to help the participant stay below the grip force breaking threshold, however, when the decaying sinusoid contact cue is combined with shear-only skin deformation (Condition 6), the max grip force is significantly lower than the no feedback condition. Because there is no significant effect of either contact cue on their own, the significant effect of Conditions 8 and 9 are a result of the shear-plus-normal skin deformation feedback which provides the user with constant feedback on grip force throughout the task.

The results of the post hoc analysis on realism shows that reducing the degrees of freedom of skin deformation feedback reduces the realism of the interaction with the

virtual environment in a grasp-lift-and-place task. It is surprising that the addition of contact cues did not have a significant effect on realism in this experiment as it has in past studies [38]. This could be due to the relatively low displacement amplitude of the piezoelectric actuator or not varying the amplitude of each contact cue condition with velocity. There does appear to be more of an effect on realism with contact cue over the no feedback condition, but once combined with skin deformation, that effect is minimized.

It is worth noting that we see a rise in the number of breaks that occur based on the order of haptic condition (Fig. 3.7). This suggests that participants may have experienced some fatigue toward the end of the experiment. We do not believe this has an effect on the analysis, as the order of the haptic conditions were presented based on a Latin squares.

3.5 Conclusion

We performed an experiment to determine if augmenting or replacing the normal degree of freedom of skin deformation feedback with contact cues had any effect on the ability to complete a grasp-lift-and-place task with a "fragile" virtual block. We modified an existing fingertip wearable skin deformation device with a piezoelectric actuator embedded in the end-effector. During the experiment, we asked participants to grasp, lift, and place a "fragile" virtual block without breaking the object when receiving nine different combinations of skin deformation feedback and contact cues.

We fit two different generalized linear mixed-effect models to the maximum grip force during the task, the maximum grip force before liftoff, and the number of broken blocks to assess the effects of each feedback modality and the combinations of feedback modalities. We found that shear-plus-normal skin deformation feedback significantly improves users' ability to grasp, lift, and place a "fragile" virtual block without breaking it, compared to receiving no feedback or contact cues. We also found that providing shear-only skin deformation feedback with a sinusoidal contact cue, rendered through a piezoelectric actuator embedded in the end-effector, improves users' ability to complete the grasp-lift-and-place task without breaking the

virtual block compared to receiving no feedback. We also found that providing shear-plus-normal skin deformation feedback lowered the maximum grip force that occurs throughout the grasp-lift-and-place task. When analyzing the grasping element of the task, we found that all feedback modalities except for the shear-only skin deformation feedback condition (Condition 5) had a significant effect lowering the maximum grip forces that occur before liftoff of the virtual block. Lastly, we asked participants to give a realism rating on each haptic condition and found that both shear-only skin deformation feedback and shear-plus-normal skin deformation feedback increase the realism of the haptic interactions with the virtual blocks, while the contact cues did not have a significant effect on realism.

These results suggest that it is possible to replace the normal degree of freedom on a 3-DoF skin deformation device and still be able to provide useful haptic feedback for a fine manipulation task. This could lead to cheaper and lighter wearable haptic devices, as it would reduce the complexity by eliminating a degree of freedom.

Chapter 4

Altering Virtual Weight Perception when using Skin Deformation Feedback

When designing wearable skin deformation devices, the term "lightweight" is often stated as a design goal. A device that is too heavy can be cumbersome for users and can affect their experience and perception. Thus, designers often choose small motors that have limited force output. This, in turn, places a limit on the virtual weight that is able to be rendered when manipulating objects in virtual reality using these devices. Adding gearboxes would increase the maximum available force but would decrease bandwidth and increase the weight of the device. Therefore, there is a need for methods to increase the virtual weight that can be conveyed without radical changes to hardware. In this chapter, we explore using weight illusions in virtual reality to alter the weight perception of virtual objects when being manipulated using skin deformation feedback devices. In the first of two studies, we describe and implement a novel haptic weight illusion in which we scale the inertial force that occurs during object manipulation to increase the perceived virtual weight by increasing the mass of the virtual object and decreasing the gravity of the virtual environment. From previous work described in Section 1.3.1, we know that inertia tensors have an effect on the perceived weight, or heaviness, of an object [27]. While the contribution of inertia

tensors in weight perception is presented in the context of increased muscular forces required to move an object in a controlled manner, we believe the tactile sensation will be enough to effect users' weight perception in virtual reality when using wearable skin deformation devices. In the second study, we investigate using scaled inertial forces for decreasing virtual weight by decreasing the mass of the virtual object and increasing the gravity of the virtual environment. In parallel, we measure the effects of the combinations of scaled inertial forces with a visuo-haptic weight illusion, non-unity control-to-display ratio, in both complementary and conflicting manners. The use of a non-unity control-to-display ratio was first introduced by Dominjon et al. [31] with a kinesthetic haptic device. The use of non-unity control-to-display ratio was expanded upon by Schorr [14] with wearable skin deformation haptic devices. The inertial scaling study (Section 4.2) was published in [15].

4.1 Device

The skin deformation haptic feedback device used in this study is similar to the device described in Chapter 2, with the main difference being the end-effector; for the following two studies in this chapter, the end-effector used did not have a piezoelectric actuator. The modified device can be seen in Fig. 4.1.

4.2 Study 1: Inertial Scaling

4.2.1 Study Description

The purpose of this study was to determine the effect of scaled inertial forces on virtual weight perception with skin deformation feedback. The experiment consisted of three parts: an open response exercise, training trials, and experiment trials. The open response portion of the experiment was used to assess how participants interpreted the difference between virtual blocks when one of the blocks has scaled inertial force. The training trials were used to familiarize the participants with performing virtual weight discrimination using the wearable skin deformation devices. The open response

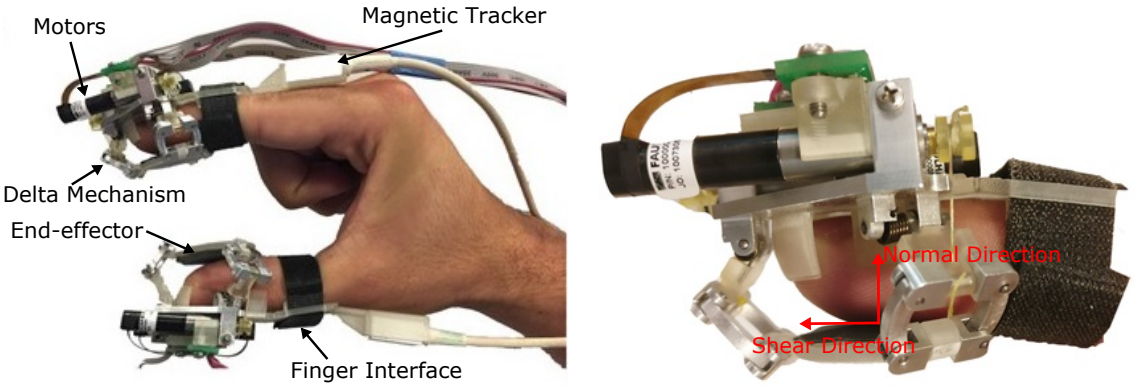

Figure 4.1: (a) Participants wore two 3-DoF skin deformation devices, one on their right hand index finger and thumb, during the experiment [14]. (b) The device renders normal and shear forces to the fingerpad through the end-effector covered with gecko-inspired dry adhesive. [15] © 2018 IEEE

portion was completed before the training trials so as not to influence the participants' responses.

A total of 11 participants (8 male and 3 female) between the ages of 23 and 45 participated in this experiment after giving informed consent. 8 participants were right-hand dominant and 3 participants were left-hand dominant. The protocol was approved by the Stanford University Institutional Review Board.

4.2.1.1 Scaled Inertial Forces Rendering Algorithm

All blocks rendered throughout the experiment were cubes with 50 mm sides and a virtual stiffness of 175 N/m.

To scale the inertial forces felt by the user, we first break down the desired rendered weight, $\vec{w}_{rendered}$, into its mass and gravity components; $m_{desired\ weight}$ and $\vec{g}_{Earth} = (0, 0, -9.8)$ m/s^2.

$$\vec{w}_{rendered} = m_{desired\ weight} \cdot \vec{g}_{Earth} \tag{4.1}$$

The mass of a virtual block is then scaled by the scaling factor, SF.

$$m_{rendered} = m_{desired\ weight} \cdot SF \tag{4.2}$$

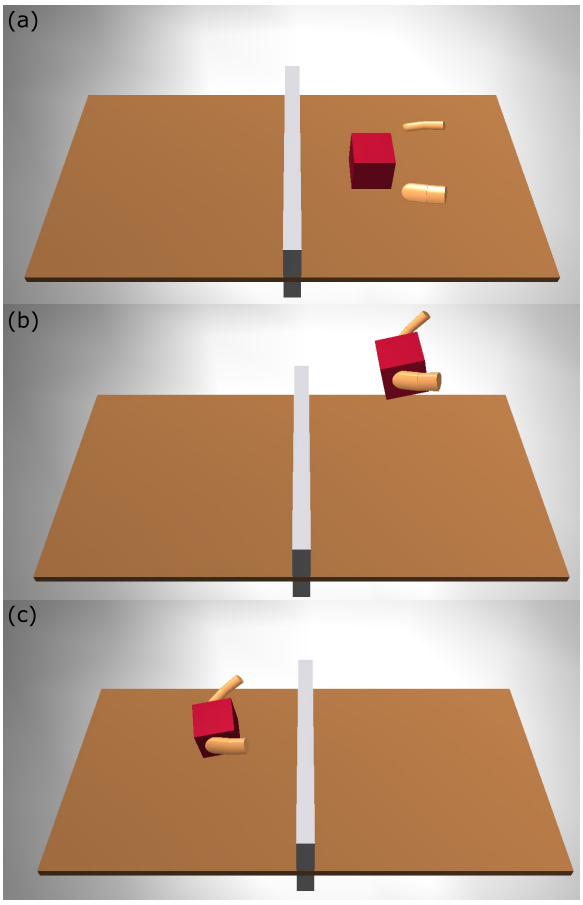

Figure 4.2: Participants were asked to (a) grasp, (b) lift, and then (c) place each virtual block on the other side of a virtual wall while determining which virtual block felt heavier.

The virtual weight is then set to desired weight by scaling the gravitational acceleration vector as shown below and in Fig. 4.3.

$$\vec{g}_{rendered} = \frac{1}{SF} \cdot \vec{g}_{Earth} \tag{4.3}$$

Therefore,

$$m_{rendered} \cdot \vec{g}_{rendered} = m_{desired\ weight} \cdot \vec{g}_{Earth} \tag{4.4}$$

With the altered gravitation vectors used in this algorithm, virtual blocks will fall

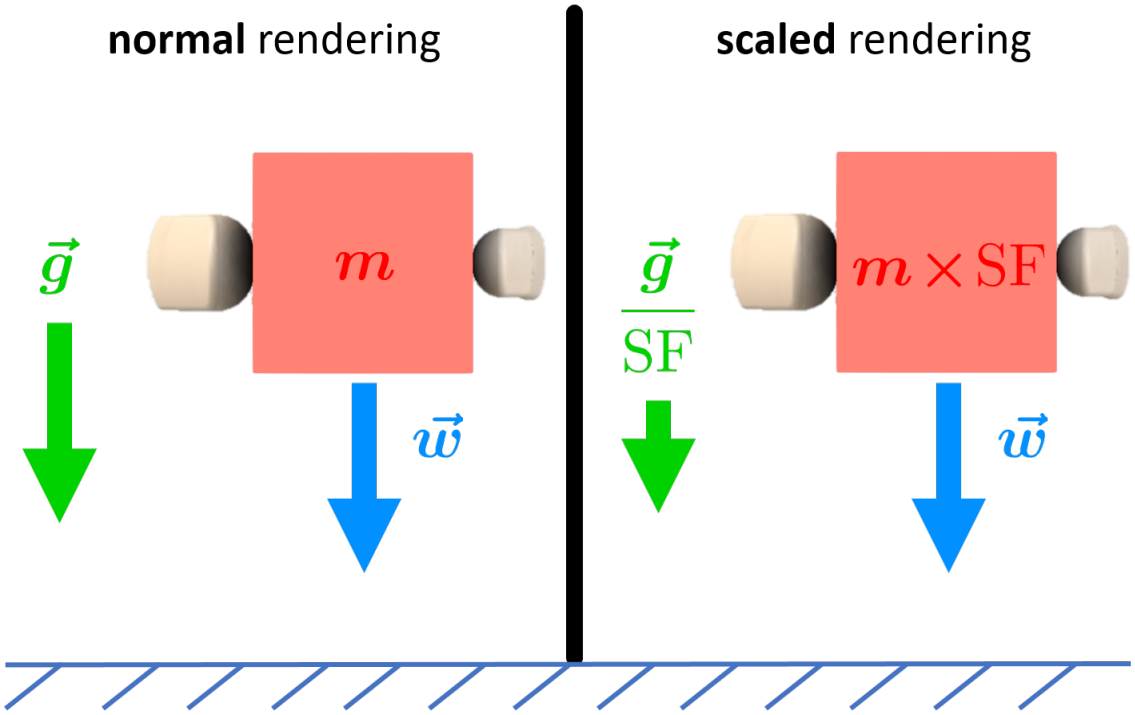

Figure 4.3: To scale the inertial forces of the virtual block, we increase the mass, m, by a inertial scaling factor, SF, and decrease the gravity, $\vec{g}$ of the virtual environment by that same factor to keep the virtual weight, $\vec{w}$ constant. [15] © 2018 IEEE

at potentially noticeably different rates than a block under Earth's gravity. To prevent this visual cue from affecting the results, the mass of the block and the gravitation vector are returned to their unscaled values when the user is not contacting the virtual block.

As the virtual scene updates, the CHAI3D framework calculates interaction forces between the virtual object and the haptic proxy point associated with each finger. We transform these forces into desired positions using the following equation

$$\vec{x}_{desired} = \alpha \cdot \vec{F}_{Interaction} \tag{4.5}$$

where $\vec{x}_{Desired}$ is the desired position of the end-effector, α is the force to position gain (2.1 mm/N in our case as mentioned previously), and $\vec{F}_{Interaction}$ is the interaction

forces calculated by the CHAI3D framework. The inverse kinematics for the delta mechanism are then solved to get desired joint angles. A proportional controller with a gain of 1200 mNm/deg on the joint angle error is used to command motor torques.

4.2.1.2 Procedure

After familiarizing themselves with the devices, participants began the open response portion of the experiment. Two virtual blocks, distinguished as "Block 1" and "Block 2", were presented one at a time to the participant. Both blocks were rendered with a weight corresponding to 200 g on Earth, with one block having a mass of 200 g and the other block having a mass of 600 g. This scales the inertial forces by a factor of 3. Participants were instructed to grasp and lift the block presented to them, and then place the block on the opposite side of a visually rendered wall, as shown in Fig. 4.2. Once the virtual block was placed, the experimenter presented the participant with the next virtual block and asked the participant to perform the same movement. Participants were asked if there was any difference between the two blocks as the experimenter switched between blocks several times, informing the participant of which block was currently being rendered. We did not prompt participants to think about weight, rather we wanted to know their first impression about what was different between the two blocks. Participants' responses to this open response exercise were recorded by the experimenter and categorized.

The weight discrimination portion of the experiment consisted of 40 training trials and two sets of 50 experiment trials using a two-alternative, forced-choice paradigm. Each trial consisted of a reference block and comparison block presented in random order. The training trials were rendered using standard gravitation forces, while the experiment trials used the scaled inertial forces when rendering the comparison weight. Data was not recorded during the training trials; subjects were given the correct answer after answering which block felt heavier. Inertial scaling factors of 2 and 3 were used for the experiment. All trials used a reference weight of 200 g. The training trials used comparison weights of 50, 125, 275, and 350 g and the experiment trials used comparison weights of 50, 125, 200, 275, and 350 g. The comparison weights were presented 10 times each in a randomized order.

Table 4.1: PSEs and JNDs of virtual weight for each subject.

Subject	Scaling Factor 2		Scaling Factor 3	
	PSE (g)	JND (g)	PSE (g)	JND (g)
1	203.5	9.6	171.0	22.9
2	211.8	28.9	189.3	35.0
3	179.2	26.5	162.4	19.0
4	184.7	22.6	162.8	19.2
5	126.9	28.5	70.8	27.0
6	162.5	18.7	171.3	34.5
7	129.7	62.6	88.3	31.7
8	145.8	26.5	125.0	9.3
9	203.4	9.2	201.9	28.5
10	162.5	18.7	18.7	4.6
Mean	171.0	25.2	150.5	23.2
Std. Dev.	30.6	15.0	42.6	10.3

Participants were asked to grasp and lift the virtual block presented, then place the virtual block on the opposite side of a visually rendered wall while determining which block "overall felt heavier." After grasping, lifting, and placing the first block, participants pressed a button on a keyboard to switch to the second block. There was no restriction on how many times the participant could grasp, lift, and place each block before recording their answer using buttons on a keyboard. Answers were only accepted when the second block of the pair was being rendered to ensure each block in the pair was presented an equal number of times. The first block in the pair was colored blue and the second block was colored red to give visual indication to the participant which block they were lifting. The entire experiment took approximately 1 hour with two 10 min breaks: one between training and the first 50 experiment trials, and one after the first 50 experiment trials. The scaling factor was fixed for each block of 50 experiment trials.

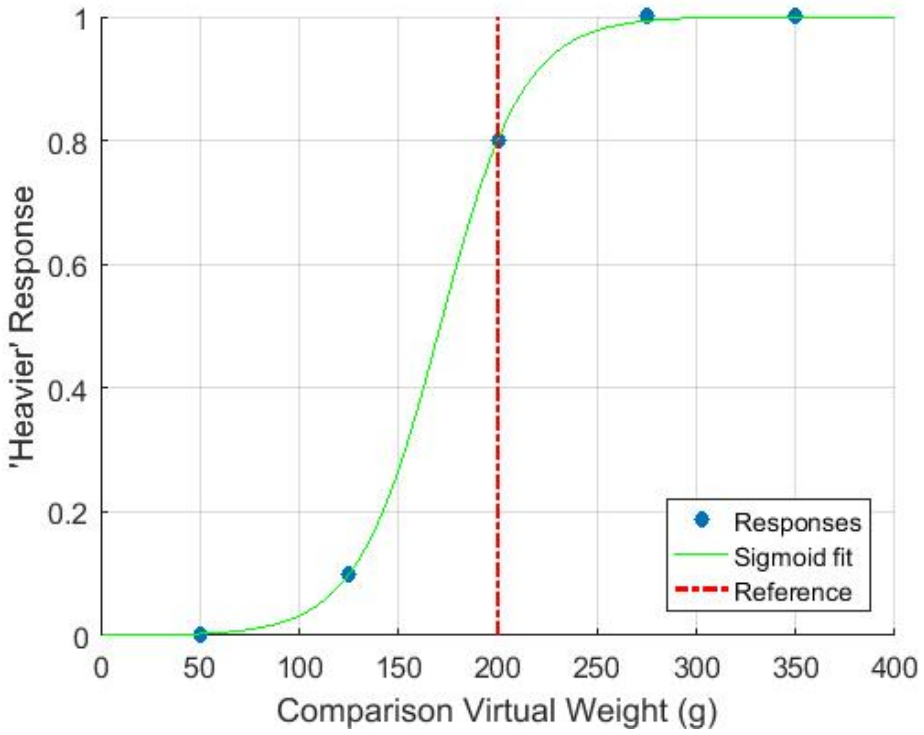

Figure 4.4: A sample psychometric curve from one participant's data with an inertial scaling factor of 3. Pyschometric curves were fit to each participant's data to calculate the PSE and JND for each scaling factor. [15] © 2018 IEEE

4.2.2 Result

Of the 11 participants in this study, 9 responded that the virtual block with inertial scaling felt "heavier" during the open response exercise portion of the experiment, with one participant responding that the block with inertial scaling felt "bigger" and one participant unable to describe any difference between the two virtual blocks.

Points of subjective equality (PSEs) and just noticeable differences (JNDs) were calculated for each inertial scaling factor by fitting a psychometric curve to proportion of "heavier" responses data using the sigmoid function:

$$y = \frac{1}{\left(1 + e^{\frac{-(x-\alpha)}{\beta}}\right)}, \tag{4.6}$$

where y is the proportion of "heavier" responses, x is the comparison weight, α is the PSE, and β is a slope fitting parameter. The values of α and β are results of the sigmoid function fit. From this fit, the JND is calculated by subtracting the PSE, α, from the comparison weight, $x_{0.75}$, corresponding to the 0.75 proportion of "heavier" responses, $y = 0.75$.

We were unable to fit a psychometric curve to the data provided by the one participant who was unable to detect a difference between the two virtual blocks in the open response exercise portion of the experiment. We classified this participant as a "non-responder" and did not include their data in the results of this study. An example of another participant's psychometric curve fit for an inertial scaling factor of 3 is shown in Fig. 4.4.

Calculated PSEs for each participant are shown in Table 4.1. PSEs were then averaged across all responding participants. Fig. 4.5 shows the average PSE for both scaling factors along with error bars representing plus/minus one standard deviation. The average PSEs for inertial scaling factors of 2 and 3 were 171.0 g and 150.5 g, respectively. Table 4.1 shows the PSEs and JNDs, as well as the standard deviation for each. A t-test was performed between the PSEs and the reference weight for each scaling factor to determine whether scaling inertial forces had a significant effect on virtual weight perception. Scaling inertial forces did have a significant effect on perceived virtual weight, with p-values of 0.015 and 0.005 for scaling factors of 2 and 3, respectively. A t-test was also performed to determine any significant difference in the effect of weight perception between a scaling factor of 2 and a scaling factor of 3. A p-value of 0.01 shows that there was a difference between scaling inertial forces by a factor of 2 and 3.

4.2.3 Discussion

The results show that scaling inertial forces has a significant effect on virtual weight perception when using skin deformation feedback during a grasp-lift-and-place task. This was done by increasing the mass of the virtual blocks while decreasing the gravitation force acting on it such that the weight of the virtual block remains the

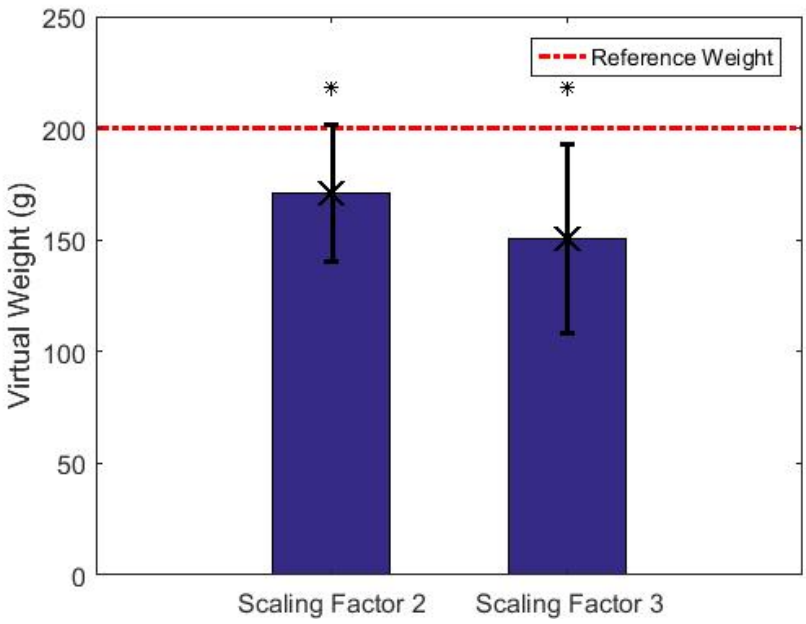

Figure 4.5: The effect of scaled inertial forces can be seen from graphing the PSE of virtual weight for a reference virtual weight of 200 g with scaling factors of 2 and 3. A t-test showed significance for both scaling factors with p-values less than 0.05. [15]

same. A grasp-lift-and-place task was chosen to elicit more of the inertial force cues to the participants.

The effect is validated in two ways. First, 9 of 11 participants responded that virtual block with scaled inertial forces felt "heavier" than the normally rendered virtual block in the open response portion of the experiment. One participant responded that the virtual block with scaled inertial forces felt "bigger". Still, this participant did show a shift in PSE during the weight discrimination task. As described earlier, we were unable to fit a psychometric curve to the weight discrimination data for a participant who was unable to notice any difference in the two virtual blocks during the open response portion of the experiment. This suggests that the participant had trouble with the virtual weight discrimination task using skin deformation as a whole, rather than only not responding to inertial scaling effect. This led us to classifying this participant as a "non-responder" and not using their data in the weight

discrimination analysis.

Second, the PSEs generated from the two-alternative forced choice paradigm portion of the experiment show that scaling the inertial forces has significant effects on perceived weight. The magnitude of the shift is reasonable given that the inertial forces are smaller in magnitude than the weight of the virtual object during this task.

Interestingly, while the results seem to agree with prior work done by Turvey et al. [27] to show an object's inertia contributes to the object's perceived weight, Turvey et al. focus on inertia in the context of wieldability, or the level of muscular forces required to move the object in a controlled fashion, where as using our method of inertial scaling with wearable skin deformation feedback devices, there is no net force on the user and thus no resistance to the movement of the users muscles. Thus we show that there is a tactile component to the influence of inertia on perceived weight.

4.3 Study 2: Complementary and Conflicting Weight Illusions using Haptics and Visuo-Haptics

In this study, we want to investigate the combination of a haptic and visuo-haptic weight illusion in both a complementary and conflicting manner using scaled inertial forces and non-unity control-to-display ratio. To do this, we also need to investigate the use of scaled inertial forces to make a virtual object feel lighter.

4.3.1 Study Description

The purpose of this study was to determine the effect of complementary and conflicting haptic and visuo-haptic weight illusions on weight perception in virtual realty using scaled inertial forces and non-unity control-to-display ratio and, in parallel, investigate if using scaled inertial forces with a scaling factor of 0.5 had an effect on virtual weight perception. The experiment consisted of three parts, for each participant, that spanned three one-hour sessions over three days. The first part of the experiment was an open response exercise, followed by training trials, and then experiment trials. The open response portion of the experiment was done only on the

first day before the training trials so as not to influence participants' responses. The second and third day consisted only of training and experiment trials. The purpose of the open response exercise was to assess how participants interpreted the difference between two virtual blocks, one of which has a inertial scaling factor of 0.5.

A total of 10 participants (4 male and 6 female) between the ages of 24 and 28 participated in this experiment after giving informed consent. All participants were right hand dominant. The protocol was approved by the Stanford University Institutional Review Board.

4.3.1.1 Algorithms

We now present the two algorithms used to alter virtual weight perception in virtual reality when using skin deformation feedback devices. The first algorithm is scaled inertial forces. The second algorithm is non-unity control-to-display ratio.

Scaled Inertial Forces This experiment uses the same inertial scaling algorithm presented in Section 4.2.1.1.

Non-unity Control-to-display Ratio The implementation of a non-unity control-to-display ratio used for this experiment is based of the generalized approach for fingertip wearable tactile devices found in [14]. This method used the underlying physics framework, CHAI3D in this case, to calculate the interaction forces between the avatars of the user's fingers and the virtual block with a unity control-to-display ratio. The virtual block has an associated scaled visual avatar that is displayed to the user. Under unity control-to-display ratio, the scaled visual avatar's position coincides with the virtual blocks position. When the control-to-display ratio is not unity, the position of the visual avatar of the virtual block is described by:

$$\vec{p}_{os} = \vec{p}_{oi} + \frac{1}{r_{\text{C/D}}}(\vec{p}_{oc} - \vec{p}_{oi}) \tag{4.7}$$

where $\vec{p}_{os}$ is the position of the scaled visual avatar of the virtual block, $\vec{p}_{oi}$ is the initial position in the virtual environment when the scaling begins, $\vec{p}_{oc}$ is the current

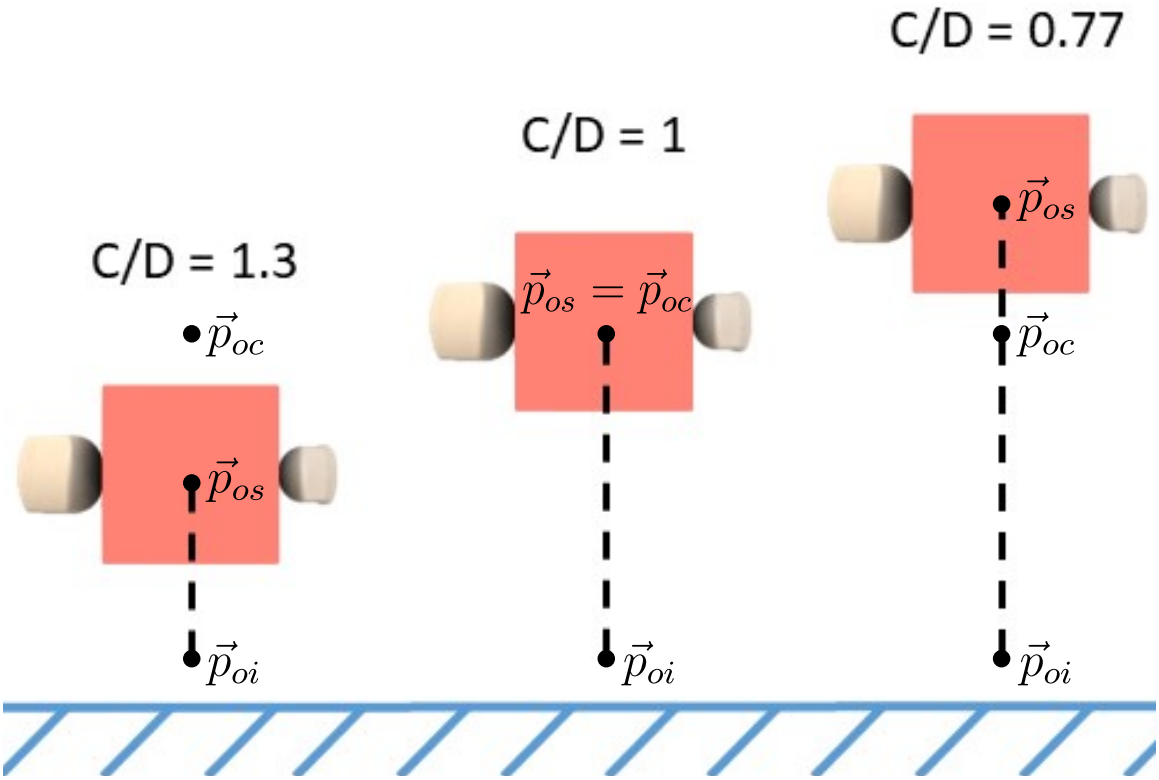

Figure 4.6: The control-to-display ratio, C/D, scales the displayed position of the virtual block when lifted by the user.Example positions of the virtual block for three control-to-display ratios are shown, for the same vertical movement by the user. In this diagram, $\vec{p}_{os}$ is the position of the scaled visual avatar of the virtual block, $\vec{p}_{oi}$ is the initial position in the virtual environment when the scaling begins, and $\vec{p}_{oc}$ is the current position of the virtual object.

position of the virtual object, and $r_{C/D}$ is the control-to-display ratio. A graphical example of the scaling can be seen in Fig. 4.6 with the points $\vec{p}_{os}$, $\vec{p}_{oc}$, and $\vec{p}_{oi}$ shown. This approach cannot be used without modification on the visual avatars of the user's virtual fingers.

The first modification necessary for implementation on the visual avatars of the virtual fingers is to only scale the visual avatars when the user is in contact with the virtual object. This allows the visual avatars to move in an unaltered motion in free space when not interacting with the virtual object. The second modification involves

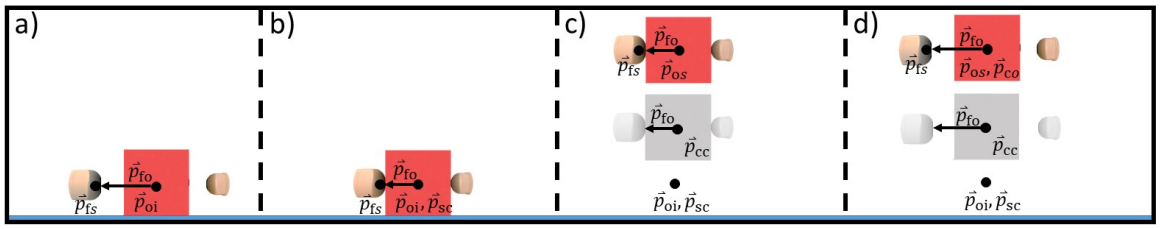

Figure 4.7: An example of the visual avatar scaling for the fingers during a grasping and lifting. (a) The user prepares to grasp the block located at $\vec{p}_{oi}$ with the visual avatars of the fingers at $\vec{p}_{fs}$, a distance of $\vec{p}_{fo}$ from $\vec{p}_{oi}$. (b) As the user makes contact with the virtual block, $\vec{p}_{sc}$, the center point between the two fingers, is set to $\vec{p}_{oi}$. (c) The gray block and fingers represent the unscaled position of the user and the virtual block, while the colored fingers and block represent the scaled visual avatars of the finger and block displayed to the user. As the block is lifted, the vertical position of the fingers is scaled by the C/D ratio, along with the block, while the horizontal distance between the visual avatar of the finger and the center point, $\vec{p}_{fo}$, is unscaled. (d) When the block is released, the clutch offset, $\vec{p}_{co}$, is calculated and used to maintain visual continuity of the visual avatar of the fingers.

preserving the distance between the two virtual fingers. If the above approach is naively applied to each visual avatar of the user's fingers, then the distance between the two fingers will change in an scaled manner that is unnatural for the user. To address this, a center point, placed between the two virtual fingers, was visually scaled while the distance between the center point and the visual avatars of the fingers is left unscaled to match the distance between virtual fingers in the underlying physical simulation. The scaled position of the visual avatars for the virtual fingers can be described as:

$$\vec{p}_{fs} = \vec{p}_{sc} + \vec{p}_{co} + \vec{p}_{fo} + \frac{1}{r_{\text{C/D}}}(\vec{p}_{cc} - \vec{p}_{sc}) \tag{4.8}$$

where $\vec{p}_{fs}$ is the position of the visual avatar, $\vec{p}_{sc}$ is the finger scaling center reference point set to the center point between the two virtual fingers when they make initial contact with the virtual object, $\vec{p}_{cc}$ is the current center point between the two fingers in physical space, $\vec{p}_{fo}$ is the distance between the center of the two fingers and individual finger of interest, and $\vec{p}_{co}$ is a clutch offset, set as the difference between

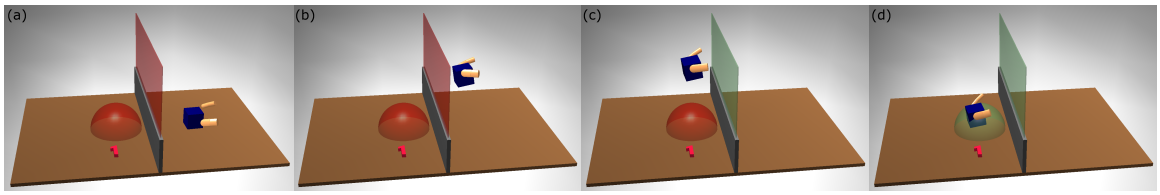

Figure 4.8: Participants were asked to grasp each virtual block (a), lift it up (b), pass it through a semi-transparent plane above a virtual wall(c), and then place the virtual block in a semi-transparent hemisphere on the other side of the virtual wall (d) to determining which block felt "heavier."

$\vec{p}_{fs}$ and $\vec{p}_{cc}$ when the fingers break contact with the virtual object.

With this implementation, the user only experiences scaled motion when interacting with the virtual block. The clutch offset, $\vec{p}_{co}$, is used to guarantee visual continuity after the virtual block is released by the user. Without this, the virtual avatar of the fingers would instantly return to the actual position of the user, possibly alerting them to the illusion taking place. To better compare results with [14], which restricted the lifting of the virtual block by participants to the vertical direction, we decided to only scale the vertical motion of the virtual fingers and block.

When changing the virtual environment to render the next block for the experiment trials, the clutch offset is reset to zero which can create a small visual discontinuity, manifesting as the instantaneous movement of the visual avatars of the virtual fingers. This happens when the virtual block is released at a point that is above the starting point of the grasp. The effect of this visual cue was minimized by introducing a short visual freeze of the simulation for 0.25 s before rendering the next virtual block.

4.3.1.2 Procedure

Throughout the experiment, all virtual blocks rendered were cubes with 50 mm sides and a stiffness of 175 N/m.

Each session began with an exploratory session for five minutes during which participantsv manipulated a single virtual block to familiarize themselves with the skin deformation devices. After this, for the first session only, participants took

part in the open response portion of the experiment. Two blocks were presented one at a time to the participant on the right side of a virtual table. The blocks were identified verbally as "Block 1" and "Block 2." Each block was rendered with a weight corresponding to 200 g on Earth. One block had a mass of 200 g, rendered with Earth's gravity, while the other block had a mass of 100 g, rendered with two times Earth's gravity, thus, rendered with an inertial scaling factor of 0.5.

Participants began by grasping the block presented to them, which appears on the right side of the virtual table, and lifting it up and through a red semi-transparent plane, centered above the virtual table. When the block passed through the plane, the color changed from red to green and participants then moved the block to a red semi-transparent hemisphere, 7.5 cm in diameter, located on the left side of the table. When the block entered the hemisphere, it changed color from red to green, signalling to participants they could release the block. This movement was repeated for each block presented to the participant. Fig. 4.8 shows the virtual table with the via points during an example grasp, lift, and placement. The experimenter switched between "Block 1" and "Block 2" after the completion of the grasp-lift-and-place task repeatedly for two minutes, verbally identifying each block as it was presented. At the end of the two minutes, participants were asked if they noticed "any differences" between the two blocks. The purpose of this portion of the experiment was to assess what effects scaling the inertial forces of the virtual block by a scaling factor less than 1 would have on the perception of the virtual block. The experimenters were careful not to bias participants to think about weight but instead gathered their first impressions on the differences between the two blocks. Each response was recorded and categorized into different physical properties by the experimenters.

After the open response portion of the experiment, the weight discrimination portion of the experiment during the first session consisted of one set of 16 training trials and one set of 50 experiment trials. The second and third sessions each consisted of one set of 16 training trials and two sets of 50 experiment trials. A two-alternative forced-choice paradigm was used for all training and experiment trials; each consisting of a reference block and a comparison block presented sequentially in random order. Participants were asked to determine which block "overall felt heavier" while

performing the same grasp-lift-and-place motion used during the open response with the restriction that each block can only be lifted once before making a decision. A unity inertial scaling factor and control-to-display ratio were used during the training trials, while the comparison blocks were scaled according to the haptic condition for the experiment trials. At the end of each trial, the answer was recorded, and, for training trials, participants were informed of the correct answer before the next sequential pair of blocks were presented.

All trials used a reference weight of 200 g. Comparison weights of 50, 125, 275, and 350 g were presented four times each during each set of training trials. Comparison weights of 50, 125, 200, 275, and 350 g were presented ten times each for each set of experiment trials. The complementary and conflicting weight illusions made up four haptic conditions which consisted of the combination of inertial scaling factors of 0.5 and 2 and control-to-display ratios of 0.77 and 1.3. A fifth haptic condition consisted of an inertial scaling factor of 0.5 with a unity control-to-display. The haptic conditions were presented to participants in an order based on Latin squares to minimize any effects of presentation order. Between each set of experiment trials, users were given a 5-minute break. The first session took approximately 45 minutes and the second and third sessions took approximately 60 minutes each.

4.3.2 Results

During the open response portion of the experiment, all 10 participants responded that they felt the virtual block with no inertial scaling "felt" heavier than the virtual block with an inertial scaling factor of 0.5.

Participants' answers for the training trials of the weight discrimination portion of the experiment were averaged across participants for each day and plotted in Fig. 4.9. The average accuracy during training for all participants across the three days was 81.7%. A one-way ANOVA was performed on the training accuracy data and showed no significant effect of the day on participants' accuracy during training ($F_{2,27} = 0.31, p = 0.74$).

The points of subjective equality (PSEs) and just noticeable differences (JNDs)

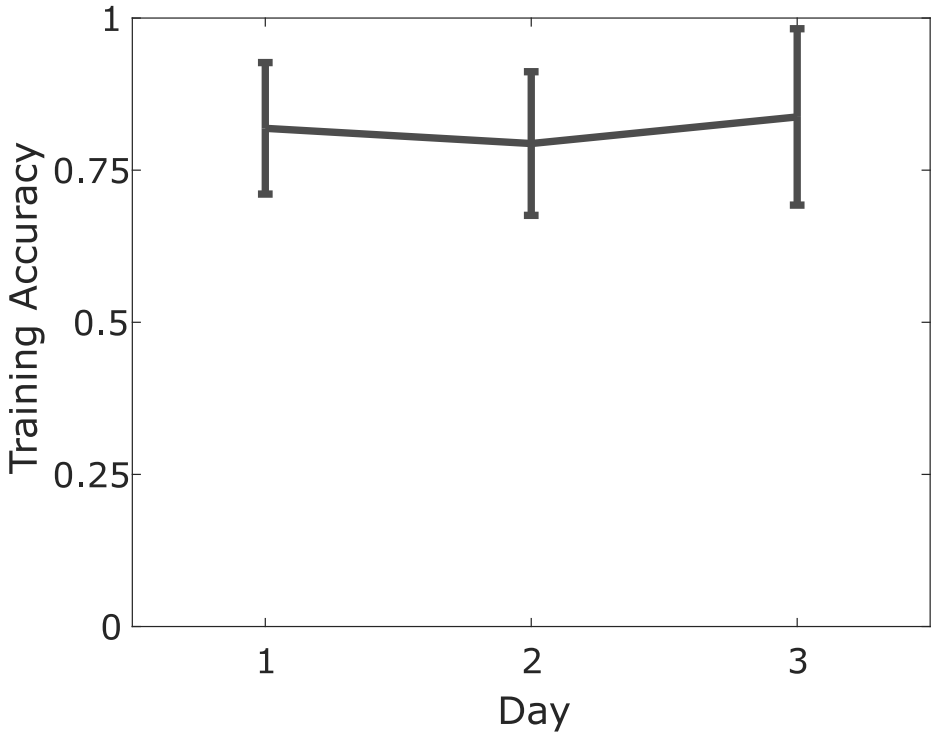

Figure 4.9: There was no significant change in participants' accuracy during the training trials across the three days (n=10). The error bars represent plus/minus one standard deviation.

were calculated from the responses during the experiment trials using a psychometric curve which was fit to each participant's proportion of "heavier" responses for each haptic condition using the sigmoid function:

$$y = \frac{1}{\left(1 + e^{\frac{-(x-\alpha)}{\beta}}\right)}, \tag{4.9}$$

where y is the proportion of "heavier" responses, x is the comparison weight, α is the PSE, and β is a slope fitting parameter. The values of α and β are determined from the fit of the sigmoid function. The JND is calculated by subtracting the PSE, α, from the comparison weight corresponding to the 0.75 proportion of "heavier" responses. Sample psychometric curves fit to a single participant's responses for each haptic condition can be seen in Fig. 4.10.

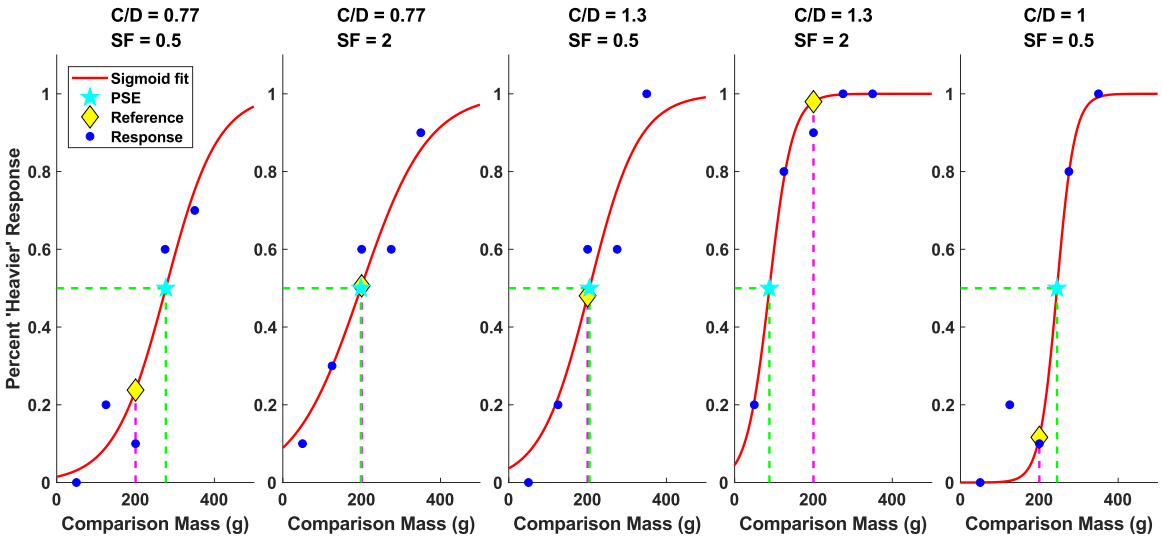

Figure 4.10: Sample psychometric curves from one participant for each of the five haptic conditions. The psychometric curves were fit to the participant's responses and used to calculate the PSE and JND for each haptic condition.

The resulting PSEs and JNDs for each condition were averaged across participants and are plotted in Fig. 4.11 and Fig. 4.12 with error bars representing plus/minus one standard deviation. The PSE and JND for an inertial scaling factor of 0.5 with unity C/D ratio were 231.2 g and 55.3 g. The PSEs for the complementary set of conditions (SF = 0.5 with C/D = 0.77 and SF = 2 with C/D = 1.3) were 254.6 g and 95.0 g, respectively. The PSEs for the conflicting set of conditions (SF = 0.5 with C/D = 1.3 and SF = 2 with C/D = 0.77) were 140.8 g and 207.1 g, respectively. The JNDs for the complementary set of conditions (SF = 0.5 with C/D = 0.77 and SF = 2 with C/D = 1.3) were 68.5 g and 46.2 g, respectively. The JNDs for the conflicting set of conditions (SF = 0.5 with C/D = 1.3 and SF = 2 with C/D = 0.77) were 108.6 g and 68.3 g, respectively.

A t-test was performed to determine if there was any significant difference between the PSEs for each haptic condition and the reference weight. The results showed the PSE for a scaling factor of 0.5 with unity C/D was significantly different than the reference weight. Both complementary sets and one conflicting set of weight illusions (SF = 0.5 with C/D = 1.3) had a PSE that was significantly different than the

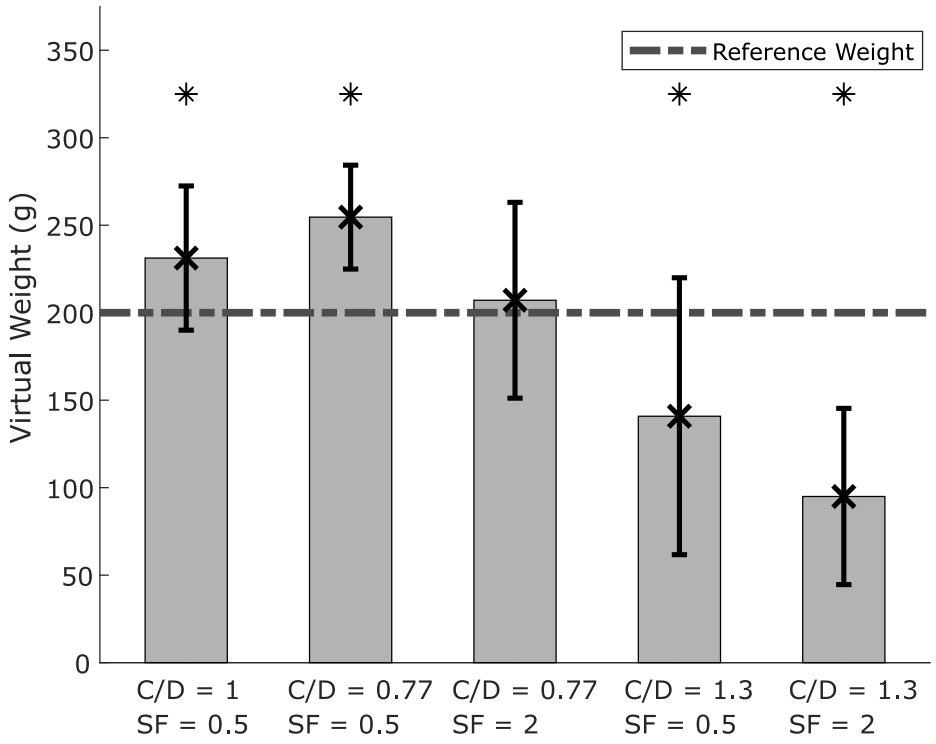

Figure 4.11: The mean PSEs for each haptic condition averaged across all participants (n = 10) with the error bars represent plus/minus one standard deviation. Each haptic condition tested, except for SF = 2 with C/D = 0.77, had a PSE significantly different from the reference weight (p-value <0.05), which is denoted by the *'s.

reference weight.

The weight shift for each haptic condition was calculated by subtracting the corresponding PSE from the reference weight. The resulting weight shifts from this experiment are plotted in Fig 4.13 with the previously reported weight shifts of C/D values of 0.77 and 1.3 from [14] and an SF of 2 from Section 4.2. Also plotted are the predicted weight shifts, which are calculated using the sum of the measured weight shifts from the individual weight illusions.

We fit a generalized linear mixed-effects model (GLME) to the measured PSEs using the inertial scaling factor, control-to-display ratio, and the interaction between the inertial scaling factor and control-to-display ratio as fixed effects with subject as a random effect. A similar GLME was fit to the measured JNDs of each haptic

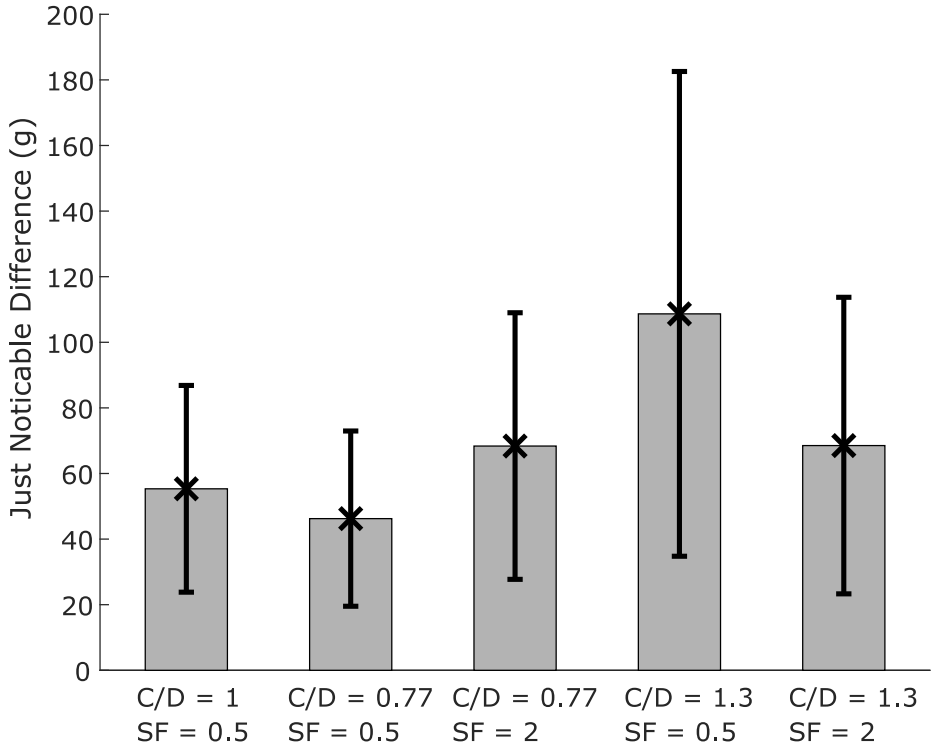

Figure 4.12: The mean JNDs averaged across all participants (n = 10) for each haptic condition plotted with error bars representing plus/minus one standard deviation.

condition. For both models, the fit was computed using C/D-1 and SF-1, so the intercept represents the reference weight and JND when C/D and SF are both 1. The results from each fit can be seen in Table 4.2.

4.3.3 Discussion

The results of the one-way ANOVA suggest there was no significant learning effect day to day for the participants. This result combined with the Latin squares ordering gives confidence to the measurements obtained for the effect of each haptic condition.

The results from both the open-response paradigm portion of the experiment and the two-alternative forced choice paradigm portion show that scaling inertial forces using a scaling factor of 0.5 can make a virtual object was perceived as lighter when

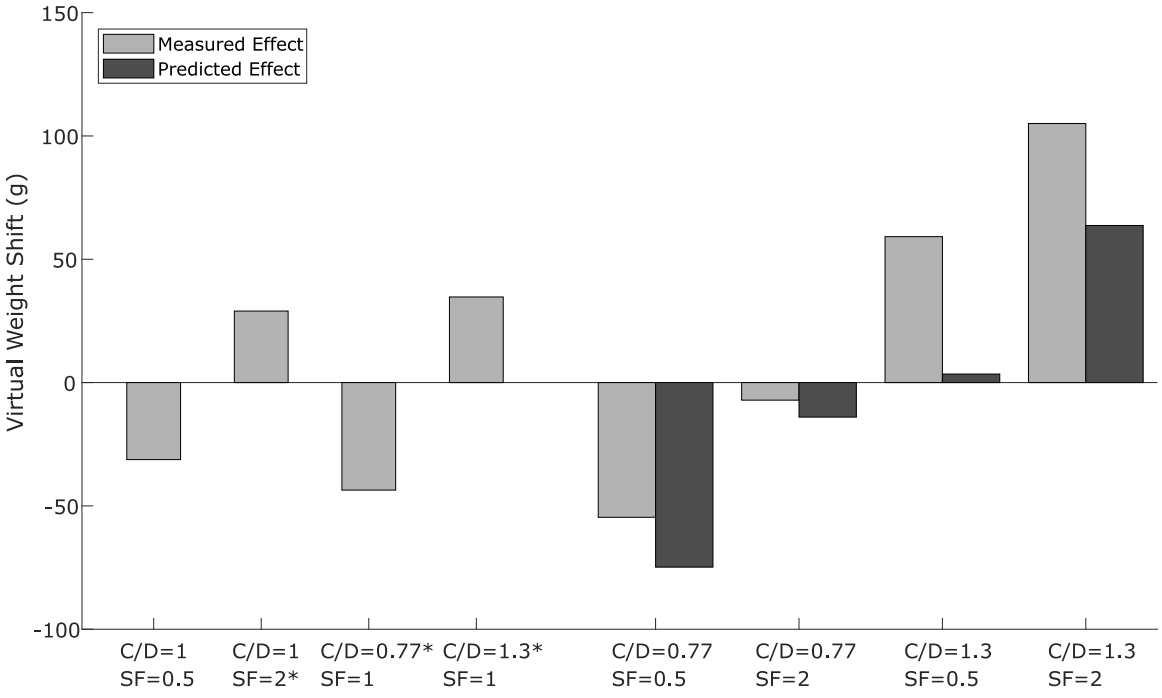

Figure 4.13: The shift in perceived virtual weight due to scaled inertial forces and non-unity control-to-display ratio compared to the predicted and measured shifts in perceived weight due to the complementary and conflicting combination of scaled inertial forces and non-unity control-to-display ratio. The *'s denote values reported in [14] and the ** denotes values reported in [15].

using skin deformation haptic devices. Furthermore, when combining the use of scaled inertial forces with a non-unity control-to-display ratio in a complementary manner to increase the perceived virtual weight, the measured weight shift, 105 g, is larger than the expected weight shift calculated as a sum of the individual effects, 63.7 g. When combining the two weight illusions to decrease the perceived virtual weight, the magnitude of the measured weight shift, 54.6 g, is smaller than the sum of the individual effects, 74.8 g. But, the overall range of shifted weights measured, 159.6 g, is greater than the expected range based on the sum of the individual effects, 138 g. This suggests that the effects can be used together to further increase the range of virtual weights that can be conveyed to a user. In a practical sense, only increasing the perceived weight would be of use for most applications as the haptic devices can

Table 4.2: Summary of generalized linear mixed effect model

PSE				
Variable	Coefficient (g)	t-stat	df	p-value
Intercept	195.5	26.18	46	2.8e-29
SF	-37.0	-3.68	46	6.2e-4
C/D	-216.5	-6.64	46	3.2e-8
SF:C/D	4.9	0.05	46	0.91
JND				
Variable	Coefficient (g)	t-stat	df	p-value
Intercept	67.6	7.9	46	4.9e-10
SF	0.8	0.1	46	0.92
C/D	80.6	3.2	46	2.3e-3
SF:C/D	-80.3	-2.5	46	0.01

already convey a range of virtual virtual weights and could only increase the range of virtual weights that can be conveyed by increasing the maximum virtual weight that can be conveyed. The magnitude of the effect of each weight illusion on their own, as well as when in complementary manners, is far greater than reported values for the weight shift when using a non-unity control-to-display ratio in [56]. This could be because the reported values in [56] are when using a kinesthetic haptic device where as the values reported from this study and [14] are when using a wearable skin deformation haptic device.

When rendering SF = 0.5 with C/D = 1.3, we see a significant shift in virtual weight perception, showing that the object is perceived as heavier. This, by itself, would suggest that the vision-based illusion dominates the effect on perceived weight. However, when the opposite conflicting pair of illusions is rendered, SF = 2 and C/D = 0.77, there is no significant change in perceived weight. This suggests the individual effects on weight perception cancel out. The results of the GLME analysis of the PSEs for all five haptic conditions show there is no significant interaction effect between scaled inertial forces and a non-unity control-to-display ratio. The large JND (108.7 g) for the conflicting haptic condition SF = 0.5 and C/D = 1.3 is the only haptic condition with a JND greater than the 75 g difference in comparison weight levels from the experiment. Another potential reason for this disparity in the conflicting

combination of illusions could be the discrepancy between the haptic rendering and the visual rendering resulted in reaching the "uncanny valley of haptics" [57]. Berger et al. [57] suggest the integration of these conflicting cues could lead to a reduced subjective experience which, in turn, could affect the user's perception.

There also could be a separate underlying interaction effect between inertial scaling factors below 1 and control-to-display ratios above 1 that resulted in the magnitude of the combined effect in this experiment to be greater than the effect of a control-to-display ratio of 1.3, but it would require measuring the perceived weight shift for more conflicting combinations.

The results of the GLME analysis on JND combined with Fig. 4.12 show that when the two weight illusions are in conflict or in complement to increase the perceived weight, the JND increases.

This work could be furthered by measuring the effects using scaled rotational inertia, implemented in virtual reality using the same principal found in [29], and rotational non-unity control-to-display ratio, like that shown in [30], in complementary and conflicting manners.

Its worth noting that when trying to decrease the perceived weight of an object, there is an inherent "floor" to the effect due to an object not being able to have negative weight. Thus the magnitude of the effect will have a dependence on the reference weight chosen for the experiment. This limitation does not exist when trying to increase the perceived weight of a virtual object. However, there are different limitations for both scaled inertial forces and non-unity control-to-display ratio when trying to increase perceived weight. The limitation for scaling inertial forces come from the skin deformation haptic device's force output. Just like virtual weight rendered when using the devices can saturate the motor output, so too can scaling the inertial forces of a virtual object, albeit at a much larger perceived virtual weight. Altering the control-to-display ratio to increase perceived virtual weight also has an upper limit that occurs when the effect becomes noticeable to the user and can even hinder their ability to manipulate a virtual object in a desired manner.

4.4 Conclusion

In this chapter, we first performed an experiment to show that scaling inertial forces in a virtual environment can alter the weight perception of virtual objects while using skin deformation feedback. Participants were asked to discriminate weight during a grasp-lift-and-place task. An open response exercise showed that scaling inertial forces of a virtual block has a noticeable effect on perceived weight. From a series of two-alternative forced-choice paradigm trials using a reference weight of 200 g, we calculated PSEs of weight for inertial scaling factors of 2 and 3. We showed that scaling the inertial forces by factors of 2 and 3 has a significant effect on the weight perception of a virtual block.

We then performed an experiment to show that scaling inertial forces can be used to decrease the perceived weight of a virtual object when using skin deformation haptic devices and to measure the change in perceived weight from the combination of scaled inertial forces and non-unity control-to-display ratio in complementary and conflicting manners. Participants indicated during the open response paradigm portion of the experiment that a block with a inertial scaling factor of 0.5 felt lighter than the reference block of equal weight. Participants then took part in the weight discrimination portion of the experiment in which they performed a grasp-lift-and-place task before discriminating between two blocks. The responses from this two-alternative forced-choice paradigm were used to calculate the PSEs and JNDs for five haptic conditions.

The results show that an inertial scaling factor of 0.5 with unity control-to-display ratio does significantly decrease the perceived weight of a virtual block. Furthermore, the combination of scaled inertial forces and non-unity control-to-display ratio increase the perceived weight more than the sum of the individual effects when both the inertial scaling factor and control-to-display ratio are greater than one. Conversely, the combination of scaled inertial forces and non-unity control-to-display ratio does not decrease the perceived weight of the virtual block as much as the sum of the individual effects when both the inertial scaling factor and control-to-display ratio are less than one.

The combination of scaled inertial forces and a non-unity control-to-display ratio in a conflicting manner had a similar effect as the sum of the individual effects for one of the combinations but not the other.

Chapter 5

Conclusion

This thesis has examined the role of skin deformation haptic feedback in virtual reality perception. This chapter summarizes the results laid out in the previous chapters, reviews the contributions of this thesis, and expounds on ideas for future work.

5.1 Summary of Results

The main results from this thesis form a better understanding of skin deformation feedback's role in virtual reality perception. We first measured the relative contribution of skin deformation and kinesthetic forces in forming weight percepts during a grasp-and-lift task when using a set of mechanical thimbles that amplified the amount of shear force on the fingerpad relative to the kinesthetic force experienced during the interaction and found that weight perception is dominated by kinesthetic forces. We then augmented an existing wearable skin deformation feedback device with a vibrotactile actuator to augment or replace the normal-to-the-fingerpad degree of freedom of skin deformation feedback. We found that shear-only skin deformation feedback with a vibrotactile contact cue can be considered an alternative feedback modality to shear-plus-normal skin deformation feedback. Lastly, we developed a haptic weight illusion which scales the inertial forces experienced when interacting with a virtual object. We combined it with a visuo-haptic weight illusion, non-unity control-to-display ratio, and showed we could further alter the perceived weight of

virtual objects. These results give insight into the role of skin deformation feedback in virtual reality perception.

The major contributions of this dissertation are summarized as follows:

- *Designed mechanical thimbles that amplify the amount of skin deformation when picking up real-world objects and measured, through human participant experiments, the relative contributions of skin deformation and kinesthetic forces for object weight perception.* In Chapter 2, a set of mechanical thimbles was developed to increase the shear skin deformation forces felt when lifting a real world object using a simple gear train. We demonstrated, through a human participant experiment, an increase in perceived weight for various gear ratios during a grasp-and-lift task. From these results, we calculated the relative contributions of kinesthetic and skin deformation forces in weight perception, showing that weight perception is dominated by kinesthetic forces.

- *Integration and validation of contact-event based haptics with a wearable skin deformation haptic device.* In Chapter 3, we integrated a piezoelectric actuator with an existing three degree-of-freedom skin deformation device for additional vibrotactile feedback for testing combinations of three-degree-of-freedom, two-degree-of-freedom shear-only, and no skin deformation feedback with either an impulse-based or decaying sinusoid contact cue. We demonstrated, through human participant experiments, that augmenting three translational degrees of freedom of skin deformation feedback on the fingerpad with a contact-event based cue did not improve task performance of a grasp-lift-and-place task of a "fragile" virtual object. We also showed that adding a high frequency vibrotactile contact cue to two shear degrees of freedom of skin deformation feedback improved task performance and could serve as an alternative to three-degree-of-freedom skin deformation feedback.

- *Implemented haptic illusions to alter virtual weight perception during a grasp-lift-and-place task.* In Chapter 4, we developed an inertial scaling haptic weight illusion which leveraged an existing physics framework for virtual reality environments to alter a user's virtual weight perception. We demonstrated and

measured, through human participant experiments, the change in perceived virtual weight when using the inertial scaling method with wearable skin deformation haptic feedback devices, increasing the range of perceivable virtual weight that can be rendered. We also demonstrated and measured, through human participant experiments, the change in virtual weight perception when combining two haptic and visuo-haptic weight illusions methods, scaled inertial forces and non-unity control-to-display ratio, in complementary and conflicting manners, further increasing the range of perceivable weights that can be rendered.

5.2 Future Work

5.2.1 Rotational (Twisting) Skin Deformation

While adding complexity to existing skin deformation devices is not desirable because it often adds to the device cost and weight, it may prove useful when it comes to providing a rotational (twisting) degree of freedom to skin deformation feedback, shown in Fig. 5.1. When interacting with virtual objects with wearable haptic devices that use the fundamental god-object [58] or proxy-based algorithm [59] for computing forces, the interaction between the haptic device and virtual object is often treated as a singular point. Thus, if grasping a virtual object using, for instance, the thumb and index finger at points that do not form a line intersecting the center of mass, the virtual object will rotate upon liftoff. Visually, this rotation prompts a user to grasp the virtual object with more force, as in the real world, this rotation could indicate that the object is about to slip from the user's grasp, which often is not the case in the virtual environment.

Many fingertip wearable haptic devices use a parallel mechanism to apply forces to the user's fingerpad. Following this trend, a rotational (twisting) degree of freedom could be added using one of the parallel mechanisms found in [60]. Combining this new device with more advanced contact interaction algorithms, such as the one presented in [61], which uses a god-finger method to emulate the presence of a contact area

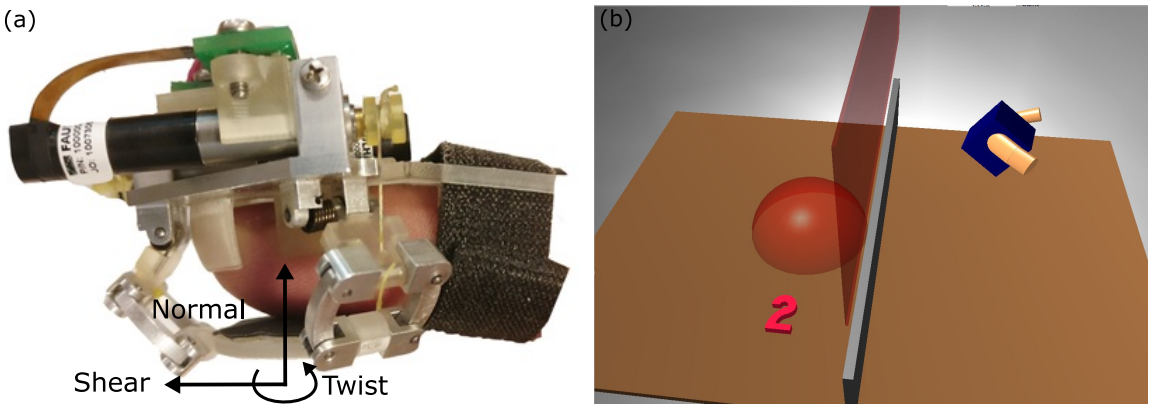

Figure 5.1: (a) Future development of wearable skin deformation devices could investigate adding a rotational (twisting) degree of freedom. (b) Common single-point contact rendering methods lead to virtual objects twisting when grasped and lifted.

between the user's proxy and the virtual object, or implementing a different friction model, such as the one presented in [62], can lead to new haptic experiences for users. Adding this twisting degree of freedom to existing three-degree-of-freedom capable devices will increase their mechanical complexity; thus motivating the need for designing and fabricating new lightweight mechanisms. One possible existing solution is to use layer-by-layer manufacturing techniques used in origami-inspired robots to create these new mechanisms [63]. An example of a four-degree-of freedom parallel mechanism fabricated with layer-by-layer manufacturing can be seen in Fig. 5.2.

Such a device could allow us to measure the effect of rotational inertia on virtual weight perception as an extension of the work found in [29]. We could then implement a similar rotational non-unity control-to-display ratio, like that found in [30], and measure the effects of each on virtual weight perception separately as well as in complementary and conflicting manners.

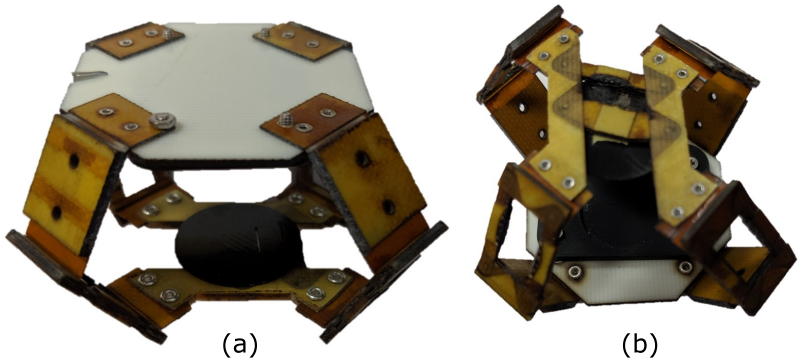

Figure 5.2: (a) Top and (b) side view of a four-degree-of-freedom mechanism made with layer-by-layer manufacturing to achieve three translational degrees of freedom and one twisting degree of freedom.

5.2.2 User-grounded Kinesthetic Feedback Integration

An important limitation of wearable skin deformation feedback devices is the force saturation that most often occurs when users penetrate too deep into a virtual surface, often in the normal to the fingerpad direction shown in Fig. 5.1. Many of these devices use a parallel mechanism to apply forces to the user's fingerpad; therefore, saturation in the normal-to-the-fingerpad direction limits the amount of shear forces that can be displayed simultaneously and causes a potentially uncomfortable pinching between the user's fingernail and fingerpad. One solution to this problem is to uncouple the normal-to-the-fingerpad degree of freedom from the shear degrees of freedom. This solves the problem of limited shear force when rendering max normal-to-the-fingerpad force but it does not eliminate the pinching sensation. For that, a user-ground kinesthetic force feedback component, as shown in Fig. 5.3, could be integrated with a shear-only skin deformation feedback device to apply the normal-to-the-fingerpad direction interaction forces on the fingerpad. This kinesthetic component could be added in multiple ways such as the cable/tendon system described in [64] or a finger-to-finger display, such as the one shown in [65].

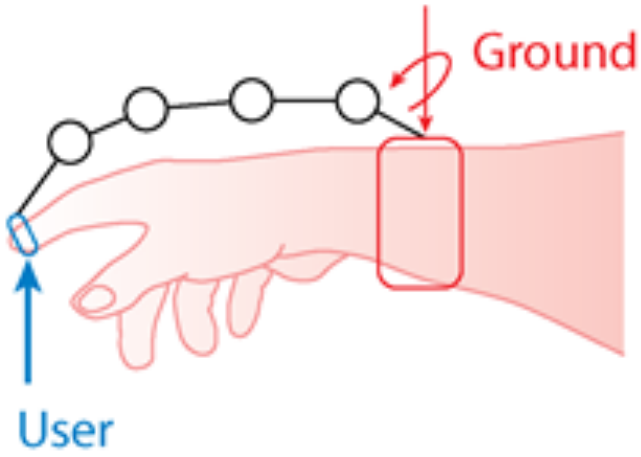

Figure 5.3: Preventing unrealistic virtual object penetration in the normal-to-the-fingerpad direction could be achieved by adding a user-grounded, kinesthetic force feedback component. Adapted from [1] © 2013 IEEE.

5.2.3 Device Weight

When designing fingertip wearable devices, we often think of minimizing device weight as a major design objective. This goal influences the choice of motors and gearboxes, and thus directly affects the maximum force capabilities of the device. While it is clear that users would likely prefer lighter devices based on comfort, there is little work done on understanding the effect of a wearable device's weight on virtual weight perception. We naturally integrate kinesthetic and tactile force information to form a weight percept, as shown in Chapter 2, but how does a constant kinesthetic force, i.e. the device weight, affect the ability to distinguish between the weight of virtual objects? This effect could be measured by attaching weights to an existing wearable skin deformation feedback device and measuring the just noticeable difference of virtual weight during a grasp-and-lift task. If it is shown to have little effect, it could give designers less of a restriction on motor selection, thus increasing the potential maximum force that can be rendered.

Bibliography

[1] D. Prattichizzo, F. Chinello, C. Pacchierotti, and M. Malvezzi, "Towards wearability in fingertip haptics: A 3-dof wearable device for cutaneous force feedback," *IEEE Transactions on Haptics*, vol. 6, no. 4, pp. 506–516, 2013.

[2] A. Charpentier, "Analyse experimentale de quelques elements de la sensation de poids," *Archives de Physiologie Normale et Pathologique*, vol. 3, pp. 122–135, 1891.

[3] H. K. Wolfe, "Some effects of size on judgments of weight," *Psychological Review*, vol. 5, pp. 25–54, 1898.

[4] G. Buckingham, N. S. Ranger, and M. A. Goodale, "The material–weight illusion induced by expectations alone," *Attention, Perception, & Psychophysics*, vol. 73, no. 1, pp. 36–41, 2011.

[5] J. R. Flanagan, A. M. Wing, S. Allison, and A. Spenceley, "Effects of surface texture on weight perception when lifting objects with a precision grip," *Perception & Psychophysics*, vol. 57, no. 3, pp. 282–290, 1995.

[6] G. Rinkenauer, S. Mattes, and R. Ulrich, "The surface—weight illusion: On the contribution of grip force to perceived heaviness," *Perception & Psychophysics*, vol. 61, no. 1, pp. 23–30, 1999.

[7] P. Walker, B. J. Francis, and L. Walker, "The brightness-weight illusion," *Experimental Psychology*, vol. 57, no. 6, pp. 462–469, 2010.

[8] Z. F. Quek, S. B. Schorr, I. Nisky, A. M. Okamura, and W. R. Provancher, "Augmentation of stiffness perception with a 1-degree-of-freedom skin stretch device," *IEEE Transactions on Human-Machine Systems*, vol. 44, no. 6, pp. 731–742, 2014.

[9] Z. F. Quek, S. B. Schorr, I. Nisky, W. R. Provancher, and A. M. Okamura, "Sensory substitution and augmentation using 3-degree-of-freedom skin deformation feedback," *IEEE Transactions on Haptics*, vol. 8, no. 2, pp. 209–221, 2015.

[10] K. Minamizawa, D. Prattichizzo, and S. Tachi, "Simplified design of haptic display by extending one-point kinesthetic feedback to multipoint tactile feedback," in *IEEE Haptics Symposium*, 2010, pp. 257–260.

[11] D. Tsetserukou, S. Hosokawa, and K. Terashima, "Linktouch: A wearable haptic device with five-bar linkage mechanism for presentation of two-dof force feedback at the fingerpad," in *IEEE Haptics Symposium*, 2014, pp. 307–312.

[12] M. Solazzi, A. Frisoli, and M. Bergamasco, "Design of a cutaneous fingertip display for improving haptic exploration of virtual objects," in *International Symposium in Robot and Human Interactive Communication*, 2010, pp. 1–6.

[13] D. Leonardis, M. Solazzi, I. Bortone, and A. Frisoli, "A 3-RSR haptic wearable device for rendering fingertip contact forces," *IEEE Transactions on Haptics*, vol. 10, no. 3, pp. 305–316, 2017.

[14] S. B. Schorr, "Fingerpad skin deformation for sensory substitution of force in teleoperation and virtual reality," Ph.D. dissertation, Mechanical Engineering Department, Stanford University, May 2017.

[15] J. M. Suchoski, S. Martínez, and A. M. Okamura, "Scaling inertial forces to alter weight perception in virtual reality," *2018 IEEE International Conference on Robotics and Automation*, pp. 484–489, 2018.

[16] I. Hwang, H. Son, and J. R. Kim, "Airpiano: Enhancing music playing experience in virtual reality with mid-air haptic feedback," in *IEEE World Haptics Conference*, 2017, pp. 213–218.

[17] R. J. Adams, D. Klowden, and B. Hannaford, "Virtual training for a manual assembly task," *Haptics-e*, 2001. [Online]. Available: http://hdl.handle.net/1773/34884

[18] O. A. J. van der Meijden and M. P. Schijven, "The value of haptic feedback in conventional and robot-assisted minimal invasive surgery and virtual reality training: a current review," *Surgical Endoscopy*, vol. 23, no. 6, pp. 1180–1190, Jun 2009.

[19] P. Lamata, E. J. Gómez, F. M. Sánchez-Margallo, F. Lamata, F. del Pozo, and J. Usón, "Tissue consistency perception in laparoscopy to define the level of fidelity in virtual reality simulation," *Surgical Endoscopy and Other Interventional Techniques*, vol. 20, no. 9, pp. 1368–1375, 2006.

[20] D. M. Vo, J. M. Vance, and M. G. Marasinghe, "Assessment of haptics-based interaction for assembly tasks in virtual reality," in *World Haptics 2009 - Third Joint EuroHaptics conference and Symposium on Haptic Interfaces for Virtual Environment and Teleoperator Systems*, 2009, pp. 494–499.

[21] B. T. Gleeson, S. K. Horschel, and W. R. Provancher, "Perception of direction for applied tangential skin displacement: Effects of speed, displacement, and repetition," *IEEE Transactions on Haptics*, vol. 3, no. 3, pp. 177–188, 2010.

[22] K. Drewing, M. Fritschi, R. Zopf, M. O. Ernst, and M. Buss, "First evaluation of a novel tactile display exerting shear force via lateral displacement," *ACM Transactions on Applied Perception*, vol. 2, no. 2, pp. 118–131, 2005.

[23] S. J. Lederman and R. L. Klatzky, "Haptic classification of common objects: Knowledge-driven exploration," *Cognitive Psychology*, vol. 22, no. 4, pp. 421 – 459, 1990.

[24] R. S. Johansson and K. J. Cole, "Sensory-motor coordination during grasping and manipulative actions," *Current Opinion in Neurobiology*, vol. 2, no. 6, pp. 815–823, 1992.

[25] A. D. Waller, "The sense of effort: An objective study 1," *Brain*, vol. 14, no. 2–3, pp. 179–249, 1891.

[26] J. J. Gibson, "The senses considered as perceptual systems." 1966.

[27] M. Turvey, K. Shockley, and C. Carello, "Affordance, proper function, and the physical basis of perceived heaviness," *Cognition*, vol. 73, no. 2, pp. B17 – B26, 1999.

[28] C. Carello, K. Shockley, S. Harrison, M. Richardson, and M. Turvey, "Heaviness perception depends on movement," *Studies in Perception and Action, VII*, pp. 87–90, 2003.

[29] E. L. Amazeen and M. T. Turvey, "Weight perception and the haptic size–weight illusion are functions of the inertia tensor." *Journal of Experimental Psychology: Human Perception and Performance*, vol. 22, no. 1, p. 213, 1996.

[30] M. Streit, K. Shockley, M. A. Riley, and A. W. Morris, "Rotational kinematics influence multimodal perception of heaviness," *Psychonomic Bulletin & Review*, vol. 14, no. 2, pp. 363–367, 2007.

[31] L. Dominjon, A. Lecuyer, J. . Burkhardt, P. Richard, and S. Richir, "Influence of control/display ratio on the perception of mass of manipulated objects in virtual environments," in *IEEE Virtual Reality*, 2005, pp. 19–25.

[32] J. R. Flanagan and M. A. Beltzner, "Independence of perceptual and sensorimotor predictions in the size–weight illusion," *Nature Neuroscience*, vol. 3, no. 7, p. 737, 2000.

[33] M. C. Payne, Jr., "Apparent weight as a function of hue." *The American Journal of Psychology*, vol. 71, no. 3, pp. 104–105, 1961.

[34] M. C. Payne, "Apparent weight as a function of color," *The American Journal of Psychology*, vol. 71, no. 4, pp. 725–730, 1958.

[35] T. H. Massie and J. K. Salisbury, "The PHANTOM haptic interface: A device for probing virtual objects," in *Proceedings of the ASME Winter Annual Meeting, Symposium on Haptic Interfaces for Virtual Environment and Teleoperator Systems*, vol. 55, no. 1, 1994, pp. 295–300.

[36] K. O. Johnson, "The roles and functions of cutaneous mechanoreceptors," *Current Opinion in Neurobiology*, vol. 11, no. 4, pp. 455–461, 2001.

[37] I. Birznieks, P. Jenmalm, A. W. Goodwin, and R. S. Johansson, "Encoding of direction of fingertip forces by human tactile afferents," *Journal of Neuroscience*, vol. 21, no. 20, pp. 8222–8237, 2001.

[38] K. J. Kuchenbecker, J. Fiene, and G. Niemeyer, "Improving contact realism through event-based haptic feedback," *IEEE Transactions on Visualization and Computer Graphics*, vol. 12, no. 2, pp. 219–230, 2006.

[39] W. McMahan, J. Gewirtz, D. Standish, P. Martin, J. A. Kunkel, M. Lilavois, A. Wedmid, D. I. Lee, and K. J. Kuchenbecker, "Tool contact acceleration feedback for telerobotic surgery," *IEEE Transactions on Haptics*, vol. 4, no. 3, pp. 210–220, 2011.

[40] R. E. Schoonmaker and C. G. L. Cao, "Vibrotactile force feedback system for minimally invasive surgical procedures," in *IEEE International Conference on Systems, Man and Cybernetics*, 2006, pp. 2464–2469.

[41] W. R. Provancher and N. D. Sylvester, "Fingerpad skin stretch increases the perception of virtual friction," *IEEE Transactions on Haptics*, vol. 2, no. 4, pp. 212–223, 2009.

[42] K. Minamizawa, K. Tojo, H. Kajimoto, N. Kawakami, and S. Tachi, "Haptic interface for middle phalanx using dual motors," in *Proc. EuroHaptics International Conference*, 2006, pp. 235–240.

[43] M. Bianchi, E. Battaglia, M. Poggiani, S. Ciotti, and A. Bicchi, "A wearable fabric-based display for haptic multi-cue delivery," in *IEEE Haptics Symposium*, 2016, pp. 277–283.

[44] M. Gabardi, M. Solazzi, D. Leonardis, and A. Frisoli, "A new wearable fingertip haptic interface for the rendering of virtual shapes and surface features," in *IEEE Haptics Symposium*, 2016, pp. 140–146.

[45] C. Pacchierotti, D. Prattichizzo, and K. J. Kuchenbecker, "Displaying sensed tactile cues with a fingertip haptic device," *IEEE Transactions on Haptics*, vol. 8, no. 4, pp. 384–396, 2015.

[46] F. Chinello, M. Malvezzi, C. Pacchierotti, and D. Prattichizzo, "Design and development of a 3-RRS wearable fingertip cutaneous device," in *IEEE International Conference on Advanced Intelligent Mechatronics*, 2015, pp. 293–298.

[47] S. B. Schorr and A. M. Okamura, "Three-dimensional skin deformation as force substitution: Wearable device design and performance during haptic exploration of virtual environments," *IEEE Transactions on Haptics*, vol. 10, no. 3, pp. 418–430, 2017.

[48] A. Parness, D. Soto, N. Esparza, N. Gravish, M. Wilkinson, K. Autumn, and M. Cutkosky, "A microfabricated wedge-shaped adhesive array displaying gecko-like dynamic adhesion, directionality and long lifetime," *Journal of the Royal Society Interface*, vol. 6, no. 41, pp. 1223–1232, 2009.

[49] J. M. Suchoski, M. Di Luca, R. King, S. Keller, and A. M. Okamura, "Effects of amplified skin deformation forces onweight perception during a grasp-and-lift task," Under Review.

[50] X. A. Wu, S. A. Suresh, H. Jiang, J. V. Ulmen, E. W. Hawkes, D. L. Christensen, and M. R. Cutkosky, "Tactile sensing for gecko-inspired adhesion," in *IEEE/RSJ International Conference on Intelligent Robots and Systems*, 2015, pp. 1501–1507.

[51] A. M. Okamura, J. T. Dennerlein, and R. D. Howe, "Vibration feedback models for virtual environments," in *IEEE International Conference on Robotics and Automation*, 1998, pp. 674–679.

[52] A. M. Okamura, M. R. Cutkosky, and J. T. Dennerlein, "Reality-based models for vibration feedback in virtual environments," *IEEE/ASME Transactions on Mechatronics*, vol. 6, no. 3, pp. 245–252, 2001.

[53] J. D. Hwang, M. D. Williams, and G. Niemeyer, "Toward event-based haptics: Rendering contact using open-loop force pulses," in *International Symposium on Haptic Interfaces for Virtual Environment and Teleoperator Systems.*, 2004, pp. 24–31.

[54] F. Conti, F. Barbagli, D. Morris, and C. Sewell, "CHAI3D: an open-source library for the rapid development of haptic scenes," *IEEE World Haptics Conference*, pp. 21–29, 2005.

[55] N. Nakazawa, R. Ikeura, and H. Inooka, "Characteristics of human fingertips in the shearing direction," *Biological Cybernetics*, vol. 82, no. 3, pp. 207–214, 2000.

[56] M. Samad, E. Gatti, A. Hermes, H. Benko, and C. Parise, "Pseudo-haptic weight: Changing the perceived weight of virtual objects by manipulating control-display ratio," in *Proceedings of the 2019 CHI Conference on Human Factors in Computing Systems*. ACM, 2019, p. 320.

[57] C. C. Berger, M. Gonzalez-Franco, E. Ofek, and K. Hinckley, "The uncanny valley of haptics," *Science Robotics*, vol. 3, no. 17, 2018. [Online]. Available: https://robotics.sciencemag.org/content/3/17/eaar7010

[58] C. B. Zilles and J. K. Salisbury, "A constraint-based god-object method for haptic display," in *IEEE/RSJ International Conference on Intelligent Robots and Systems*, vol. 3, 1995, pp. 146–151.

[59] D. C. Ruspini, K. Kolarov, and O. Khatib, "The haptic display of complex graphical environments," in *SIGGRAPH*, vol. 97, 1997, pp. 345–352.

[60] F. Pierrot, V. Nabat, O. Company, S. Krut, and P. Poignet, "Optimal design of a 4-dof parallel manipulator: From academia to industry," *IEEE Transactions on Robotics*, vol. 25, no. 2, pp. 213–224, 2009.

[61] A. Talvas, M. Marchal, and A. Lécuyer, "The god-finger method for improving 3d interaction with virtual objects through simulation of contact area," in *2013 IEEE Symposium on 3D User Interfaces*, 2013, pp. 111–114.

[62] R. D. Howe and M. R. Cutkosky, "Practical force-motion models for sliding manipulation," *The International Journal of Robotics Research*, vol. 15, no. 6, pp. 557–572, 1996.

[63] Z. Zhakypov, M. Falahi, M. Shah, and J. Paik, "The design and control of the multi-modal locomotion origami robot, tribot," in *IEEE/RSJ International Conference on Intelligent Robots and Systems (IROS)*, 2015, pp. 4349–4355.

[64] P. Kammermeier, A. Kron, J. Hoogen, and G. Schmidt, "Display of holistic haptic sensations by combined tactile and kinesthetic feedback," *Presence: Teleoperators and Virtual Environments*, vol. 13, no. 1, pp. 1–15, 2004.

[65] I. Choi, H. Culbertson, M. R. Miller, A. Olwal, and S. Follmer, "Grabity: A wearable haptic interface for simulating weight and grasping in virtual reality," in *ACM Symposium on User Interface Software and Technology*, 2017, pp. 119–130.